

s1: Simple test-time scaling

Niklas Muennighoff^{*134} Zitong Yang^{*1} Weijia Shi^{*2} Xiang Lisa Li^{*1} Li Fei-Fei¹ Hannaneh Hajishirzi²³
 Luke Zettlemoyer² Percy Liang¹ Emmanuel Candès¹ Tatsunori Hashimoto¹

Abstract

Test-time scaling is a promising new approach to language modeling that uses extra test-time compute to improve performance. Recently, OpenAI’s o1 model showed this capability but did not publicly share its methodology, leading to many replication efforts. We seek the simplest approach to achieve test-time scaling and strong reasoning performance. First, we curate a small dataset **s1K** of 1,000 questions paired with reasoning traces relying on three criteria we validate through ablations: difficulty, diversity, and quality. Second, we develop budget forcing to control test-time compute by forcefully terminating the model’s thinking process or lengthening it by appending “Wait” multiple times to the model’s generation when it tries to end. This can lead the model to double-check its answer, often fixing incorrect reasoning steps. After supervised finetuning the Qwen2.5-32B-Instruct language model on **s1K** and equipping it with budget forcing, our model **s1-32B** exceeds o1-preview on competition math questions by up to 27% (MATH and AIME24). Further, scaling **s1-32B** with budget forcing allows extrapolating beyond its performance without test-time intervention: from 50% to 57% on AIME24. Our model, data, and code are open-source at <https://github.com/simplescaling/s1>.

1. Introduction

Performance improvements of language models (LMs) over the past years have largely relied on scaling up train-time compute using large-scale self-supervised pretraining (Kaplan et al., 2020; Hoffmann et al., 2022). The creation of these powerful models has set the stage for a new scaling paradigm built on top of them: *test-time scaling*. The aim

^{*}Equal contribution. ZY and NM started the project. WS, NM and ZY collected the prompts, XL, ZY and NM, built the data pipeline, LZ and WS proposed using a 1K subset and ZY and NM built budget forcing. ¹ Stanford University. ² University of Washington, Seattle. ³ Allen Institute for AI. ⁴ Contextual AI.

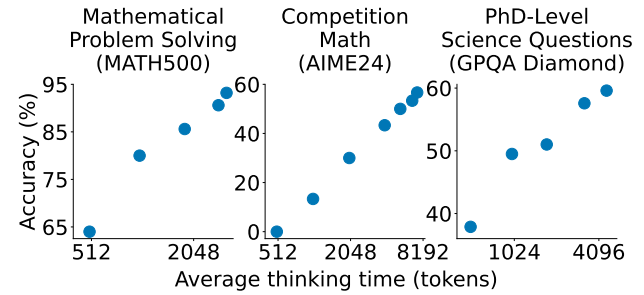


Figure 1. Test-time scaling with s1-32B. We benchmark s1-32B on reasoning-intensive tasks and vary test-time compute.

of this approach is to increase the compute at test time to get better results. There has been much work exploring this idea (Snell et al., 2024; Wu et al., 2024b; Welleck et al., 2024), and the viability of this paradigm was recently validated by OpenAI o1 (OpenAI, 2024). o1 has demonstrated strong reasoning performance with consistent gains from scaling test-time compute. OpenAI describes their approach as using large-scale reinforcement learning (RL) implying the use of sizable amounts of data (OpenAI, 2024). This has led to various attempts to replicate their models relying on techniques like Monte Carlo Tree Search (Gao et al., 2024b; Zhang et al., 2024a), multi-agent approaches (Huang et al., 2024b), and others (Huang et al., 2024b; Gao et al., 2024b; Zhang et al., 2024a; Wang et al., 2024a). Among these approaches, DeepSeek R1 (DeepSeek-AI et al., 2025) has successfully replicated o1-level performance, also employing reinforcement learning via millions of samples and multiple training stages. However, despite the large number of o1 replication attempts, none have openly replicated a clear test-time scaling behavior. Thus, we ask: what is the simplest approach to achieve both test-time scaling and strong reasoning performance?

We show that training on only 1,000 samples with next-token prediction and controlling thinking duration via a simple test-time technique we refer to as *budget forcing* leads to a strong reasoning model that scales in performance with more test-time compute. Specifically, we construct **s1K**, which consists of 1,000 carefully curated questions paired with reasoning traces and answers distilled from Gemini Thinking Experimental (Google, 2024). We perform super-

vised fine-tuning (SFT) of an off-the-shelf pretrained model on our small dataset requiring just 26 minutes of training on 16 H100 GPUs. After training, we control the amount of test-time compute our model spends using *budget forcing*: **(I)** If the model generates more thinking tokens than a desired limit, we forcefully end the thinking process by appending an end-of-thinking token delimiter. Ending the thinking this way makes the model transition to generating its answer. **(II)** If we want the model to spend more test-time compute on a problem, we suppress the generation of the end-of-thinking token delimiter and instead append “Wait” to the model’s current reasoning trace to encourage more exploration. Equipped with this simple recipe – SFT on 1,000 samples and test-time budget forcing – our model **s1-32B** exhibits test-time scaling (Figure 1). Further, **s1-32B** is the most sample-efficient reasoning model and outperforms closed-source models like OpenAI’s o1-preview (Figure 2).

We conduct extensive ablation experiments targeting (a) our selection of 1,000 (1K) reasoning samples and (b) our test-time scaling. For **(a)**, we find that jointly incorporating difficulty, diversity, and quality measures into our selection algorithm is important. Random selection, selecting samples with the longest reasoning traces, or only selecting maximally diverse samples all lead to significantly worse performance (around -30% on AIME24 on average). Training on our full data pool of 59K examples, a superset of **s1K**, does not offer substantial gains over our 1K selection. This highlights the importance of careful data selection and echoes prior findings for instruction tuning (Zhou et al., 2023). For **(b)**, we define desiderata for test-time scaling methods to compare different approaches. Budget forcing leads to the best scaling as it has perfect controllability with a clear positive slope leading to strong performance.

In summary, our contributions are: We develop simple methods for creating a sample-efficient reasoning dataset (§2) and test-time scaling (§3); Based on these we build **s1-32B** which is competitive with o1-preview (§4); We ablate subtleties of data (§5.1) and test-time scaling (§5.2). We end with a discussion to motivate future work on simple reasoning (§6). Our code, model, and data will be open-source.

2. Reasoning data curation to create s1K

In this section, we describe our process for creating a large dataset first in §2.1 and then filtering it down to **s1K** in §2.2.

2.1. Initial collection of 59K samples

We collect an initial 59,029 questions from 16 diverse sources following three guiding principles. **Quality**: Datasets should be of high quality; we always inspect samples and ignore datasets with, e.g., poor formatting; **Difficulty**: Datasets should be challenging and require significant

reasoning effort; **Diversity**: Datasets should stem from different fields to cover different reasoning tasks. We collect datasets of two categories:

Curation of existing datasets Our largest source is NuminaMATH (LI et al., 2024) with 30,660 mathematical problems from online websites. We also include historical AIME problems (1983-2021). To enhance diversity, we add OlympicArena (Huang et al., 2024a) with 4,250 questions spanning Astronomy, Biology, Chemistry, Computer Science, Geography, Mathematics, and Physics from various Olympiads. OmniMath (Gao et al., 2024a) adds 4,238 competition-level mathematics problems. We also include 2,385 problems from AGIEval (Zhong et al., 2023), which features questions from standardized tests like SAT and LSAT, covering English, Law, and Logic. We refer to Table 6 in §B for our other sources.

New datasets in quantitative reasoning To complement these existing datasets, we create two original datasets. s1-prob consists of 182 questions from the probability section of Stanford University’s Statistics Department’s PhD Qualifying Exams (<https://statistics.stanford.edu>), accompanied by handwritten solutions that cover difficult proofs. The probability qualifying exam is held yearly and requires professional-level mathematical problem-solving. s1-teasers comprises 23 challenging brain-teasers commonly used in interview questions for quantitative trading positions. Each sample consists of a problem and solution taken from PuzzledQuant (<https://www.puzzledquant.com/>). We only take examples with the highest difficulty level (“Hard”).

For each question, we generate a reasoning trace and solution using the Google Gemini Flash Thinking API (Google, 2024) extracting its reasoning trace and response. This yields 59K triplets of a question, generated reasoning trace, and generated solution. Examples from our dataset are in §C.2. We decontaminate all samples against our evaluation questions (MATH500, GPQA Diamond, AIME24; §B.5) using 8-grams and deduplicate the data.

2.2. Final selection of 1K samples

We could directly train on our pool of 59K questions, however, our goal is to find the *simplest* approach with minimal resources. Thus, we go through three stages of filtering to arrive at a minimal set of 1,000 samples relying on our three guiding data principles: Quality, Difficulty, and Diversity.

Quality We first remove any questions where we ran into any API errors reducing our dataset to 54,116 samples. Next, we filter out low-quality examples by checking if they contain any string patterns with formatting issues, such as ASCII art diagrams, non-existent image references, or inconsistent

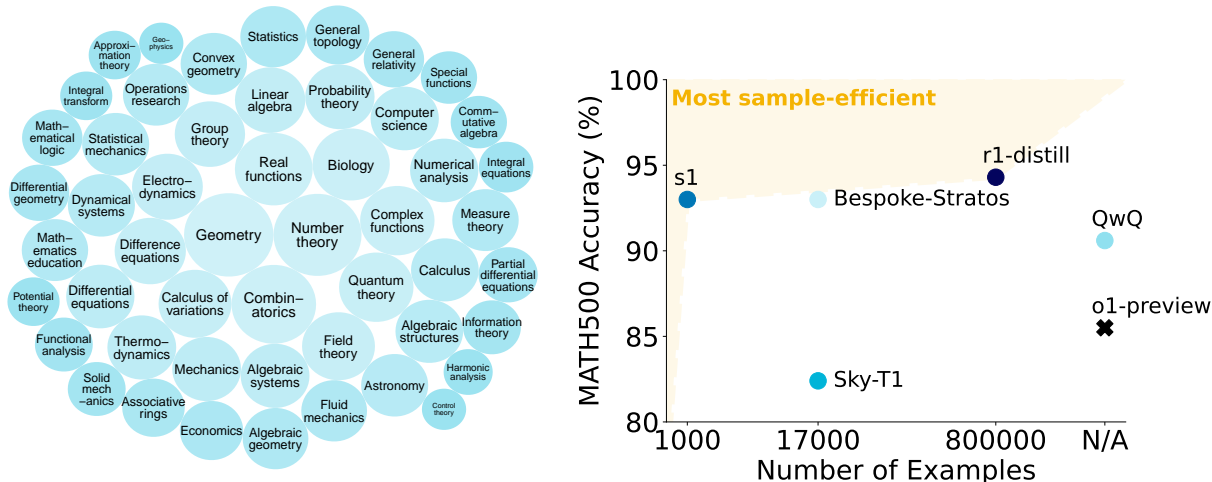


Figure 2. **s1K** and **s1-32B**. (left) **s1K** is a dataset of 1,000 high-quality, diverse, and difficult questions with reasoning traces. (right) **s1-32B**, a 32B parameter model finetuned on **s1K** is on the sample-efficiency frontier. See Table 1 for details on other models.

question numbering reducing our dataset to 51,581 examples. From this pool, we identify 384 samples for our final 1,000 samples from datasets that we perceive as high-quality and not in need of further filtering (see §B.4 for details).

Difficulty For difficulty, we use two indicators: model performance and reasoning trace length. We evaluate two models on each question: Qwen2.5-7B-Instruct and Qwen2.5-32B-Instruct (Qwen et al., 2024), with correctness assessed by Claude 3.5 Sonnet comparing each attempt against the reference solution (see §B.3 for the grading protocol). We measure the token length of each reasoning trace to indicate problem difficulty using the Qwen2.5 tokenizer. This relies on the assumption that more difficult problems require more thinking tokens. Based on the grading, we remove questions that either Qwen2.5-7B-Instruct or Qwen2.5-32B-Instruct can solve correctly and thus may be too easy. By using two models we reduce the likelihood of an easy sample slipping through our filtering due to a rare mistake on an easy question of one of the models. This brings our total samples down to 24,496, setting the stage for the next round of subsampling based on diversity. While filtering with these two models may be optimized for our setup as we will also use Qwen2.5-32B-Instruct as our model to finetune, the idea of model-based filtering generalizes to other setups.

Diversity To quantify diversity we classify each question into specific domains using Claude 3.5 Sonnet based on the Mathematics Subject Classification (MSC) system (e.g., geometry, dynamic systems, real analysis, etc.) from the American Mathematical Society.¹ The taxonomy focuses

¹<https://mathscinet.ams.org/mathscinet/msc/msc2020.html>

on topics in mathematics but also includes other sciences such as biology, physics, and economics. To select our final examples from the pool of 24,496 questions, we first choose one domain uniformly at random. Then, we sample one problem from this domain according to a distribution that favors longer reasoning traces (see §B.4 for details) as motivated in *Difficulty*. We repeat this process until we have 1,000 total samples.

This three-stage process yields a dataset spanning 50 different domains (see Table 5). In §5.1, we will show that using our three criteria in combination is important, as only relying on quality, diversity, or difficulty in isolation leads to worse datasets. Examples from our dataset are in §C.2.

3. Test-time scaling

3.1. Method

We classify test-time scaling methods into **1) Sequential**, where later computations depend on earlier ones (e.g., a long reasoning trace), and **2) Parallel**, where computations run independently (e.g., majority voting) (Snell et al., 2024; Brown et al., 2024). We focus on sequential scaling as intuitively we believe it should scale better, since later computations can build on intermediate results, allowing for deeper reasoning and iterative refinement. We propose new sequential scaling methods and ways to benchmark them.

Budget forcing We propose a simple decoding-time intervention by forcing a maximum and/or minimum number of thinking tokens at test time. Specifically, we enforce a maximum token count by simply appending the end-of-thinking token delimiter and “Final Answer:” to early exit the

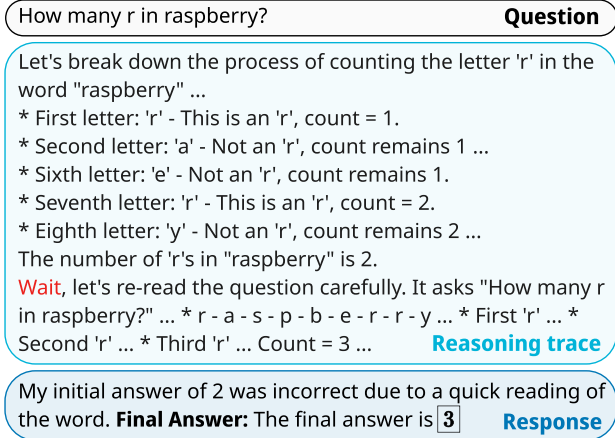


Figure 3. **Budget forcing with s1-32B.** The model tries to stop after "...is 2.", but we suppress the end-of-thinking token delimiter instead appending "Wait" leading s1-32B to self-correct its answer.

thinking stage and make the model provide its current best answer. To enforce a minimum, we suppress the generation of the end-of-thinking token delimiter and optionally append the string "Wait" to the model's current reasoning trace to encourage the model to reflect on its current generation. Figure 3 contains an example of how this simple approach can lead the model to arrive at a better answer.

Baselines We benchmark budget forcing with: **(I) Conditional length-control methods**, which rely on telling the model in the prompt how long it should generate for. We group them by granularity into (a) Token-conditional control: We specify an upper bound of thinking tokens in the prompt; (b) Step-conditional control: We specify an upper bound of thinking steps, where each step is around 100 tokens; (c) Class-conditional control: We write two generic prompts that tell the model to either think for a short or long amount of time (see §D.1 for details). **(II) Rejection sampling**, which samples until a generation fits a predetermined compute budget. This oracle captures the posterior over responses conditioned on its length.

3.2. Metrics

We establish a set of desiderata as evaluation metrics to measure test-time scaling across methods. Importantly, we do not only care about the accuracy a method can achieve but also its controllability and test-time scaling slope. For each method we consider, we run a set of evaluations $a \in \mathcal{A}$ varying test-time compute on a fixed benchmark, e.g. AIME24. This produces a piece-wise linear function f with compute as the x-axis measured in thinking tokens and accuracy as the y-axis (see Figure 1, where the rightmost dot for AIME24 corresponds to $f(7320) = 57\%$). We measure

three metrics:

$$\text{Control} = \frac{1}{|\mathcal{A}|} \sum_{a \in \mathcal{A}} \mathbb{1}(a_{\min} \leq a \leq a_{\max}) \quad (1)$$

where a_{\min}, a_{\max} refer to a pre-specified minimum and maximum amount of test-time compute; in our case thinking tokens. We usually only constrain a_{\max} . As tokens generated correspond to the amount of test-time compute spent, this metric measures the extent to which a method allows controllability over the use of that test-time compute. We report it as a percentage with 100% being perfect control.

$$\text{Scaling} = \frac{1}{\binom{|\mathcal{A}|}{2}} \sum_{\substack{a, b \in \mathcal{A} \\ b > a}} \frac{f(b) - f(a)}{b - a} \quad (2)$$

Scaling is the average slope of the piece-wise linear function. It must be positive for useful methods and larger is better.

$$\text{Performance} = \max_{a \in \mathcal{A}} f(a) \quad (3)$$

Performance is simply the maximum performance the method achieves on the benchmark. A method with monotonically increasing scaling achieves 100% performance on any benchmark in the limit. However, the methods we investigate eventually flatten out or further scaling fails due to control or context window limitations.

4. Results

4.1. Setup

Training We perform supervised finetuning on Qwen2.5-32B-Instruct using s1K to obtain our model s1-32B using basic hyperparameters outlined in §C. Finetuning took 26 minutes on 16 NVIDIA H100 GPUs with PyTorch FSDP.

Evaluation We select three representative reasoning benchmarks widely used in the field: **AIME24** (of America, 2024) consists of 30 problems that were used in the 2024 American Invitational Mathematics Examination (AIME) held from Wednesday, January 31 – Thursday, February 1, 2024. AIME tests mathematical problem-solving with arithmetic, algebra, counting, geometry, number theory, probability, and other secondary school math topics. High-scoring high school students in the test are invited to participate in the United States of America Mathematics Olympiad (USAMO). All AIME answers are integers ranging from 000 to 999, inclusive. Some AIME problems rely on figures that we provide to our model using the vector graphics language Asymptote as it cannot take image inputs. **MATH500** (Hendrycks et al., 2021) is a benchmark of competition math problems of varying difficulty. We evaluate on the same 500 samples selected by OpenAI in prior work (Lightman et al., 2023). **GPQA Diamond** (Rein et al., 2023) consists of 198

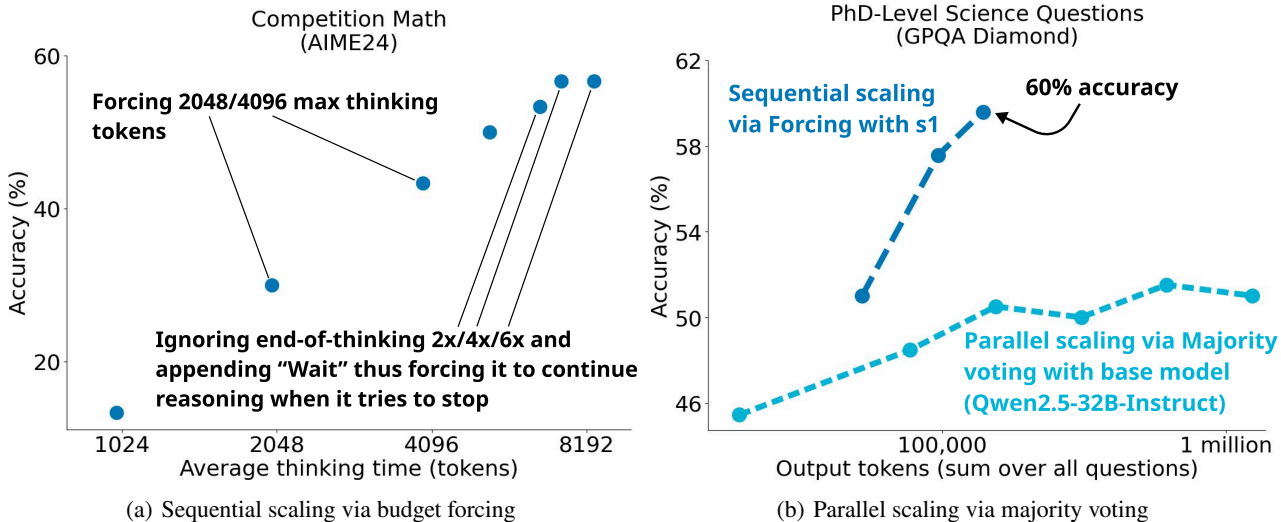


Figure 4. **Sequential and parallel test-time scaling.** (a): Budget forcing shows clear scaling trends and extrapolates to some extent. For the three rightmost dots, we prevent the model from stopping its thinking 2/4/6 times, each time appending “Wait” to its current reasoning trace. (b): For Qwen2.5-32B-Instruct we perform 64 evaluations for each sample and visualize the performance when majority voting across 2, 4, 8, 16, 32, and 64 of these.

PhD-level science questions from Biology, Chemistry and Physics. Experts with PhDs in the corresponding domains only achieved 69.7% on GPQA Diamond (OpenAI, 2024). When we write “GPQA” in the context of evaluation in this work, we always refer to the Diamond subset. We build on the “lm-evaluation-harness” framework (Gao et al., 2021; Biderman et al., 2024).

Other models We benchmark **s1-32B** against: **OpenAI o1 series** (OpenAI, 2024), which are closed-source models that popularized the idea of test-time scaling; **DeepSeek r1 series** (Team, 2024a), which are open-weight reasoning models with up to o1-level performance, concurrently released to ours; Qwen’s **QwQ-32B-preview** (Team, 2024b), a 32B open-weight reasoning model without disclosed methodology; **Sky-T1-32B-Preview**, which is an open-weight and open reasoning data model distilled from QwQ-32B-preview; **Google Gemini 2.0 Flash Thinking Experimental**, the API that we are distilling from. As there are no official evaluation scores, we use the Gemini API to benchmark it ourselves. However, the “recitation error” associated with the Gemini API makes evaluation challenging.² We circumvent this, by manually inserting all 30 AIME24 questions in its web interface where the error does not appear. However, we leave out MATH500 (500 questions) and GPQA Diamond (198 questions), thus they are N.A. in Table 1. Our model, **s1-32B**, is fully open including weights, reasoning data, and code.

²<https://github.com/google/generative-ai-docs/issues/257>

Table 1. **s1-32B is an open and sample-efficient reasoning model.** We evaluate **s1-32B**, Qwen, and Gemini (some entries are unknown (N.A.), see §4). Other results are from the respective reports (Qwen et al., 2024; Team, 2024b; OpenAI, 2024; DeepSeek-AI et al., 2025; Labs, 2025; Team, 2025). # ex. = number examples used for reasoning finetuning; BF = budget forcing.

Model	# ex.	AIME 2024	MATH-500	GPQA Diamond
API only				
o1-preview	N.A.	44.6	85.5	73.3
o1-mini	N.A.	70.0	90.0	60.0
o1	N.A.	74.4	94.8	77.3
Gemini 2.0 Flash Think.	N.A.	60.0	N.A.	N.A.
Open Weights				
Qwen2.5-32B-Instruct	N.A.	26.7	84.0	49.0
QwQ-32B	N.A.	50.0	90.6	65.2
r1	≥800K	79.8	97.3	71.5
r1-distill	800K	72.6	94.3	62.1
Open Weights and Open Data				
Sky-T1	17K	43.3	82.4	56.8
Bespoke-32B	17K	63.3	93.0	58.1
s1 w/o BF	1K	50.0	92.6	56.6
s1-32B	1K	56.7	93.0	59.6

4.2. Performance

Test-time scaling Figure 1 shows the performance of **s1-32B** with budget forcing scales with more test-time compute. In Figure 4 (left), we expand the plot from Figure 1 (middle) showing that while we can improve AIME24 performance using our budget forcing technique (§3) and more test-time compute it does eventually flatten out at six times. Suppressing the end-of-thinking token delimiter too often can lead the model into repetitive loops instead of continued reasoning. In Figure 4 (right), we show that after training Qwen2.5-32B-Instruct on our 1,000 samples to produce **s1-32B** and equipping it with the simple budget forcing technique, it operates in a different scaling paradigm. Scaling test-time compute on the base model via majority voting cannot catch up with the performance of **s1-32B** which validates our intuition from §3 that sequential scaling is more effective than parallel. We provide example generations of **s1-32B** in Figure 5.

Sample-efficiency In Figure 2 (right) and Table 1 we compare **s1-32B** with other models. We find that **s1-32B** is the most sample-efficient open data reasoning model. It performs significantly better than our base model (Qwen2.5-32B-Instruct) despite just training it on an additional 1,000 samples. The concurrently released r1-32B shows stronger performance than **s1-32B** while also only using SFT (DeepSeek-AI et al., 2025). However, it is trained on $800 \times$ more reasoning samples. It is an open question whether one can achieve their performance with just 1,000 samples. Finally, our model nearly matches Gemini 2.0 Thinking on AIME24, as **s1-32B** is distilled from Gemini 2.0, this shows that our distillation procedure was likely effective.

5. Ablations

5.1. Data Quantity, Diversity, and Difficulty

Table 2. **s1K data ablations.** We budget force (BF) a maximum of 32,000 thinking tokens for scores in this table. This performs slightly better than the scores without BF (Table 1) as it allows the model to finish with a best guess when stuck in an infinite loop. We report 95% Wilson confidence intervals with \pm .

Model	AIME 2024	MATH- 500	GPQA Diamond
1K-random	36.7 \pm 14.8	90.6 \pm 2.3	52.0 \pm 6.9
1K-diverse	26.7 \pm 12.5	91.2 \pm 2.2	54.6 \pm 6.8
1K-longest	33.3 \pm 14.0	90.4 \pm 2.3	59.6 \pm 6.6
59K-full	53.3 \pm 16.8	92.8 \pm 2.0	58.1 \pm 6.9
s1K	50.0 \pm 16.8	93.0 \pm 1.9	57.6 \pm 6.7

In §2 we outlined our three guiding principles in curating

s1K: Quality, Difficulty, and Diversity. Here we test the importance of combining them and the overall efficacy of our selection. **Only Quality (1K-random)**: After obtaining our high-quality reasoning chains from Gemini, we select 1,000 samples at random; not relying on our difficulty and diversity filtering at all. Table 2 shows this approach performs much worse than **s1K** across all benchmarks. **Only Diversity (1K-diverse)**: For this dataset, we sample uniformly across domains to maximize diversity disregarding any notion of difficulty. This approach also leads to poor performance similar to 1K-random. **Only Difficulty (1K-longest)**: Here we rely on one of our difficulty indicators introduced in §2 by selecting the 1,000 samples with the longest reasoning traces. This approach significantly boosts GPQA performance but overall still falls short of using **s1K**. **Maximize Quantity**: Finally, we compare with just training on all of our 59K samples, a superset of all the 1K-sample versions. This leads to a strong model but uses much more resources. To finetune on 59K samples, we use 394 H100 GPU hours while **s1-32B** only required 7 H100 GPU hours. Moreover, relying only on **s1K** is extremely competitive as shown in §2. Overall, combining all three criteria – *Quality*, *Difficulty*, *Diversity* – via our methodology in §2 is key for sample-efficient reasoning training.

5.2. Test-time scaling methods

Table 3. **Ablations on methods to scale test-time compute on AIME24.** $|A|$ refers to the number of evaluation runs used to estimate the properties; thus a higher value indicates more robustness. **Bold** indicates our chosen method and the best values. BF = budget forcing, TCC/SCC/CCC = token/step/class-conditional control, RS = rejection sampling.

Method	Control	Scaling	Performance	$ A $
BF	100%	15	56.7	5
TCC	40%	-24	40.0	5
TCC + BF	100%	13	40.0	5
SCC	60%	3	36.7	5
SCC + BF	100%	6	36.7	5
CCC	50%	25	36.7	2
RS	100%	-35	40.0	5

Budget forcing In Table 3 we compare the test-time scaling methods we have introduced in §3. Overall, we find that *budget forcing* provides perfect control, good scaling, and leads to our best AIME24 score. Thus, this is the method we use for **s1-32B** in Figure 1 and in §4. In Table 4, we compare different strings for extrapolating performance. We find that “Wait” generally gives the best performance.

Class-conditional control We provide benchmark scores for this method in §D.1 and summarize three findings here:

[AIME24]

Alice and Bob play the following game. A stack of n tokens lies before them. The players take turns with Alice going first. On each turn, the player removes either 1 token or 4 tokens from the stack. Whoever removes the last token wins. Find the number of positive integers n less than or equal to 2024 for which there exists a strategy for Bob that guarantees that Bob will win the game regardless of Alice's play.

The problem asks for the number of positive integers $n \leq 2024$ such that Bob has a winning strategy. This is a typical impartial game that can be analyzed using the Sprague-Grundy theorem or by directly finding the winning and losing positions. Let W be the set of winning positions (number of tokens n such that the player whose turn it is can force a win) and L be the set of losing positions. [...]

Let $P(n)$ be the statement "the player whose turn it is when there are n tokens has a winning strategy. $P(0)$ is false (the player whose turn it is and faces 0 tokens has already lost). Consider the small values of n :
 $n = 1$: The player whose turn it is can take 1 token and win. So $P(1)$ is true. $1 \in W$.
 $n = 2$: The player whose turn it is can take 1 token, leaving 1 token for the opponent. Since $1 \in W$, the opponent wins. So $P(2)$ is false. $2 \in L$.
 $n = 3$: The player whose turn it is can take 1 token, leaving 2 tokens for the opponent. Since $2 \in L$, the player whose turn it is wins. So $P(3)$ is true. $3 \in W$. [...]

We are looking for the number of positive integers $n \leq 2024$ for which Bob has a winning strategy. This means that if the game starts with n tokens, and Alice goes first, Bob can win. This happens if and only if n is a losing position (because if $n \in L$, then Alice's first move must lead to a winning position for Bob). [...]

Let's try to find a pattern in the losing positions $L = \{0, 2, 5, 7, 10, 12, 15, 17, 20, 22, \dots\}$. Differences between consecutive terms: 2, 3, 2, 3, 2, 3, 2, 3, ... The pattern of differences is alternating 2, 3. [...]

The losing positions are of the form $5m$ or $5m + 2$, where $m \geq 0$. We need to find the number of positive integers $n \leq 2024$ that are in the set of losing positions L . [...]

Case 1: $n = 5m$, where $m \geq 1$. $1 \leq 5m \leq 2024$
 $1/5 \leq m \leq 2024/5 = 404.8$ Since m is an integer, $1 \leq m \leq 404$. The number of values of m is 404.

Case 2: $n = 5m + 2$, where $m \geq 0$. $5m + 2 \leq 2024$
 $5m \leq 2022$ $m \leq 2022/5 = 404.4$ Since m is an integer, $0 \leq m \leq 404$. The number of values of m is $404 - 0 + 1 = 405$.

The total number of positive integers $n \leq 2024$ that are losing positions is $404 + 405 = \boxed{809}$.

[MATH]

Find the projection of a onto $b = \begin{pmatrix} 2 \\ 6 \\ 3 \end{pmatrix}$ if $a \cdot b = 8$.

The projection of vector \mathbf{a} onto vector \mathbf{b} is given by the formula:

$$\text{proj}_{\mathbf{b}} \mathbf{a} = \frac{\mathbf{a} \cdot \mathbf{b}}{\|\mathbf{b}\|^2} \mathbf{b}$$

We are given $\mathbf{b} = \begin{pmatrix} 2 \\ 6 \\ 3 \end{pmatrix}$ and $\mathbf{a} \cdot \mathbf{b} = 8$.

First, we need to find the magnitude squared of \mathbf{b} , which is $\|\mathbf{b}\|^2$.

$$\|\mathbf{b}\|^2 = \mathbf{b} \cdot \mathbf{b} = 2^2 + 6^2 + 3^2 = 4 + 36 + 9 = 49.$$

Now we can plug the values into the projection formula:

$$\text{proj}_{\mathbf{b}} \mathbf{a} = \frac{8}{49} \mathbf{b}$$

Substitute the vector \mathbf{b} :

$$\text{proj}_{\mathbf{b}} \mathbf{a} = \frac{8}{49} \begin{pmatrix} 2 \\ 6 \\ 3 \end{pmatrix}$$

Multiply the scalar by each component of the vector:

$$\text{proj}_{\mathbf{b}} \mathbf{a} = \begin{pmatrix} \frac{8}{49} \times 2 \\ \frac{8}{49} \times 6 \\ \frac{8}{49} \times 3 \end{pmatrix} = \begin{pmatrix} \frac{16}{49} \\ \frac{48}{49} \\ \frac{24}{49} \end{pmatrix}$$

Final Answer: The final answer is

$$\boxed{\begin{pmatrix} \frac{16}{49} \\ \frac{48}{49} \\ \frac{24}{49} \end{pmatrix}}$$

[GPQA]

A quantum mechanical particle of mass m moves in two dimensions in the following potential, as a function of the polar coordinates (r, θ) :

$$V(r, \theta) = \frac{1}{2}kr^2 + \frac{3}{2}kr^2 \cos^2(\theta)$$

Find the energy spectrum. Hint: Write the potential in Cartesian coordinates.

The problem asks for the energy spectrum of a particle in a given 2D potential. The potential is given in polar coordinates (r, θ) :

$$V(r, \theta) = \frac{1}{2}kr^2 + \frac{3}{2}kr^2 \cos^2(\theta).$$

We can rewrite the potential as:

$$V(r, \theta) = \frac{1}{2}kr^2(1 + 3 \cos^2(\theta)).$$

The Hamiltonian for a particle in 2D is given by:

$$H = -\frac{\hbar^2}{2m} \left(\frac{\partial^2}{\partial x^2} + \frac{\partial^2}{\partial y^2} \right) + V(x, y).$$

In polar coordinates (r, θ) , the Laplacian operator is:

$$\nabla^2 = \frac{1}{r} \frac{\partial}{\partial r} \left(r \frac{\partial}{\partial r} \right) + \frac{1}{r^2} \frac{\partial^2}{\partial \theta^2}.$$

So the Hamiltonian in polar coordinates is:

$$H = -\frac{\hbar^2}{2m} \left[\frac{1}{r} \frac{\partial}{\partial r} \left(r \frac{\partial}{\partial r} \right) + \frac{1}{r^2} \frac{\partial^2}{\partial \theta^2} \right] + V(r, \theta).$$

The time-independent Schrödinger equation is $H\psi = E\psi$. We can try to separate variables by assuming a solution of the form $\psi(r, \theta) = R(r)\Theta(\theta)$. [...]

This confirms the energy spectrum is:

$$E = \hbar \sqrt{\frac{k}{m}} \left(2n_x + n_y + \frac{3}{2} \right).$$

Final Answer: $E = \hbar \sqrt{\frac{k}{m}} \left(2n_x + n_y + \frac{3}{2} \right).$

Figure 5. Example model outputs. We pick a question from AIME24 (left), MATH (middle), and GPQA (right), where our model generates the correct answer. The black text is the prompt, the light blue text is the reasoning trace, and the blue text is the answer of s1-32B. The gray ellipsis [...] indicates that the text was trimmed to fit this page, but the generated text is actually longer.

(1) Token-conditional control fails without budget forcing, as our model cannot reliably count tokens - even when trained to do so. (2) Under step-conditional control, the model generates a similar total number of tokens when given different step targets, as the model goes from few steps with many tokens per step, to many steps with few tokens in each step. Thus, the model learns to hack its way around the compute constraint making the controllability of this method mediocre. (3) Class-conditional control can work - telling a model to simply think longer can increase its test-time compute and performance, which leads good scaling in Table 3.

Table 4. **Budget forcing extrapolation ablations.** We compare ignoring the end-of-thinking delimiter twice and appending none or various strings.

Model	AIME 2024	MATH -500	GPQA Diamond
No extrapolation	50.0	93.0	57.6
2x without string	50.0	90.2	55.1
2x "Alternatively"	50.0	92.2	59.6
2x "Hmm"	50.0	93.0	59.6
2x "Wait"	53.3	93.0	59.6

Rejection sampling Surprisingly, we find that simply sampling until the generation fits a specific length leads to an inverse scaling trend as depicted in Figure 6. In §D.2 we inspect a question, which was answered correctly by the model when rejection sampling for ≤ 4000 , but not for the ≤ 8000 token setting. In the ≤ 4000 setting the model directly jumps to the correct approach, while for the ≤ 8000 setting it backtracks a lot. We hypothesize that there is a correlation such that shorter generations tend to be the ones where the model was on the right track from the start, whereas longer ones tend to be ones where the model made mistakes and thus backtracks or questions itself. This leads to longer samples

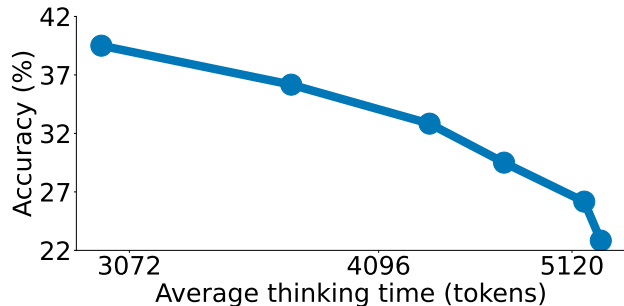


Figure 6. **Rejection sampling on AIME24 with s1-32B.** We sample with a temperature of 1 until all generations have less than (from left to right) 3500, 4000, 5000, 8000, and 16000 thinking tokens requiring an average of 655, 97, 8, 3, 2, and 1 tries per sample.

often being wrong when rejection sampling and thus the inverse scaling trend.

6. Discussion and related work

6.1. Sample-efficient reasoning

Models There are a number of concurrent efforts to build models that replicate the performance of o1 (OpenAI, 2024). For example, DeepSeek-r1 and k1.5 (DeepSeek-AI et al., 2025; Team et al., 2025) are built with reinforcement learning methods, while others rely on SFT using tens of thousands of distilled examples (Team, 2025; Xu et al., 2025; Labs, 2025). We show that SFT on only 1,000 examples suffices to build a competitive reasoning model matching o1-preview and produces a model that lies on the pareto frontier (Figure 2). Further, we introduce budget forcing which combined with our reasoning model leads to the first reproduction of OpenAI’s test-time scaling curves (OpenAI, 2024). Why does supervised finetuning on just 1,000 samples lead to such performance gains? We hypothesize that the model is already exposed to large amounts of reasoning data during pretraining which spans trillions of tokens. Thus, the ability to perform reasoning is already present in our model. Our sample-efficient finetuning stage just activates it and we scale it further at test time with budget forcing. This is similar to the "Superficial Alignment Hypothesis" presented in LIMA (Zhou et al., 2023), where the authors find that 1,000 examples can be sufficient to align a model to adhere to user preferences.

Benchmarks and methods To evaluate and push the limits of these models, increasingly challenging benchmarks have been introduced, such as Olympiad-level science competitions (He et al., 2024a; Jain et al., 2024a; Zhong et al., 2023) and others (Srivastava et al., 2023; Glazer et al., 2024; Su et al., 2024; Kim et al., 2024; Phan et al., 2025). To enhance models’ performance on reasoning-related tasks, researchers have pursued several strategies: Prior works have explored continuing training language models on specialized corpora related to mathematics and science (Azerbaiyev et al., 2023; Yang et al., 2024), sometimes even synthetically generated data (Yu et al., 2024). Others have developed training methodologies specifically aimed at reasoning performance (Zelikman et al., 2022; 2024; Luo et al., 2025; Yuan et al., 2025). Another significant line of work focuses on prompting-based methods to elicit and improve reasoning abilities, including methods like Chain-of-Thought prompting (Wei et al., 2023; Yao et al., 2023a;b; Bi et al., 2023; Fu et al., 2023; Zhang et al., 2024b; Hu et al., 2024). These combined efforts aim to advance the reasoning ability of language models, enabling them to handle more complex and abstract tasks effectively.

6.2. Test-time scaling

Methods As we introduce in §3, we differentiate two methods to scale test-time compute: **parallel** and **sequential**. The former relies on multiple solution attempts generated in parallel and selecting the best outcome via specific criteria. These criteria include choosing the most frequent response for majority voting or the best response based on an external reward for Best-of-N (Brown et al., 2024; Irvine et al., 2023; Snell et al., 2024). Unlike repeated sampling, previous sequential scaling methods let the model generate solution attempts sequentially based on previous attempts, allowing it to refine each attempt based on previous outcomes (Snell et al., 2024; Hou et al., 2025; Lee et al., 2025). Tree-based search methods (Gandhi et al., 2024; Wu et al., 2024a) offer a hybrid approach between sequential and parallel scaling, such as Monte-Carlo Tree Search (MCTS) (Liu et al., 2024; Zhang et al., 2023; Zhou et al., 2024; Choi et al., 2023) and guided beam search (Xie et al., 2023). REBASE (Wu et al., 2024a) employs a process reward model to balance exploitation and pruning during tree search. Empirically, REBASE has been shown to outperform sampling-based methods and MCTS (Wu et al., 2024a). Reward models (Lightman et al., 2023; Wang et al., 2024b;c) play a key role in these methods. They come in two variants: outcome reward models and process reward models. Outcome reward models (Xin et al., 2024; Ankner et al., 2024) assign a score to complete solutions and are particularly useful in Best-of-N selection, while process reward models (Lightman et al., 2023; Wang et al., 2024b; Wu et al., 2024a) assess individual reasoning steps and are effective in guiding tree-based search methods.

Limits to further test-time scaling We have shown that budget forcing allows extrapolating test-time compute in §4, e.g., improving AIME24 performance from 50% to 57%. However, it has two key limitations when scaling further: it eventually **flattens out** (Figure 4), and the **context window** of the underlying language model constrains it. Despite these constraints, our work shows test-time scaling across a wide range of accuracies (Figure 1), partly because scaling down test-time compute behaves predictably and does not suffer from these constraints.

Continuing test-time scaling will require approaches that can further extrapolate test-time compute. How can we get such extrapolation? There may be improvements to budget forcing such as rotating through different strings, not only “Wait”, or combining it with frequency penalties or higher temperature to avoid repetitive loops. An exciting direction for future work is also researching whether applying budget forcing to a reasoning model trained with reinforcement learning yields better extrapolation; or if RL allows for new ways of test-time scaling beyond budget forcing. Our work defines the right metrics (§3.2) – Control, Scaling, and Performance – to enable future research and progress on

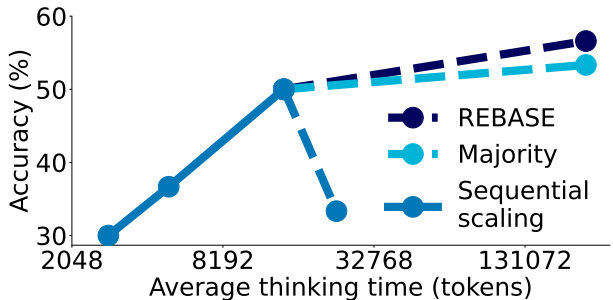


Figure 7. **Scaling further with parallel scaling methods.** All metrics averaged over the 30 questions in AIME24. Average thinking tokens for REBASE do not account for the additional compute from the reward model. For sequential scaling, we prompt the model to use up to (from left to right) 32, 64, 256, and 512 steps. For REBASE and majority voting we generate 16 parallel trajectories to aggregate across.

extrapolating test-time compute.

Parallel scaling as a solution Parallel scaling offers one solution to the limits of sequential scaling, thus we augment our sequentially scaled model with two methods: **(I) Majority voting:** After generating k solutions, the final solution is the most frequent one across generations; **(II) Tree search via REBASE:** We use the REBASE process reward model, which is initialized from LLaMA-34B and further finetuned on a synthetic process reward modeling dataset (Wu et al., 2024a). We then aggregate the solutions generated by REBASE via majority voting. As shown in Figure 7, augmenting our model with REBASE scales better than majority voting, and even sequential scaling in this scenario. However, REBASE requires an additional forward pass at each step for the reward model adding some computation overhead. For sequential scaling, when prompted to use up to 512 steps, for 12 out of the 30 evaluation questions the model generates a response that exceeds the context window leading to a large performance drop. Overall, we find that these parallel scaling methods complement sequential scaling thus they offer an avenue for scaling test-time compute even further; beyond fixed context windows.

Impact Statement

Language models with strong reasoning capabilities have the potential to greatly enhance human productivity, from assisting in complex decision-making to driving scientific breakthroughs. However, recent advances in reasoning, such as OpenAI’s o1 and DeepSeek’s r1, lack transparency, limiting broader research progress. Our work aims to push the frontier of reasoning in a fully open manner, fostering innovation and collaboration to accelerate advancements that ultimately benefit society.

Acknowledgements

This work was partly conducted using the Stanford Marlowe GPU cluster (Kapfer et al., 2025) made possible by financial support from Stanford University. We thank Alexander M. Rush, Andrew Ilyas, Banghua Zhu, Chenglei Si, Chunting Zhou, John Yang, Ludwig Schmidt, Samy Jelassi, Tengyu Ma, Xuechen Li, Yu Sun and Yue Zhang for very constructive discussions.

References

- Ankner, Z., Paul, M., Cui, B., Chang, J. D., and Ammanabrolu, P. Critique-out-loud reward models, 2024. URL <https://arxiv.org/abs/2408.11791>.
- Arora, D., Singh, H. G., and Mausam. Have llms advanced enough? a challenging problem solving benchmark for large language models, 2023. URL <https://arxiv.org/abs/2305.15074>.
- Azerbaiyev, Z., Schoelkopf, H., Paster, K., Santos, M. D., McAleer, S., Jiang, A. Q., Deng, J., Biderman, S., and Welleck, S. Llemma: An open language model for mathematics, 2023.
- Bi, Z., Zhang, N., Jiang, Y., Deng, S., Zheng, G., and Chen, H. When do program-of-thoughts work for reasoning?, 2023. URL <https://arxiv.org/abs/2308.15452>.
- Biderman, S., Schoelkopf, H., Sutawika, L., Gao, L., Tow, J., Abbasi, B., Aji, A. F., Ammanamanchi, P. S., Black, S., Clive, J., DiPofi, A., Etxaniz, J., Fattori, B., Forde, J. Z., Foster, C., Hsu, J., Jaiswal, M., Lee, W. Y., Li, H., Lovering, C., Muennighoff, N., Pavlick, E., Phang, J., Skowron, A., Tan, S., Tang, X., Wang, K. A., Winata, G. I., Yvon, F., and Zou, A. Lessons from the trenches on reproducible evaluation of language models, 2024.
- Brown, B., Juravsky, J., Ehrlich, R., Clark, R., Le, Q. V., Ré, C., and Mirhoseini, A. Large language monkeys: Scaling inference compute with repeated sampling, 2024. URL <https://arxiv.org/abs/2407.21787>.
- Chen, W., Yin, M., Ku, M., Lu, P., Wan, Y., Ma, X., Xu, J., Wang, X., and Xia, T. Theoremqa: A theorem-driven question answering dataset, 2023. URL <https://arxiv.org/abs/2305.12524>.
- Choi, S., Fang, T., Wang, Z., and Song, Y. Kcts: Knowledge-constrained tree search decoding with token-level hallucination detection, 2023. URL <https://arxiv.org/abs/2310.09044>.
- DeepSeek-AI, Guo, D., Yang, D., Zhang, H., Song, J., Zhang, R., Xu, R., Zhu, Q., Ma, S., Wang, P., Bi, X., Zhang, X., Yu, X., Wu, Y., Wu, Z. F., Gou, Z., Shao, Z., Li, Z., Gao, Z., Liu, A., Xue, B., Wang, B., Wu, B., Feng, B., Lu, C., Zhao, C., Deng, C., Zhang, C., Ruan, C., Dai, D., Chen, D., Ji, D., Li, E., Lin, F., Dai, F., Luo, F., Hao, G., Chen, G., Li, G., Zhang, H., Bao, H., Xu, H., Wang, H., Ding, H., Xin, H., Gao, H., Qu, H., Li, H., Guo, J., Li, J., Wang, J., Chen, J., Yuan, J., Qiu, J., Li, J., Cai, J. L., Ni, J., Liang, J., Chen, J., Dong, K., Hu, K., Gao, K., Guan, K., Huang, K., Yu, K., Wang, L., Zhang, L., Zhao, L., Wang, L., Zhang, L., Xu, L., Xia, L., Zhang, M., Zhang, M., Tang, M., Li, M., Wang, M., Li, M., Tian, N., Huang, P., Zhang, P., Wang, Q., Chen, Q., Du, Q., Ge, R., Zhang, R., Pan, R., Wang, R., Chen, R. J., Jin, R. L., Chen, R., Lu, S., Zhou, S., Chen, S., Ye, S., Wang, S., Yu, S., Zhou, S., Pan, S., Li, S. S., Zhou, S., Wu, S., Ye, S., Yun, T., Pei, T., Sun, T., Wang, T., Zeng, W., Zhao, W., Liu, W., Liang, W., Gao, W., Yu, W., Zhang, W., Xiao, W. L., An, W., Liu, X., Wang, X., Chen, X., Nie, X., Cheng, X., Liu, X., Xie, X., Liu, X., Yang, X., Li, X., Su, X., Lin, X., Li, X. Q., Jin, X., Shen, X., Chen, X., Sun, X., Wang, X., Song, X., Zhou, X., Wang, X., Shan, X., Li, Y. K., Wang, Y. Q., Wei, Y. X., Zhang, Y., Xu, Y., Li, Y., Zhao, Y., Sun, Y., Wang, Y., Yu, Y., Zhang, Y., Shi, Y., Xiong, Y., He, Y., Piao, Y., Wang, Y., Tan, Y., Ma, Y., Liu, Y., Guo, Y., Ou, Y., Wang, Y., Gong, Y., Zou, Y., He, Y., Xiong, Y., Luo, Y., You, Y., Liu, Y., Zhou, Y., Zhu, Y. X., Xu, Y., Huang, Y., Li, Y., Zheng, Y., Zhu, Y., Ma, Y., Tang, Y., Zha, Y., Yan, Y., Ren, Z. Z., Ren, Z., Sha, Z., Fu, Z., Xu, Z., Xie, Z., Zhang, Z., Hao, Z., Ma, Z., Yan, Z., Wu, Z., Gu, Z., Zhu, Z., Liu, Z., Li, Z., Xie, Z., Song, Z., Pan, Z., Huang, Z., Xu, Z., Zhang, Z., and Zhang, Z. Deepseek-r1: Incentivizing reasoning capability in llms via reinforcement learning, 2025. URL <https://arxiv.org/abs/2501.12948>.
- Fu, Y., Peng, H., Sabharwal, A., Clark, P., and Khot, T. Complexity-based prompting for multi-step reasoning, 2023. URL <https://arxiv.org/abs/2210.00720>.
- Gandhi, K., Lee, D., Grand, G., Liu, M., Cheng, W., Sharma, A., and Goodman, N. D. Stream of search (sos): Learning to search in language, 2024. URL <https://arxiv.org/abs/2404.03683>.
- Gao, B., Song, F., Yang, Z., Cai, Z., Miao, Y., Dong, Q., Li, L., Ma, C., Chen, L., Xu, R., Tang, Z., Wang, B., Zan, D., Quan, S., Zhang, G., Sha, L., Zhang, Y., Ren, X., Liu, T., and Chang, B. Omni-math: A universal olympiad level mathematics benchmark for large language models, 2024a. URL <https://arxiv.org/abs/2410.07985>.
- Gao, L., Tow, J., Biderman, S., Black, S., DiPofi, A., Foster, C., Golding, L., Hsu, J., McDonell, K., Muennighoff, N., Phang, J., Reynolds, L., Tang, E., Thite, A., Wang, B., Wang, K., and Zou, A. A framework for few-shot language

- model evaluation, September 2021. URL <https://doi.org/10.5281/zenodo.5371628>.
- Gao, Z., Niu, B., He, X., Xu, H., Liu, H., Liu, A., Hu, X., and Wen, L. Interpretable contrastive monte carlo tree search reasoning, 2024b. URL <https://arxiv.org/abs/2410.01707>.
- Glazer, E., Erdil, E., Besiroglu, T., Chicharro, D., Chen, E., Gunning, A., Olsson, C. F., Denain, J.-S., Ho, A., de Oliveira Santos, E., Järvineniemi, O., Barnett, M., Sandler, R., Vrzsala, M., Sevilla, J., Ren, Q., Pratt, E., Levine, L., Barkley, G., Stewart, N., Grechuk, B., Grechuk, T., Enugandla, S. V., and Wildon, M. Frontiermath: A benchmark for evaluating advanced mathematical reasoning in ai, 2024. URL <https://arxiv.org/abs/2411.04872>.
- Google. Gemini 2.0 flash thinking mode (gemini-2.0-flash-thinking-exp-1219), December 2024. URL <https://cloud.google.com/vertex-ai/generative-ai/docs/thinking-mode>.
- He, C., Luo, R., Bai, Y., Hu, S., Thai, Z. L., Shen, J., Hu, J., Han, X., Huang, Y., Zhang, Y., Liu, J., Qi, L., Liu, Z., and Sun, M. Olympiadbench: A challenging benchmark for promoting agi with olympiad-level bilingual multimodal scientific problems, 2024a. URL <https://arxiv.org/abs/2402.14008>.
- He, C., Luo, R., Bai, Y., Hu, S., Thai, Z. L., Shen, J., Hu, J., Han, X., Huang, Y., Zhang, Y., Liu, J., Qi, L., Liu, Z., and Sun, M. Olympiadbench: A challenging benchmark for promoting agi with olympiad-level bilingual multimodal scientific problems, 2024b. URL <https://arxiv.org/abs/2402.14008>.
- Hendrycks, D., Burns, C., Kadavath, S., Arora, A., Basart, S., Tang, E., Song, D., and Steinhardt, J. Measuring mathematical problem solving with the math dataset, 2021. URL <https://arxiv.org/abs/2103.03874>.
- Hoffmann, J., Borgeaud, S., Mensch, A., Buchatskaya, E., Cai, T., Rutherford, E., de Las Casas, D., Hendricks, L. A., Welbl, J., Clark, A., Hennigan, T., Noland, E., Millican, K., van den Driessche, G., Damoc, B., Guy, A., Osindero, S., Simonyan, K., Elsen, E., Rae, J. W., Vinyals, O., and Sifre, L. Training compute-optimal large language models, 2022. URL <https://arxiv.org/abs/2203.15556>.
- Hou, Z., Lv, X., Lu, R., Zhang, J., Li, Y., Yao, Z., Li, J., Tang, J., and Dong, Y. Advancing language model reasoning through reinforcement learning and inference scaling, 2025. URL <https://arxiv.org/abs/2501.11651>.
- Hu, Y., Shi, W., Fu, X., Roth, D., Ostendorf, M., Zettlemoyer, L., Smith, N. A., and Krishna, R. Visual sketchpad: Sketching as a visual chain of thought for multimodal language models, 2024. URL <https://arxiv.org/abs/2406.09403>.
- Huang, Z., Wang, Z., Xia, S., Li, X., Zou, H., Xu, R., Fan, R.-Z., Ye, L., Chern, E., Ye, Y., Zhang, Y., Yang, Y., Wu, T., Wang, B., Sun, S., Xiao, Y., Li, Y., Zhou, F., Chern, S., Qin, Y., Ma, Y., Su, J., Liu, Y., Zheng, Y., Zhang, S., Lin, D., Qiao, Y., and Liu, P. Olympicarena: Benchmarking multi-discipline cognitive reasoning for superintelligent ai, 2024a. URL <https://arxiv.org/abs/2406.12753>.
- Huang, Z., Zou, H., Li, X., Liu, Y., Zheng, Y., Chern, E., Xia, S., Qin, Y., Yuan, W., and Liu, P. O1 replication journey – part 2: Surpassing o1-preview through simple distillation, big progress or bitter lesson?, 2024b. URL <https://arxiv.org/abs/2411.16489>.
- Irvine, R., Boubert, D., Raina, V., Liusie, A., Zhu, Z., Mudupalli, V., Korshuk, A., Liu, Z., Cremer, F., Assassi, V., Beauchamp, C.-C., Lu, X., Rialan, T., and Beauchamp, W. Rewarding chatbots for real-world engagement with millions of users, 2023. URL <https://arxiv.org/abs/2303.06135>.
- Jain, N., Han, K., Gu, A., Li, W.-D., Yan, F., Zhang, T., Wang, S., Solar-Lezama, A., Sen, K., and Stoica, I. Livecodebench: Holistic and contamination free evaluation of large language models for code, 2024a. URL <https://arxiv.org/abs/2403.07974>.
- Jain, N., Han, K., Gu, A., Li, W.-D., Yan, F., Zhang, T., Wang, S., Solar-Lezama, A., Sen, K., and Stoica, I. Livecodebench: Holistic and contamination free evaluation of large language models for code, 2024b. URL <https://arxiv.org/abs/2403.07974>.
- Kapfer, C., Stine, K., Narasimhan, B., Mentzel, C., and Candes, E. Marlowe: Stanford’s gpu-based computational instrument, January 2025. URL <https://doi.org/10.5281/zenodo.14751899>.
- Kaplan, J., McCandlish, S., Henighan, T., Brown, T. B., Chess, B., Child, R., Gray, S., Radford, A., Wu, J., and Amodei, D. Scaling laws for neural language models, 2020. URL <https://arxiv.org/abs/2001.08361>.
- Kim, E., Suk, J., Kim, S., Muennighoff, N., Kim, D., and Oh, A. Llm-as-an-interviewer: Beyond static testing through dynamic llm evaluation, 2024. URL <https://arxiv.org/abs/2412.10424>.

- Kwon, W., Li, Z., Zhuang, S., Sheng, Y., Zheng, L., Yu, C. H., Gonzalez, J. E., Zhang, H., and Stoica, I. Efficient memory management for large language model serving with pagedattention, 2023. URL <https://arxiv.org/abs/2309.06180>.
- Labs, B. Bespoke-stratos: The unreasonable effectiveness of reasoning distillation, 2025. URL <https://hf.co/bespokelabs/Bespoke-Stratos-32B>. Accessed: 2025-01-22.
- Lee, K.-H., Fischer, I., Wu, Y.-H., Marwood, D., Baluja, S., Schuurmans, D., and Chen, X. Evolving deeper llm thinking, 2025. URL <https://arxiv.org/abs/2501.09891>.
- LI, J., Beeching, E., Tunstall, L., Lipkin, B., Soletskyi, R., Huang, S. C., Rasul, K., Yu, L., Jiang, A., Shen, Z., Qin, Z., Dong, B., Zhou, L., Fleureau, Y., Lample, G., and Polu, S. Numinamath, 2024. URL https://github.com/project-numina/aimo-progress-prize/blob/main/report/numina_dataset.pdf.
- Lightman, H., Kosaraju, V., Burda, Y., Edwards, H., Baker, B., Lee, T., Leike, J., Schulman, J., Sutskever, I., and Cobbe, K. Let’s verify step by step, 2023. URL <https://arxiv.org/abs/2305.20050>.
- Ling, W., Yogatama, D., Dyer, C., and Blunsom, P. Program induction by rationale generation : Learning to solve and explain algebraic word problems, 2017. URL <https://arxiv.org/abs/1705.04146>.
- Liu, J., Cui, L., Liu, H., Huang, D., Wang, Y., and Zhang, Y. Logiqa: A challenge dataset for machine reading comprehension with logical reasoning, 2020. URL <https://arxiv.org/abs/2007.08124>.
- Liu, J., Cohen, A., Pasunuru, R., Choi, Y., Hajishirzi, H., and Celikyilmaz, A. Don’t throw away your value model! generating more preferable text with value-guided monte-carlo tree search decoding, 2024. URL <https://arxiv.org/abs/2309.15028>.
- Loshchilov, I. and Hutter, F. Decoupled weight decay regularization, 2019.
- Luo, H., Sun, Q., Xu, C., Zhao, P., Lou, J., Tao, C., Geng, X., Lin, Q., Chen, S., Tang, Y., and Zhang, D. Wizardmath: Empowering mathematical reasoning for large language models via reinforced evol-instruct, 2025. URL <https://arxiv.org/abs/2308.09583>.
- of America, M. A. Aime, February 2024. URL https://artofproblemsolving.com/wiki/index.php/AIME_Problems_and_Solutions/.
- OpenAI. Learning to reason with llms, September 2024. URL <https://openai.com/index/learning-to-reason-with-llms/>.
- Phan, L., Gatti, A., Han, Z., Li, N., Hu, J., Zhang, H., Shi, S., Choi, M., Agrawal, A., Chopra, A., Khoja, A., Kim, R., Hausenloy, J., Zhang, O., Mazeika, M., Anderson, D., Nguyen, T., Mahmood, M., Feng, F., Feng, S. Y., Zhao, H., Yu, M., Gangal, V., Zou, C., Wang, Z., Wang, J. P., Kumar, P., Pokutnyi, O., Gerbicz, R., Popov, S., Levin, J.-C., Kazakov, M., Schmitt, J., Galgon, G., Sanchez, A., Lee, Y., Yeadon, W., Sauers, S., Roth, M., Agu, C., Riis, S., Giska, F., Utpala, S., Giboney, Z., Goshu, G. M., of Arc Xavier, J., Crowson, S.-J., Naiya, M. M., Burns, N., Finke, L., Cheng, Z., Park, H., Fournier-Facio, F., Wydallis, J., Nandor, M., Singh, A., Gehringer, T., Cai, J., McCarty, B., Duclosel, D., Nam, J., Zampese, J., Hoerr, R. G., Bacho, A., Loume, G. A., Galal, A., Cao, H., Garretson, A. C., Sileo, D., Ren, Q., Cojoc, D., Arkhipov, P., Qazi, U., Li, L., Motwani, S., de Witt, C. S., Taylor, E., Veith, J., Singer, E., Hartman, T. D., Rissone, P., Jin, J., Shi, J. W. L., Willcocks, C. G., Robinson, J., Mikov, A., Prabhu, A., Tang, L., Alapont, X., Uro, J. L., Zhou, K., de Oliveira Santos, E., Maksimov, A. P., Vendrow, E., Zenitani, K., Guillod, J., Li, Y., Vendrow, J., Kuchkin, V., Ze-An, N., Marion, P., Efremov, D., Lynch, J., Liang, K., Gritsevskiy, A., Martinez, D., Pageler, B., Crispino, N., Zvonkine, D., Fraga, N. W., Soori, S., Press, O., Tang, H., Salazar, J., Green, S. R., Brüssel, L., Twayana, M., Dieuleveut, A., Rogers, T. R., Zhang, W., Li, B., Yang, J., Rao, A., Loiseau, G., Kalinin, M., Lukas, M., Manolescu, C., Mishra, S., Kamdoun, A. G. K., Kreiman, T., Hogg, T., Jin, A., Bosio, C., Sun, G., Coppola, B. P., Tarver, T., Heidinger, H., Sayous, R., Ivanov, S., Cavanagh, J. M., Shen, J., Imperial, J. M., Schwaller, P., Senthilkuma, S., Bran, A. M., Dehghan, A., Algaba, A., Verbeken, B., Noever, D., V. R. P., Schut, L., Sucholutsky, I., Zheltonozhskii, E., Lim, D., Stanley, R., Sivarajan, S., Yang, T., Maar, J., Wykowski, J., Oller, M., Sandlin, J., Sahu, A., Hu, Y., Fish, S., Heydari, N., Apronti, A., Rawal, K., Vilchis, T. G., Zu, Y., Lackner, M., Koppel, J., Nguyen, J., Antonenko, D. S., Chern, S., Zhao, B., Arsene, P., Goldfarb, A., Ivanov, S., Poświata, R., Wang, C., Li, D., Crisostomi, D., Achilleos, A., Myklebust, B., Sen, A., Perrella, D., Kaparov, N., Inlow, M. H., Zang, A., Thornley, E., Orel, D., Poritski, V., Ben-David, S., Berger, Z., Whitfill, P., Foster, M., Munro, D., Ho, L., Hava, D. B., Kuchkin, A., Lauff, R., Holmes, D., Sommerhage, F., Schneider, K., Kazibwe, Z., Stambaugh, N., Singh, M., Magoulas, I., Clarke, D., Kim, D. H., Dias, F. M., Elser, V., Agarwal, K. P., Vilchis, V. E. G., Klose, I., Demian, C., Anantheswaran, U., Zweiger, A., Albani, G., Li, J., Daans, N., Radionov, M., Rozhoň, V., Ma, Z., Stump, C., Berkani, M., Platnick, J., Nevirkovets, V., Basler, L., Piccardo, M., Jeanplong, F.,

- Cohen, N., Tkadlec, J., Rosu, P., Padlewski, P., Barzowski, S., Montgomery, K., Menezes, A., Patel, A., Wang, Z., Tucker-Foltz, J., Stade, J., Goertzen, T., Kazemi, F., Milbauer, J., Ambay, J. A., Shukla, A., Labrador, Y. C. L., Givré, A., Wolff, H., Rossbach, V., Aziz, M. F., Kaddar, Y., Chen, Y., Zhang, R., Pan, J., Terpin, A., Muennighoff, N., Schoelkopf, H., Zheng, E., Carmi, A., Jones, A., Shah, J., Brown, E. D. L., Zhu, K., Bartolo, M., Wheeler, R., Ho, A., Barkan, S., Wang, J., Stehberger, M., Kretov, E., Sridhar, K., EL-Wasif, Z., Zhang, A., Pyda, D., Tam, J., Cunningham, D. M., Goryachev, V., Patramanis, D., Krause, M., Redenti, A., Bugas, D., Aldous, D., Lai, J., Coleman, S., Bahaloo, M., Xu, J., Lee, S., Zhao, S., Tang, N., Cohen, M. K., Carroll, M., Paradise, O., Kirchner, J. H., Steinerberger, S., Ovchynnikov, M., Matos, J. O., Shenoy, A., de Oliveira Junior, B. A., Wang, M., Nie, Y., Giordano, P., Petersen, P., Szyber-Betley, A., Shukla, P., Crozier, J., Pinto, A., Verma, S., Joshi, P., Yong, Z.-X., Tee, A., Andréoletti, J., Weller, O., Singhal, R., Zhang, G., Ivanov, A., Khoury, S., Mostaghimi, H., Thaman, K., Chen, Q., Khánh, T. Q., Loader, J., Cavalleri, S., Szlyk, H., Brown, Z., Roberts, J., Alley, W., Sun, K., Stendall, R., Lamparth, M., Reuel, A., Wang, T., Xu, H., Raparathi, S. G., Hernández-Cámara, P., Martin, F., Malishev, D., Preu, T., Korbak, T., Abramovitch, M., Williamson, D., Chen, Z., Bálint, B., Bari, M. S., Kassani, P., Wang, Z., Ansarinejad, B., Goswami, L. P., Sun, Y., Elgnainy, H., Tordera, D., Balabani, G., Anderson, E., Kvistad, L., Moyano, A. J., Maheshwari, R., Sakor, A., Eron, M., McAlister, I. C., Gimenez, J., Enyekwe, I. O., A. F. D., Shah, S., Zhou, X., Kamalov, F., Clark, R., Abdoli, S., Santens, T., Meer, K., Wang, H. K., Ramakrishnan, K., Chen, E., Tomasiello, A., Luca, G. B. D., Looi, S.-Z., Le, V.-K., Kolt, N., Mündler, N., Semler, A., Rodman, E., Drori, J., Fossum, C. J., Jagota, M., Pradeep, R., Fan, H., Shah, T., Eicher, J., Chen, M., Thaman, K., Merrill, W., Harris, C., Gross, J., Gusev, I., Sharma, A., Agnihotri, S., Zhelnov, P., Usawasutsakorn, S., Mofayezi, M., Bogdanov, S., Piperski, A., Carauleanu, M., Zhang, D. K., Ler, D., Leventov, R., Soroko, I., Jansen, T., Lauer, P., Duersch, J., Taamazyan, V., Morak, W., Ma, W., Held, W., Duc Huy, T., Xian, R., Zebaze, A. R., Mohamed, M., Leser, J. N., Yuan, M. X., Yacar, L., Lengler, J., Shahrtash, H., Oliveira, E., Jackson, J. W., Gonzalez, D. E., Zou, A., Chidambaram, M., Manik, T., Haffenden, H., Stander, D., Dasouqi, A., Shen, A., Duc, E., Golshani, B., Stap, D., Uzhou, M., Zhidkovskaya, A. B., Lewark, L., Vincze, M., Wehr, D., Tang, C., Hossain, Z., Phillips, S., Muzhen, J., Ekström, F., Hammon, A., Patel, O., Remy, N., Farhidi, F., Medley, G., Mohammadzadeh, F., Peñaflo, M., Kassahun, H., Friedrich, A., Sparrow, C., Sakal, T., Dhamane, O., Mirabadi, A. K., Hallman, E., Battaglia, M., Magsoudimehrabani, M., Hoang, H., Amit, A., Hulbert, D., Pereira, R., Weber, S., Mensah, S., Andre, N., Peristyy, A., Harjadi, C., Gupta, H., Malina, S., Albanie, S., Cai, W., Mehkary, M., Reidegeld, F., Dick, A.-K., Friday, C., Sidhu, J., Kim, W., Costa, M., Gurdogan, H., Weber, B., Kumar, H., Jiang, T., Agarwal, A., Ceconello, C., Vaz, W. S., Zhuang, C., Park, H., Tawfeek, A. R., Aggarwal, D., Kirchof, M., Dai, L., Kim, E., Ferret, J., Wang, Y., Yan, M., Burdzy, K., Zhang, L., Franca, A., Pham, D. T., Loh, K. Y., Robinson, J., Gul, S., Chhablani, G., Du, Z., Cosma, A., White, C., Riblet, R., Saxena, P., Votava, J., Vinnikov, V., Delaney, E., Halasyamani, S., Shahid, S. M., Mourrat, J.-C., Vetoshkin, L., Bacho, R., Ginis, V., Maksapetyan, A., de la Rosa, F., Li, X., Malod, G., Lang, L., Laurendeau, J., Adesanya, F., Portier, J., Hollom, L., Souza, V., Zhou, Y. A., Yalın, Y., Obikoya, G. D., Arnaboldi, L., Rai, Bigi, F., Bacho, K., Clavier, P., Recchia, G., Popescu, M., Shulga, N., Tanwie, N. M., Lux, T. C. H., Rank, B., Ni, C., Yakimchik, A., Huanxu, Liu, Häggström, O., Verkama, E., Narayan, H., Gundlach, H., Brito-Santana, L., Amaro, B., Vajipey, V., Grover, R., Fan, Y., e Silva, G. P. R., Xin, L., Kratish, Y., Łucki, J., Li, W.-D., Xu, J., Scaria, K. J., Vargus, F., Habibi, F., Long, Lian, Rodolà, E., Robins, J., Cheng, V., Grabb, D., Bosio, I., Fruhauff, T., Akov, I., Lo, E. J. Y., Qi, H., Jiang, X., Segev, B., Fan, J., Martinson, S., Wang, E. Y., Hausknecht, K., Brenner, M. P., Mao, M., Jiang, Y., Zhang, X., Avagian, D., Scipio, E. J., Siddiqi, M. R., Ragoler, A., Tan, J., Patil, D., Plecnik, R., Kirtland, A., Montecillo, R. G., Durand, S., Bodur, O. F., Adoul, Z., Zekry, M., Douville, G., Karakoc, A., Santos, T. C. B., Shamseldeen, S., Karim, L., Liakhovitskaia, A., Resman, N., Farina, N., Gonzalez, J. C., Maayan, G., Hoback, S., Pena, R. D. O., Sherman, G., Mariji, H., Pouriamanesh, R., Wu, W., Demir, G., Mendoza, S., Alarab, I., Cole, J., Ferreira, D., Johnson, B., Milliron, H., Safdari, M., Dai, L., Arthornthurasuk, S., Pronin, A., Fan, J., Ramirez-Trinidad, A., Cartwright, A., Pottmaier, D., Taheri, O., Outevsky, D., Stepanic, S., Perry, S., Askew, L., Rodríguez, R. A. H., Dendane, A., Ali, S., Lorena, R., Iyer, K., Salauddin, S. M., Islam, M., Gonzalez, J., Ducey, J., Campbell, R., Somrak, M., Mavroudis, V., Vergo, E., Qin, J., Borbás, B., Chu, E., Lindsey, J., Radhakrishnan, A., Jallon, A., McInnis, I. M. J., Hoover, A., Möller, S., Bian, S., Lai, J., Patwardhan, T., Yue, S., Wang, A., and Hendrycks, D. Humanity's last exam, 2025. URL <https://arxiv.org/abs/2501.14249>.
- Qwen, :, Yang, A., Yang, B., Zhang, B., Hui, B., Zheng, B., Yu, B., Li, C., Liu, D., Huang, F., Wei, H., Lin, H., Yang, J., Tu, J., Zhang, J., Yang, J., Yang, J., Zhou, J., Lin, J., Dang, K., Lu, K., Bao, K., Yang, K., Yu, L., Li, M., Xue, M., Zhang, P., Zhu, Q., Men, R., Lin, R., Li, T., Xia, T., Ren, X., Ren, X., Fan, Y., Su, Y., Zhang, Y., Wan, Y., Liu, Y., Cui, Z., Zhang, Z., and Qiu, Z. Qwen2.5 technical report, 2024. URL <https://arxiv.org/abs/2412.15115>.

- Rein, D., Hou, B. L., Stickland, A. C., Petty, J., Pang, R. Y., Dirani, J., Michael, J., and Bowman, S. R. Gpqa: A graduate-level google-proof q&a benchmark, 2023. URL <https://arxiv.org/abs/2311.12022>.
- Shi, Q., Tang, M., Narasimhan, K., and Yao, S. Can language models solve olympiad programming?, 2024. URL <https://arxiv.org/abs/2404.10952>.
- Snell, C., Lee, J., Xu, K., and Kumar, A. Scaling llm test-time compute optimally can be more effective than scaling model parameters, 2024. URL <https://arxiv.org/abs/2408.03314>.
- Srivastava, A., Rastogi, A., Rao, A., Shoeb, A. A. M., Abid, A., Fisch, A., Brown, A. R., Santoro, A., Gupta, A., Garriga-Alonso, A., et al. Beyond the imitation game: Quantifying and extrapolating the capabilities of language models, 2023.
- Su, H., Yen, H., Xia, M., Shi, W., Muennighoff, N., Yu Wang, H., Liu, H., Shi, Q., Siegel, Z. S., Tang, M., Sun, R., Yoon, J., Arik, S. O., Chen, D., and Yu, T. Bright: A realistic and challenging benchmark for reasoning-intensive retrieval, 2024. URL <https://arxiv.org/abs/2407.12883>.
- Sun, L., Han, Y., Zhao, Z., Ma, D., Shen, Z., Chen, B., Chen, L., and Yu, K. Scieval: A multi-level large language model evaluation benchmark for scientific research, 2024. URL <https://arxiv.org/abs/2308.13149>.
- Team, D. Deepseek r1, November 2024a. URL https://x.com/deepseek_ai/status/1859200141355536422.
- Team, K., Du, A., Gao, B., Xing, B., Jiang, C., Chen, C., Li, C., Xiao, C., Du, C., Liao, C., Tang, C., Wang, C., Zhang, D., Yuan, E., Lu, E., Tang, F., Sung, F., Wei, G., Lai, G., Guo, H., Zhu, H., Ding, H., Hu, H., Yang, H., Zhang, H., Yao, H., Zhao, H., Lu, H., Li, H., Yu, H., Gao, H., Zheng, H., Yuan, H., Chen, J., Guo, J., Su, J., Wang, J., Zhao, J., Zhang, J., Liu, J., Yan, J., Wu, J., Shi, L., Ye, L., Yu, L., Dong, M., Zhang, N., Ma, N., Pan, Q., Gong, Q., Liu, S., Ma, S., Wei, S., Cao, S., Huang, S., Jiang, T., Gao, W., Xiong, W., He, W., Huang, W., Wu, W., He, W., Wei, X., Jia, X., Wu, X., Xu, X., Zu, X., Zhou, X., Pan, X., Charles, Y., Li, Y., Hu, Y., Liu, Y., Chen, Y., Wang, Y., Liu, Y., Qin, Y., Liu, Y., Yang, Y., Bao, Y., Du, Y., Wu, Y., Wang, Y., Zhou, Z., Wang, Z., Li, Z., Zhu, Z., Zhang, Z., Wang, Z., Yang, Z., Huang, Z., Huang, Z., Xu, Z., and Yang, Z. Kimi k1.5: Scaling reinforcement learning with llms, 2025. URL <https://arxiv.org/abs/2501.12599>.
- Team, N. Sky-t1: Fully open-source reasoning model with o1-preview performance in \$450 budget, 2025. URL <https://novasky-ai.github.io/posts/sky-t1>. Accessed: 2025-01-09.
- Team, Q. Qwq: Reflect deeply on the boundaries of the unknown, November 2024b. URL <https://qwenlm.github.io/blog/qwq-32b-preview/>.
- Wang, J., Meng, F., Liang, Y., and Zhou, J. Drt-o1: Optimized deep reasoning translation via long chain-of-thought, 2024a. URL <https://arxiv.org/abs/2412.17498>.
- Wang, P., Li, L., Shao, Z., Xu, R. X., Dai, D., Li, Y., Chen, D., Wu, Y., and Sui, Z. Math-shepherd: Verify and reinforce llms step-by-step without human annotations, 2024b. URL <https://arxiv.org/abs/2312.08935>.
- Wang, S., Liu, Z., Zhong, W., Zhou, M., Wei, Z., Chen, Z., and Duan, N. From lsat: The progress and challenges of complex reasoning, 2021. URL <https://arxiv.org/abs/2108.00648>.
- Wang, Z., Dong, Y., Delalleau, O., Zeng, J., Shen, G., Egert, D., Zhang, J. J., Sreedhar, M. N., and Kuchaiev, O. Helpsteer2: Open-source dataset for training top-performing reward models, 2024c. URL <https://arxiv.org/abs/2406.08673>.
- Wei, J., Wang, X., Schuurmans, D., Bosma, M., Ichter, B., Xia, F., Chi, E., Le, Q., and Zhou, D. Chain-of-thought prompting elicits reasoning in large language models, 2023. URL <https://arxiv.org/abs/2201.11903>.
- Welleck, S., Bertsch, A., Finlayson, M., Schoelkopf, H., Xie, A., Neubig, G., Kulikov, I., and Harchaoui, Z. From decoding to meta-generation: Inference-time algorithms for large language models, 2024. URL <https://arxiv.org/abs/2406.16838>.
- Wu, Y., Sun, Z., Li, S., Welleck, S., and Yang, Y. Inference scaling laws: An empirical analysis of compute-optimal inference for problem-solving with language models, 2024a. URL <https://arxiv.org/abs/2408.00724>.
- Wu, Y., Sun, Z., Li, S., Welleck, S., and Yang, Y. Inference scaling laws: An empirical analysis of compute-optimal inference for problem-solving with language models, 2024b. URL <https://arxiv.org/abs/2408.00724>.
- Xie, Y., Kawaguchi, K., Zhao, Y., Zhao, X., Kan, M.-Y., He, J., and Xie, Q. Self-evaluation guided beam search for reasoning, 2023. URL <https://arxiv.org/abs/2305.00633>.
- Xin, H., Guo, D., Shao, Z., Ren, Z., Zhu, Q., Liu, B., Ruan, C., Li, W., and Liang, X. Deepseek-prover: Advancing theorem proving in llms through large-scale synthetic data, 2024. URL <https://arxiv.org/abs/2405.14333>.

- Xu, H., Wu, X., Wang, W., Li, Z., Zheng, D., Chen, B., Hu, Y., Kang, S., Ji, J., Zhang, Y., Guo, Z., Yang, Y., Zhang, M., and Zhang, D. Redstar: Does scaling long-cot data unlock better slow-reasoning systems?, 2025. URL <https://arxiv.org/abs/2501.11284>.
- Yang, Z., Band, N., Li, S., Candès, E., and Hashimoto, T. Synthetic continued pretraining, 2024. URL <https://arxiv.org/abs/2409.07431>.
- Yao, S., Yu, D., Zhao, J., Shafran, I., Griffiths, T. L., Cao, Y., and Narasimhan, K. Tree of thoughts: Deliberate problem solving with large language models, 2023a. URL <https://arxiv.org/abs/2305.10601>.
- Yao, S., Zhao, J., Yu, D., Du, N., Shafran, I., Narasimhan, K., and Cao, Y. React: Synergizing reasoning and acting in language models, 2023b. URL <https://arxiv.org/abs/2210.03629>.
- Yu, L., Jiang, W., Shi, H., Yu, J., Liu, Z., Zhang, Y., Kwok, J. T., Li, Z., Weller, A., and Liu, W. Metamath: Bootstrap your own mathematical questions for large language models, 2024. URL <https://arxiv.org/abs/2309.12284>.
- Yuan, S., Chen, Z., Xi, Z., Ye, J., Du, Z., and Chen, J. Agent-r: Training language model agents to reflect via iterative self-training, 2025. URL <https://arxiv.org/abs/2501.11425>.
- Zelikman, E., Wu, Y., Mu, J., and Goodman, N. D. Star: Bootstrapping reasoning with reasoning, 2022. URL <https://arxiv.org/abs/2203.14465>.
- Zelikman, E., Harik, G., Shao, Y., Jayasiri, V., Haber, N., and Goodman, N. D. Quiet-star: Language models can teach themselves to think before speaking, 2024. URL <https://arxiv.org/abs/2403.09629>.
- Zhang, H. and Chen, C. Test-time compute scaling laws, 2024. URL https://github.com/hughbzhang/o1_inference_scaling_laws.
- Zhang, S., Chen, Z., Shen, Y., Ding, M., Tenenbaum, J. B., and Gan, C. Planning with large language models for code generation, 2023. URL <https://arxiv.org/abs/2303.05510>.
- Zhang, Y., Wu, S., Yang, Y., Shu, J., Xiao, J., Kong, C., and Sang, J. o1-coder: an o1 replication for coding, 2024a. URL <https://arxiv.org/abs/2412.00154>.
- Zhang, Y., Yang, J., Yuan, Y., and Yao, A. C.-C. Cumulative reasoning with large language models, 2024b. URL <https://arxiv.org/abs/2308.04371>.
- Zhong, H., Xiao, C., Tu, C., Zhang, T., Liu, Z., and Sun, M. Jec-qa: A legal-domain question answering dataset, 2019. URL <https://arxiv.org/abs/1911.12011>.
- Zhong, W., Cui, R., Guo, Y., Liang, Y., Lu, S., Wang, Y., Saied, A., Chen, W., and Duan, N. Agieval: A human-centric benchmark for evaluating foundation models, 2023. URL <https://arxiv.org/abs/2304.06364>.
- Zhou, A., Yan, K., Shlapentokh-Rothman, M., Wang, H., and Wang, Y.-X. Language agent tree search unifies reasoning acting and planning in language models, 2024. URL <https://arxiv.org/abs/2310.04406>.
- Zhou, C., Liu, P., Xu, P., Iyer, S., Sun, J., Mao, Y., Ma, X., Efrat, A., Yu, P., Yu, L., Zhang, S., Ghosh, G., Lewis, M., Zettlemoyer, L., and Levy, O. Lima: Less is more for alignment, 2023.

Contents

1	Introduction	1
2	Reasoning data curation to create s1K	2
2.1	Initial collection of 59K samples	2
2.2	Final selection of 1K samples	2
3	Test-time scaling	3
3.1	Method	3
3.2	Metrics	4
4	Results	4
4.1	Setup	4
4.2	Performance	6
5	Ablations	6
5.1	Data Quantity, Diversity, and Difficulty	6
5.2	Test-time scaling methods	6
6	Discussion and related work	8
6.1	Sample-efficient reasoning	8
6.2	Test-time scaling	9
A	Evaluation determinism	17
B	s1K details	17
B.1	s1K summary	17
B.2	Dataset composition for full 59K questions	17
B.3	s1K grading prompt	19
B.4	s1K diversity selection	19
B.5	Decontamination	19
C	Training details	21
C.1	Training Ablations: Sequence length	21
C.2	Training Samples	21
D	Test-time scaling details	35
D.1	Sequential scaling ablations	35
D.2	Examples for rejection sampling ablation	37

A. Evaluation determinism

We run our evaluations using vLLM (Kwon et al., 2023) as it is faster than the alternatives we tried. However, we find that even when using the same random seeds and greedy sampling, evaluation scores can change significantly across runs:

- Different batch sizes causing different results see <https://github.com/vllm-project/vllm/issues/5898>
- Continuing generations causing different results see <https://github.com/vllm-project/vllm/issues/11783>
- Changes in tensor parallelism causing different results

As our model generates long reasoning traces prior to its answer, small numeric changes can snowball into large differences. We encounter many generations that are exactly the same for thousands of tokens and then suddenly differ in one token eventually ending up with an entirely different answer. To partly counter this issue we generally run our final evaluations using full precision unless otherwise indicated.

B. s1K details

B.1. s1K summary

Table 5. **Summary of our dataset s1K.** Token count measured by the Qwen-2.5 tokenizer. We prompt Claude to produce keywords given several questions from the domain.

Domain	#questions	Total token count	Keywords
Geometry	109	560.2K	Area, Triangle, Distance
Number theory	98	522.5K	Sequences, Divisibility
Combinatorics	75	384.7K	Permutations, Counting
Real functions	43	234.8K	Trigonometry, Calculus
Biology	41	120.9K	Organic reactions
Complex functions	32	170.2K	Complex roots
Quantum theory	32	127.9K	Particles, Wave functions
Field theory	28	150.1K	Polynomials, Roots
Calculus of variations	28	155.5K	Optimization, Control
Difference equations	24	132.5K	Recurrence, Recursion
Electromagnetic theory	23	95.8K	Optics, Waves, Diffraction
Group theory	22	100.0K	Groups, Automorphisms
Linear algebra	22	128.3K	Matrices, Determinants
Probability theory	20	114.6K	Random walk, Expectation
Algebraic systems	19	109.9K	Functional equations
Mechanics	19	103.6K	Forces, Motion, Energy
Thermodynamics	19	74.2K	Heat engines, Entropy
Differential equations	18	89.6K	Substitution, Existence
Computer science	18	34.2K	Complexity theory, Algorithms
Numerical analysis	18	76.5K	Error analysis, Stability
Calculus	17	96.3K	Convergence, Summation
Algebraic structures	17	90.4K	Inequalities, Sets
Astronomy	16	37.7K	Stellar populations, Orbits
Remaining 27 domains	242	982.2K	Domains with ≤ 16 questions
All domains (51)	1000	4.7M	s1K

B.2. Dataset composition for full 59K questions

Table 6. **Composition of full 59K questions.** Thinking and response lengths are measured in tokens using the Qwen2.5-32B-Instruct tokenizer (Qwen et al., 2024). In addition to excluding our evaluation benchmark, AIME24, we also exclude AIME questions from 2022-2023 as we use these 90 questions during our development stage of s1-32B.

Source	Description	#Samples	Avg. thinking length
NuminaMATH (LI et al., 2024)	Math problems from online websites	30660	4.1K
MATH (Hendrycks et al., 2021)	Math problems from competitions	11999	2.9K
OlympicArena (Huang et al., 2024a)	Astronomy, Biology, Chemistry, Computer Science, Geography, Math, and Physics olympiad questions	4250	3.2K
OmniMath (Gao et al., 2024a)	Math problems from competitions	4238	4.4K
AGIEval (Zhong et al., 2023; Ling et al., 2017; Hendrycks et al., 2021; Liu et al., 2020; Zhong et al., 2019; Wang et al., 2021)	English, Law, Logic and Math problems from the SAT, LSAT and other exams	2385	1.2K
xword	Crossword puzzles	999	0.7K
OlympiadBench (He et al., 2024b)	Math and Physics olympiad questions	896	3.9K
AIME (1983-2021)	American Invitational Mathematics Examination	890	4.7K
TheoremQA (Chen et al., 2023)	Computer Science, Finance, Math, and Physics university-level questions relating to theorems	747	2.1K
USACO (Shi et al., 2024)	Code problems from the USA Computing Olympiad	519	3.6K
JEEBench (Arora et al., 2023)	Chemistry, Math, and Physics problems used in the university entrance examination of the Indian Institute of Technology	515	2.9K
GPQA (Rein et al., 2023)	PhD-Level Science Questions	348	2.9K
SciEval (Sun et al., 2024)	Biology, Chemistry, and Physics problems from various sources	227	0.7K
s1-prob	Stanford statistics qualifying exams	182	4.0K
LiveCodeBench (Jain et al., 2024b)	Code problems from coding websites (LeetCode, AtCoder, and CodeForces)	151	3.5K
s1-teasers	Math brain-teasers crawled from the Internet	23	4.1K
All 59K questions	Composite of the above datasets with reasoning traces and solutions	59029	3.6K

B.3. s1K grading prompt

To grade whether an example is correct for our dataset selection in §2, we use the prompt in Figure 8.

You are an AI assistant for grading a science problem. The user will provide you with the question itself, an attempt made by a student and the correct answer to the problem. Your job is to judge whether the attempt is correct by comparing it with the correct answer. If the expected solution concludes with a number or choice, there should be no ambiguity. If the expected solution involves going through the entire reasoning process, you should judge the attempt based on whether the reasoning process is correct with correct answer if helpful.

The user will provide the attempt and the correct answer in the following format:

Problem
{problem}

Attempt
{attempt}

Correct answer
{solution}

Explain your reasoning, and end your response on a new line with only "Yes" or "No" (without quotes).

Figure 8. Grading prompt.

B.4. s1K diversity selection

Algorithm 1 provides our algorithm for selecting data in our diversity selection stage. As mentioned in §2, we also include samples from some specific benchmarks we perceive as high-quality. None of the samples overlap with our final evaluation.

B.5. Decontamination

We filter all samples by checking for an 8-gram overlap between the selected examples and the evaluation benchmarks: MATH500, GPTQA Diamond, and AIME24. We exclude questions with more than an 8-gram overlap.

Algorithm 1 Two-stage sampling for s1K

```

1: Input:  $\mathcal{Q}$  := Set of 24,496 questions with features
2: Output:  $\mathcal{S}$  := Set of 1,000 selected questions
3:  $\mathcal{S} \leftarrow \emptyset$  Initialize the output set (only tracks unique elements)
4: for  $q \in \mathcal{Q}$  do
5:   if IsGeminiCorrect( $q$ ) and (IsAIME( $q$ ) or IsGPQA( $q$ )) then
6:      $\mathcal{S} \leftarrow \mathcal{S} \cup \{q\}$ 
7:   Select all correct AIME/GPQA solutions
8:   else if IsGeminiCorrect( $q$ ) and IsMATH( $q$ ) and ThinkingLength( $q$ ) > 5600 then
9:      $\mathcal{S} \leftarrow \mathcal{S} \cup \{q\}$ 
10:   Select correct MATH solutions with long chains
11:   end if
12: end for
13:  $\mathcal{D} \leftarrow$  All available domains
14: Initialize domain pool
15: while  $|\mathcal{S}| < 1000$  do
16:    $d \leftarrow$  RandomChoice( $\mathcal{D}$ )
17:   Randomly select a domain
18:    $\mathcal{Q}_d \leftarrow$  Questions in domain  $d$ 
19:   Get questions from this domain
20:   ranks  $\leftarrow$  RankByThinkingLength( $\mathcal{Q}_d$ )
21:   Rank by thinking length
22:   weights  $\leftarrow 2^{-\text{ranks}}$ 
23:   Apply power-law weighting
24:    $q \leftarrow$  WeightedSample( $\mathcal{Q}_d$ , weights)
25:   Sample favoring longer chains
26:    $\mathcal{S} \leftarrow \mathcal{S} \cup \{q\}$ 
27:   Add selected question
28:    $\mathcal{Q}_d \leftarrow \mathcal{Q}_d \setminus \{q\}$ 
29:   if  $\mathcal{Q}_d = \emptyset$  then
30:      $\mathcal{D} \leftarrow \mathcal{D} \setminus \{d\}$ 
31:   Remove exhausted domains
32:   end if
33: end while

```

C. Training details

We take a model that has already been pretrained and instruction tuned and further finetune it for reasoning. Specifically, we use Qwen2.5-32B-Instruct (Qwen et al., 2024), which generally matches or outperforms the larger Qwen2.5-72B-Instruct on math tasks (Qwen et al., 2024). We use token delimiters to separate the thinking stage from the answering stage. We enclose the thinking stage with `<|im_start|>think` and `<|im_start|>answer`; both preceded and followed by a newline. Samples from our dataset are in §C.2. We use basic fine-tuning hyperparameters: we train for 5 epochs with a batch size of 16 for a total of 315 gradient steps. We train in bfloat16 precision with a learning rate of $1e-5$ warmed up linearly for 5% (16 steps) and then decayed to 0 over the rest of training (299 steps) following a cosine schedule. We use the AdamW optimizer (Loshchilov & Hutter, 2019) with $\beta_1 = 0.9$, $\beta_2 = 0.95$ and weight decay of $1e-4$. We do not compute loss on questions, only on reasoning traces and solutions. We ensure the sequence length is large enough to avoid cutting off any samples; a setting we ablate in §C.1. The training takes just 26 minutes on 16 NVIDIA H100 GPUs.

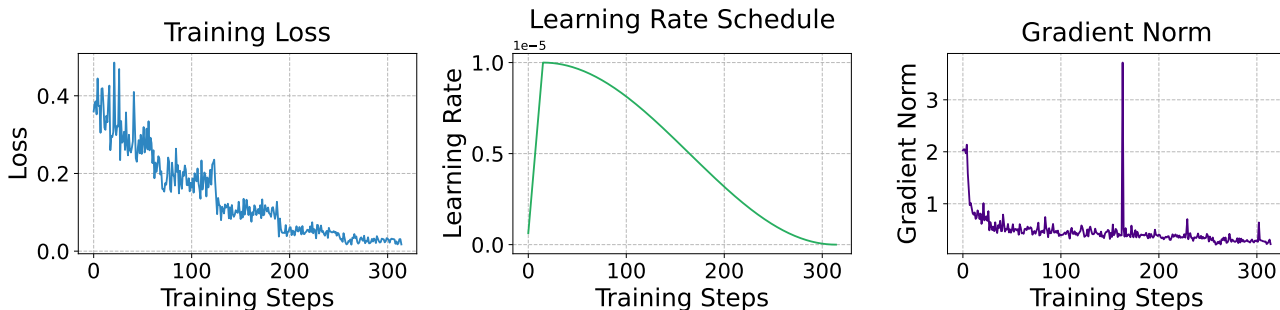


Figure 9. Training dynamics of s1-32B on s1K.

C.1. Training Ablations: Sequence length

Table 7. **Training sequence length ablation.** We report “accuracy / average thinking tokens per sample”; the higher the accuracy and the fewer the thinking tokens (inference cost) the better.

	Model A	Model B
Training sequence length	4096	32768
% training samples cutoff	74%	0%
AIME24	30.0% / 20721	50.0% / 6984
MATH	90.0% / 5324	91.0% / 3268
GPQA	52.5% / 6841	53.0% / 3568

Besides our scaling ablations in §5.2, the main training hyperparameter we ablate is the sequence length used during training. We find that a **shorter** training sequence length leads to **longer** reasoning traces at test time. This is because when training with a shorter sequence length the answer section of the training sample is more commonly cut off. Inversely, when the training sequence length is longer, more samples appear in their entirety with the section where the model answers. Thus the model receives more gradient updates where it learns to generate an answer following its chain. This in turn leads to a higher log probability of the answer section at any point during the generation and thus shorter reasoning traces at test time. Performance-wise, we find that there is no major difference when training with different sequence lengths, thus we opt for the longest training sequence length as it makes inference more efficient by leading to shorter reasoning traces.

C.2. Training Samples

Table 8, Table 9, Table 10 contain training samples from s1K.

Table 8. **s1K sample stemming from s1-prob.** The black text is the question and the yellow text is the solution. Based solely on the question we generate the light blue reasoning trace and blue response with Gemini, which we use for training.

You are given integrable random variables X, Y_0 and Z_0 on the same probability space $(\Omega, \mathcal{F}, \mathbb{P})$, and two σ -algebras $\mathcal{A} \subset \mathcal{F}, \mathcal{B} \subset \mathcal{F}$. For $k = 1, 2, \dots$, let

$$Y_k := \mathbb{E}[X | \sigma(\mathcal{A}, Z_0, \dots, Z_{k-1})], \quad Z_k := \mathbb{E}[X | \sigma(\mathcal{B}, Y_0, \dots, Y_{k-1})].$$

(a) Show that there exist integrable random variables Y_∞ and Z_∞ such that as $n \rightarrow \infty$ both $\mathbb{E}[|Y_n - Y_\infty|] \rightarrow 0$ and $\mathbb{E}[|Z_n - Z_\infty|] \rightarrow 0$. (b) Prove that almost surely $Y_\infty = Z_\infty$.

1. Introduce the notations, $\mathcal{F}_n := \sigma(\mathcal{A}, Z_0, \dots, Z_{n-1})$ and $\mathcal{G}_n := \sigma(\mathcal{B}, Y_0, \dots, Y_{n-1})$, for all $n \geq 1$ and $\mathcal{F}_0 := \mathcal{A}, \mathcal{G}_0 := \mathcal{B}$. Clearly, both are filtrations and by definition, $Y_n = \mathbb{E}[X | \mathcal{F}_n]$ and $Z_n = \mathbb{E}[X | \mathcal{G}_n]$, for all $n \geq 0$. Thus $\{Y_n\}_{n \geq 0}$ (or $\{Z_n\}_{n \geq 0}$) is a *Doob's Martingale* with respect to filtration $\{\mathcal{F}_n\}_{n \geq 0}$ (or $\{\mathcal{G}_n\}_{n \geq 0}$) and hence is U.I., X being integrable. Now apply the fact that a Martingale is U.I. if and only if it converges in L^1 and conclude.

2. We provide two different proofs.

1. Observe the following identity which follows from *Tower Property*.

$$\mathbb{E}[Y_n | \mathcal{G}_n] = \mathbb{E}[\mathbb{E}[X | \mathcal{F}_n] | \mathcal{G}_n] = \mathbb{E}[\mathbb{E}[X | \mathcal{G}_n] | \mathcal{F}_n] = \mathbb{E}[Z_n | \mathcal{F}_n]. \quad (4)$$

Note that $\mathbb{E}[|Y_n | \mathcal{G}_n - Y_\infty | \mathcal{G}_n|] \leq \mathbb{E}[|Y_n - Y_\infty|] = o(1)$ and by *Levy's Upward Theorem*, $\mathbb{E}[Y_\infty | \mathcal{G}_n] \xrightarrow{L^1} \mathbb{E}[Y_\infty | \mathcal{G}_\infty]$, where $\mathcal{G}_\infty = \sigma(\cup_{n \geq 0} \mathcal{G}_n) = \sigma(\mathcal{B}, Y_0, Y_1, \dots)$. It is evident that $Y_\infty \in m\mathcal{G}_\infty$ (since it is almost sure limit of $Y_n \in m\mathcal{G}_n$) and hence $\mathbb{E}[Y_\infty | \mathcal{G}_\infty] = Y_\infty$ almost surely. Combining the above observations we conclude that $\mathbb{E}[Y_n | \mathcal{G}_n] \xrightarrow{L^1} Y_\infty$. Similarly, $\mathbb{E}[Z_n | \mathcal{F}_n] \xrightarrow{L^1} Z_\infty$. Now invoke Equation (4), to conclude that $Y_\infty = Z_\infty$ almost surely.

2. Since X is integrable, we have by *Levy's Upward Theorem*, $Y_\infty = \lim_{n \rightarrow \infty} Y_n = \lim_{n \rightarrow \infty} \mathbb{E}[X | \mathcal{F}_n] = \mathbb{E}[X | \mathcal{F}_\infty]$. Similarly, $Z_\infty = \mathbb{E}[X | \mathcal{G}_\infty]$. On the otherhand, in first proof we have observed that $Y_\infty \in m\mathcal{G}_\infty$ and hence $Y_\infty \in m\mathcal{G}_\infty \cap m\mathcal{F}_\infty = m(\mathcal{G}_\infty \cap \mathcal{F}_\infty)$. This yields the following.

$$Y_\infty = \mathbb{E}[Y_\infty | \mathcal{G}_\infty \cap \mathcal{F}_\infty] = \mathbb{E}[\mathbb{E}[X | \mathcal{F}_\infty] | \mathcal{G}_\infty \cap \mathcal{F}_\infty] = \mathbb{E}[X | \mathcal{G}_\infty \cap \mathcal{F}_\infty].$$

Similarly, $Z_\infty = \mathbb{E}[X | \mathcal{G}_\infty \cap \mathcal{F}_\infty]$. This proves that $Y_\infty = Z_\infty$ almost surely.

Let's analyze the problem. We are given two sequences of random variables Y_k and Z_k defined by conditional expectations. We need to show that these sequences converge in L^1 and that their limits are equal almost surely.

Part (a): Convergence in L^1 .

The sigma-algebras involved are increasing:

$$\mathcal{F}_k = \sigma(\mathcal{A}, Z_0, \dots, Z_{k-1})$$

$$\mathcal{G}_k = \sigma(\mathcal{B}, Y_0, \dots, Y_{k-1})$$

For the Y_k sequence:

$$Y_1 = \mathbb{E}[X | \sigma(\mathcal{A})]$$

$$Y_2 = \mathbb{E}[X | \sigma(\mathcal{A}, Z_0)]$$

$$Y_3 = \mathbb{E}[X | \sigma(\mathcal{A}, Z_0, Z_1)]$$

...

The sequence of sigma-algebras $\sigma(\mathcal{A}, Z_0, \dots, Z_{k-1})$ is increasing. By the Martingale Convergence Theorem (for conditional expectations), since X is integrable, the sequence Y_k converges almost surely and in L^1 to $\mathbb{E}[X | \sigma(\mathcal{A}, Z_0, Z_1, \dots)]$. Let $Y_\infty = \mathbb{E}[X | \sigma(\mathcal{A}, Z_0, Z_1, \dots)]$.

Similarly, for the Z_k sequence:

$$Z_1 = \mathbb{E}[X|\sigma(\mathcal{B})]$$

$$Z_2 = \mathbb{E}[X|\sigma(\mathcal{B}, Y_0)]$$

$$Z_3 = \mathbb{E}[X|\sigma(\mathcal{B}, Y_0, Y_1)]$$

...

The sequence of sigma-algebras $\sigma(\mathcal{B}, Y_0, \dots, Y_{k-1})$ is increasing. By the Martingale Convergence Theorem, the sequence Z_k converges almost surely and in L^1 to $\mathbb{E}[X|\sigma(\mathcal{B}, Y_0, Y_1, \dots)]$. Let $Z_\infty = \mathbb{E}[X|\sigma(\mathcal{B}, Y_0, Y_1, \dots)]$.

Part (b): Prove that almost surely $Y_\infty = Z_\infty$.

We have $Y_\infty = \mathbb{E}[X|\sigma(\mathcal{A}, Z_0, Z_1, \dots)]$ and $Z_\infty = \mathbb{E}[X|\sigma(\mathcal{B}, Y_0, Y_1, \dots)]$.

Let $\mathcal{Y}_\infty = \sigma(\mathcal{A}, Z_0, Z_1, \dots)$ and $\mathcal{Z}_\infty = \sigma(\mathcal{B}, Y_0, Y_1, \dots)$.

Then $Y_\infty = \mathbb{E}[X|\mathcal{Y}_\infty]$ and $Z_\infty = \mathbb{E}[X|\mathcal{Z}_\infty]$.

Consider $Y_1 = \mathbb{E}[X|\mathcal{A}]$. $Z_1 = \mathbb{E}[X|\mathcal{B}]$.

$Y_2 = \mathbb{E}[X|\sigma(\mathcal{A}, Z_0)]$. Since $Z_0 = \mathbb{E}[X|\mathcal{B}]$, $\sigma(\mathcal{A}, Z_0) = \sigma(\mathcal{A}, \mathbb{E}[X|\mathcal{B}])$.

$Z_2 = \mathbb{E}[X|\sigma(\mathcal{B}, Y_0)]$. Since Y_0 is not defined, let's assume Y_0 and Z_0 are given.

Let's consider the sigma-algebra generated by all the Y_i and Z_i .

Let $\mathcal{G} = \sigma(Y_0, Z_0, Y_1, Z_1, \dots)$.

Both Y_k and Z_k are measurable with respect to \mathcal{G} . Thus, Y_∞ and Z_∞ are measurable with respect to \mathcal{G} .

Consider $\mathbb{E}[Y_{n+1}|\mathcal{A}, Z_0, \dots, Z_{n-1}] = \mathbb{E}[\mathbb{E}[X|\sigma(\mathcal{A}, Z_0, \dots, Z_n)]|\mathcal{A}, Z_0, \dots, Z_{n-1}] = Y_n$.

Consider $\mathbb{E}[Z_{n+1}|\mathcal{B}, Y_0, \dots, Y_{n-1}] = \mathbb{E}[\mathbb{E}[X|\sigma(\mathcal{B}, Y_0, \dots, Y_n)]|\mathcal{B}, Y_0, \dots, Y_{n-1}] = Z_n$.

Let $\mathcal{H} = \sigma(\mathcal{A} \cup \mathcal{B} \cup \sigma(Y_0, Z_0, Y_1, Z_1, \dots))$.

Consider $\mathbb{E}[X|\mathcal{A}, Z_0, \dots, Z_{k-1}] = Y_k$.

Consider $\mathbb{E}[X|\mathcal{B}, Y_0, \dots, Y_{k-1}] = Z_k$.

Let's consider the limit sigma-algebras $\mathcal{Y}_\infty = \sigma(\mathcal{A}, Z_0, Z_1, \dots)$ and $\mathcal{Z}_\infty = \sigma(\mathcal{B}, Y_0, Y_1, \dots)$.

We know that Y_∞ is \mathcal{Y}_∞ -measurable and Z_∞ is \mathcal{Z}_∞ -measurable.

Let $\mathcal{C} = \sigma(\mathcal{A} \cup \mathcal{B})$.

$Y_1 = \mathbb{E}[X|\mathcal{A}]$. $Z_1 = \mathbb{E}[X|\mathcal{B}]$.

$Y_2 = \mathbb{E}[X|\sigma(\mathcal{A}, Z_0)] = \mathbb{E}[X|\sigma(\mathcal{A}, \mathbb{E}[X|\mathcal{B}])]$.

$Z_2 = \mathbb{E}[X|\sigma(\mathcal{B}, Y_0)] = \mathbb{E}[X|\sigma(\mathcal{B}, \mathbb{E}[X|\mathcal{A}])]$.

Consider the case when \mathcal{A} and \mathcal{B} are independent. Then $Y_1 = \mathbb{E}[X|\mathcal{A}]$ and $Z_1 = \mathbb{E}[X|\mathcal{B}]$.

$Y_2 = \mathbb{E}[X|\sigma(\mathcal{A}, \mathbb{E}[X|\mathcal{B}])]$.

Let's consider the sigma-algebra generated by all the information. Let $\mathcal{F}_\infty = \sigma(\mathcal{A}, \mathcal{B}, Y_0, Z_0, Y_1, Z_1, \dots)$.

Then both Y_∞ and Z_∞ are \mathcal{F}_∞ -measurable.

We have $Y_\infty = \lim_{n \rightarrow \infty} Y_n$ and $Z_\infty = \lim_{n \rightarrow \infty} Z_n$ a.s. and in L^1 .

Consider $\mathbb{E}[X|\mathcal{A}, Z_0, Z_1, \dots] = Y_\infty$ and $\mathbb{E}[X|\mathcal{B}, Y_0, Y_1, \dots] = Z_\infty$.

Let $\mathcal{H}_\infty = \sigma(\mathcal{A} \cup \mathcal{B})$.

Consider $\mathbb{E}[X|\mathcal{H}_\infty]$.

Let's try to show that both Y_∞ and Z_∞ are equal to $\mathbb{E}[X|\sigma(\mathcal{A} \vee \mathcal{B})]$. This seems too simple.

Let's consider the definition of conditional expectation. For any set $A \in \mathcal{Y}_\infty$, $\mathbb{E}[Y_\infty 1_A] = \mathbb{E}[X 1_A]$.

For any set $B \in \mathcal{Z}_\infty$, $\mathbb{E}[Z_\infty 1_B] = \mathbb{E}[X 1_B]$.

Consider $\mathbb{E}[Y_{k+1}|\mathcal{F}_k] = Y_k$ where $\mathcal{F}_k = \sigma(\mathcal{A}, Z_0, \dots, Z_{k-1})$.

Consider $\mathbb{E}[Z_{k+1}|\mathcal{G}_k] = Z_k$ where $\mathcal{G}_k = \sigma(\mathcal{B}, Y_0, \dots, Y_{k-1})$.

Consider the sigma-algebra $\sigma(\mathcal{A} \cup \mathcal{B})$.

Let $W = \mathbb{E}[X|\sigma(\mathcal{A} \cup \mathcal{B})]$.

We have $Y_\infty = \mathbb{E}[X|\sigma(\mathcal{A}, Z_0, Z_1, \dots)]$.

Since Z_k depends on Y_{k-1} which depends on Z_{k-2} etc., it is complex.

Let's consider the case where $Y_0 = \mathbb{E}[X|\mathcal{A}]$ and $Z_0 = \mathbb{E}[X|\mathcal{B}]$.

Then $Y_1 = \mathbb{E}[X|\mathcal{A}] = Y_0$.

$Z_1 = \mathbb{E}[X|\mathcal{B}] = Z_0$.

If this were the case, then $Y_k = Y_0$ and $Z_k = Z_0$, so $Y_\infty = Y_0$ and $Z_\infty = Z_0$.

We need $Y_0 = Z_0$ a.s., i.e., $\mathbb{E}[X|\mathcal{A}] = \mathbb{E}[X|\mathcal{B}]$ a.s. This is not generally true.

Consider the sigma-algebra generated by all Y_i and Z_i , denoted by $\mathcal{G}_\infty = \sigma(Y_0, Z_0, Y_1, Z_1, \dots)$.

Then $\mathcal{Y}_\infty = \sigma(\mathcal{A}, Z_0, Z_1, \dots) \subseteq \sigma(\mathcal{A}, \mathcal{G}_\infty)$.

$\mathcal{Z}_\infty = \sigma(\mathcal{B}, Y_0, Y_1, \dots) \subseteq \sigma(\mathcal{B}, \mathcal{G}_\infty)$.

Consider $\mathbb{E}[X|\mathcal{A}, Z_0, Z_1, \dots] = Y_\infty$. This means for any $A \in \sigma(\mathcal{A}, Z_0, Z_1, \dots)$, $\mathbb{E}[X1_A] = \mathbb{E}[Y_\infty 1_A]$.

Consider $\mathbb{E}[X|\mathcal{B}, Y_0, Y_1, \dots] = Z_\infty$. This means for any $B \in \sigma(\mathcal{B}, Y_0, Y_1, \dots)$, $\mathbb{E}[X1_B] = \mathbb{E}[Z_\infty 1_B]$.

Let $\mathcal{H} = \sigma(\mathcal{A}, \mathcal{B})$.

Consider $\mathbb{E}[X|\mathcal{H}]$.

Consider $\mathbb{E}[Y_\infty|\mathcal{B}, Y_0, Y_1, \dots] = \mathbb{E}[\mathbb{E}[X|\mathcal{A}, Z_0, Z_1, \dots]|\mathcal{B}, Y_0, Y_1, \dots]$.

Let's use the fact that Y_∞ is $\sigma(\mathcal{A}, Z_0, Z_1, \dots)$ -measurable and Z_∞ is $\sigma(\mathcal{B}, Y_0, Y_1, \dots)$ -measurable.

Consider the smallest sigma-algebra containing both $\sigma(\mathcal{A}, Z_0, Z_1, \dots)$ and $\sigma(\mathcal{B}, Y_0, Y_1, \dots)$.

This is $\sigma(\mathcal{A} \cup \mathcal{B} \cup \{Y_i\}_{i \geq 0} \cup \{Z_i\}_{i \geq 0})$.

Let's try to show that $\mathbb{E}[(Y_\infty - Z_\infty)^2] = 0$.

$$\mathbb{E}[(Y_\infty - Z_\infty)^2] = \mathbb{E}[Y_\infty^2] + \mathbb{E}[Z_\infty^2] - 2\mathbb{E}[Y_\infty Z_\infty].$$

Consider the definition of Y_k and Z_k .

$$\mathbb{E}[Y_{k+1}|\mathcal{A}, Z_0, \dots, Z_{k-1}] = Y_k.$$

$$\mathbb{E}[Z_{k+1}|\mathcal{B}, Y_0, \dots, Y_{k-1}] = Z_k.$$

Consider $\mathbb{E}[Y_\infty|\mathcal{B}, Y_0, Y_1, \dots]$.

Since Y_∞ is measurable with respect to $\sigma(\mathcal{A}, Z_0, Z_1, \dots)$, this does not simplify easily.

Let's assume $Y_\infty \neq Z_\infty$ on a set of positive measure.

Consider the case where \mathcal{A} and \mathcal{B} are trivial.

Then $Y_k = \mathbb{E}[X|\sigma(Z_0, \dots, Z_{k-1})]$ and $Z_k = \mathbb{E}[X|\sigma(Y_0, \dots, Y_{k-1})]$.

Let $\mathcal{H}_\infty = \sigma(\mathcal{A} \cup \mathcal{B} \cup \{Y_i, Z_i\}_{i \geq 0})$.

Consider $\mathbb{E}[X|\mathcal{H}_\infty]$.

We have $Y_\infty = \mathbb{E}[X|\sigma(\mathcal{A}, Z_0, Z_1, \dots)]$.

By the properties of conditional expectation, $\mathbb{E}[Y_\infty|\mathcal{A}] = \mathbb{E}[\mathbb{E}[X|\mathcal{A}, Z_0, Z_1, \dots]|\mathcal{A}]$.

Consider the sigma-algebra \mathcal{D} generated by all the random variables involved.

$$\mathcal{D} = \sigma(\mathcal{A} \cup \mathcal{B} \cup \{Y_i\}_{i \geq 0} \cup \{Z_i\}_{i \geq 0}).$$

Let $M_\infty = \mathbb{E}[X|\mathcal{A} \vee \mathcal{B}]$.

Consider the limits. As $n \rightarrow \infty$, $\sigma(\mathcal{A}, Z_0, \dots, Z_{n-1}) \uparrow \sigma(\mathcal{A}, Z_0, Z_1, \dots)$.

As $n \rightarrow \infty$, $\sigma(\mathcal{B}, Y_0, \dots, Y_{n-1}) \uparrow \sigma(\mathcal{B}, Y_0, Y_1, \dots)$.

Let $\mathcal{Y}_\infty = \sigma(\mathcal{A}, Z_0, Z_1, \dots)$ and $\mathcal{Z}_\infty = \sigma(\mathcal{B}, Y_0, Y_1, \dots)$.

We have $Y_\infty = \mathbb{E}[X|\mathcal{Y}_\infty]$ and $Z_\infty = \mathbb{E}[X|\mathcal{Z}_\infty]$.

$$\begin{aligned} \text{Consider } \mathbb{E}[Y_\infty - Z_\infty]^2 &= \mathbb{E}[(Y_\infty - X) + (X - Z_\infty)]^2 \\ &= \mathbb{E}[(Y_\infty - X)^2] + \mathbb{E}[(X - Z_\infty)^2] + 2\mathbb{E}[(Y_\infty - X)(X - Z_\infty)] \\ &= \mathbb{E}[(X - \mathbb{E}[X|\mathcal{Y}_\infty])^2] + \mathbb{E}[(X - \mathbb{E}[X|\mathcal{Z}_\infty])^2] + 2\mathbb{E}[Y_\infty X - Y_\infty Z_\infty - X^2 + X Z_\infty] \\ &= \mathbb{E}[X^2] - \mathbb{E}[Y_\infty^2] + \mathbb{E}[X^2] - \mathbb{E}[Z_\infty^2] + 2\mathbb{E}[Y_\infty X] - 2\mathbb{E}[Y_\infty Z_\infty] - 2\mathbb{E}[X^2] + 2\mathbb{E}[X Z_\infty] \\ &= -\mathbb{E}[Y_\infty^2] - \mathbb{E}[Z_\infty^2] + 2\mathbb{E}[Y_\infty^2] - 2\mathbb{E}[Y_\infty Z_\infty] + 2\mathbb{E}[Z_\infty^2] \\ &= \mathbb{E}[Y_\infty^2] + \mathbb{E}[Z_\infty^2] - 2\mathbb{E}[Y_\infty Z_\infty] \end{aligned}$$

Consider the sigma-algebra $\mathcal{C} = \sigma(\mathcal{A} \cup \mathcal{B})$.

Let $W = \mathbb{E}[X|\mathcal{C}]$.

Consider the limit sigma-algebra generated by all the information.

Let $\mathcal{F}_\infty = \sigma(\mathcal{A}, \mathcal{B}, Y_0, Z_0, Y_1, Z_1, \dots)$.

Then $\mathcal{Y}_\infty \subseteq \mathcal{F}_\infty$ and $\mathcal{Z}_\infty \subseteq \mathcal{F}_\infty$.

We have $\mathbb{E}[X|\mathcal{Y}_\infty] = Y_\infty$ and $\mathbb{E}[X|\mathcal{Z}_\infty] = Z_\infty$.

Consider $\mathbb{E}[Y_\infty|\mathcal{Z}_\infty]$ and $\mathbb{E}[Z_\infty|\mathcal{Y}_\infty]$.

Let $\mathcal{H} = \sigma(\mathcal{A} \cup \mathcal{B})$.

Consider $\mathbb{E}[X|\mathcal{H}]$.

Consider the sequence of pairs (Y_k, Z_k) .

If the limits are the same, then for any bounded measurable function f , $\mathbb{E}[f(Y_\infty)] = \mathbb{E}[f(Z_\infty)]$.

Consider the sigma-algebra $\mathcal{D} = \sigma(\mathcal{A} \cup \mathcal{B} \cup \sigma(Y_0, Z_0, \dots))$.

Then both Y_∞ and Z_∞ are measurable with respect to \mathcal{D} .

Consider $\mathbb{E}[(Y_n - Z_n)^2]$.

Let $\mathcal{G} = \sigma(\mathcal{A} \cup \mathcal{B})$.

Consider $W = \mathbb{E}[X|\mathcal{G}]$.

Then $\mathbb{E}[W|\mathcal{A}] = \mathbb{E}[X|\mathcal{A}]$ and $\mathbb{E}[W|\mathcal{B}] = \mathbb{E}[X|\mathcal{B}]$.

Consider the limit sigma-algebra $\mathcal{L} = \sigma(\mathcal{A} \cup \mathcal{B} \cup \sigma(Y_0, Z_0, \dots))$.

We have $Y_\infty = \mathbb{E}[X|\sigma(\mathcal{A}, Z_0, Z_1, \dots)]$ and $Z_\infty = \mathbb{E}[X|\sigma(\mathcal{B}, Y_0, Y_1, \dots)]$.

Let $\mathcal{M} = \sigma(\mathcal{A}, Z_0, Z_1, \dots) \vee \sigma(\mathcal{B}, Y_0, Y_1, \dots)$.

Consider $\mathbb{E}[X|\mathcal{M}]$.

Consider the random variable X . Then $Y_\infty = \lim_n \mathbb{E}[X|\mathcal{F}_n]$ and $Z_\infty = \lim_n \mathbb{E}[X|\mathcal{G}_n]$.

Let $\mathcal{H}_\infty = \sigma(\mathcal{A} \cup \mathcal{B} \cup \sigma(Y_0, Z_0, \dots))$.

Consider $E = \{\omega : Y_\infty(\omega) \neq Z_\infty(\omega)\}$. Suppose $P(E) > 0$.

Consider the conditional expectation with respect to the join of the sigma-algebras.

Let $\mathcal{C}_\infty = \sigma(\mathcal{A}, \mathcal{B}, Y_0, Z_0, \dots)$.

Consider $\mathbb{E}[X|\mathcal{C}_\infty]$.

Then $\mathbb{E}[\mathbb{E}[X|\mathcal{C}_\infty]|\mathcal{A}, Z_0, \dots] = \mathbb{E}[X|\mathcal{A}, Z_0, \dots] = Y_{n+1}$.

And $\mathbb{E}[\mathbb{E}[X|\mathcal{C}_\infty]|\mathcal{B}, Y_0, \dots] = \mathbb{E}[X|\mathcal{B}, Y_0, \dots] = Z_{n+1}$.

So $Y_\infty = \mathbb{E}[X|\sigma(\mathcal{A}, Z_0, Z_1, \dots)]$ and $Z_\infty = \mathbb{E}[X|\sigma(\mathcal{B}, Y_0, Y_1, \dots)]$.

Let $\mathcal{F}_\infty = \sigma(\mathcal{A}, Z_0, Z_1, \dots)$ and $\mathcal{G}_\infty = \sigma(\mathcal{B}, Y_0, Y_1, \dots)$.

Consider $\mathbb{E}[X|\mathcal{F}_\infty \vee \mathcal{G}_\infty]$.

Then $\mathbb{E}[\mathbb{E}[X|\mathcal{F}_\infty \vee \mathcal{G}_\infty]|\mathcal{F}_\infty] = \mathbb{E}[X|\mathcal{F}_\infty] = Y_\infty$.

And $\mathbb{E}[\mathbb{E}[X|\mathcal{F}_\infty \vee \mathcal{G}_\infty]|\mathcal{G}_\infty] = \mathbb{E}[X|\mathcal{G}_\infty] = Z_\infty$.

This means $Y_\infty = \mathbb{E}[X|\mathcal{F}_\infty \vee \mathcal{G}_\infty]$ a.s. and $Z_\infty = \mathbb{E}[X|\mathcal{F}_\infty \vee \mathcal{G}_\infty]$ a.s.

Therefore, $Y_\infty = Z_\infty$ a.s.

Solution:

(a) For the sequence Y_k , the σ -algebras $\mathcal{F}_k = \sigma(\mathcal{A}, Z_0, \dots, Z_{k-1})$ are increasing as k increases. Since X is integrable, by the Martingale Convergence Theorem for conditional expectations, the sequence $Y_k = \mathbb{E}[X|\mathcal{F}_k]$ converges almost surely and in L^1 to $Y_\infty = \mathbb{E}[X|\sigma(\mathcal{A}, Z_0, Z_1, \dots)]$. Similarly, for the sequence Z_k , the σ -algebras $\mathcal{G}_k = \sigma(\mathcal{B}, Y_0, \dots, Y_{k-1})$ are increasing. Since X is integrable, by the Martingale Convergence Theorem, the sequence $Z_k = \mathbb{E}[X|\mathcal{G}_k]$ converges almost surely and in L^1 to $Z_\infty = \mathbb{E}[X|\sigma(\mathcal{B}, Y_0, Y_1, \dots)]$.

(b) Let $\mathcal{F}_\infty = \sigma(\mathcal{A}, Z_0, Z_1, \dots)$ and $\mathcal{G}_\infty = \sigma(\mathcal{B}, Y_0, Y_1, \dots)$. We have $Y_\infty = \mathbb{E}[X|\mathcal{F}_\infty]$ and $Z_\infty = \mathbb{E}[X|\mathcal{G}_\infty]$. Consider the σ -algebra $\mathcal{H} = \mathcal{F}_\infty \vee \mathcal{G}_\infty = \sigma(\mathcal{A}, \mathcal{B}, Y_0, Z_0, Y_1, Z_1, \dots)$. Consider $W = \mathbb{E}[X|\mathcal{H}]$.

We have $\mathcal{F}_\infty \subseteq \mathcal{H}$, so $\mathbb{E}[W|\mathcal{F}_\infty] = \mathbb{E}[\mathbb{E}[X|\mathcal{H}]|\mathcal{F}_\infty] = \mathbb{E}[X|\mathcal{F}_\infty] = Y_\infty$.

Since W is \mathcal{H} -measurable, $\mathbb{E}[W|\mathcal{F}_\infty] = Y_\infty$ implies that Y_∞ is the conditional expectation of W given \mathcal{F}_∞ . But since Y_∞ is already \mathcal{F}_∞ -measurable, we have $\mathbb{E}[W|\mathcal{F}_\infty] = W$ if W is \mathcal{F}_∞ -measurable, which is not necessarily true.

However, we know that $\mathbb{E}[Y_\infty|\mathcal{F}_\infty] = Y_\infty$ and $\mathbb{E}[Z_\infty|\mathcal{G}_\infty] = Z_\infty$.

Consider $\mathbb{E}[X|\mathcal{F}_\infty \vee \mathcal{G}_\infty]$.

Then $\mathbb{E}[\mathbb{E}[X|\mathcal{F}_\infty \vee \mathcal{G}_\infty]|\mathcal{F}_\infty] = \mathbb{E}[X|\mathcal{F}_\infty] = Y_\infty$.

This implies that $\mathbb{E}[X|\mathcal{F}_\infty \vee \mathcal{G}_\infty] = Y_\infty$ almost surely.

Similarly, $\mathbb{E}[\mathbb{E}[X|\mathcal{F}_\infty \vee \mathcal{G}_\infty]|\mathcal{G}_\infty] = \mathbb{E}[X|\mathcal{G}_\infty] = Z_\infty$.

This implies that $\mathbb{E}[X|\mathcal{F}_\infty \vee \mathcal{G}_\infty] = Z_\infty$ almost surely.

Therefore, $Y_\infty = Z_\infty$ almost surely.

Final Answer: The final answer is $\boxed{Y_\infty = Z_\infty}$

Table 9. **s1K sample stemming from s1-teasers.** The black text is the question and the yellow text is the solution. Based solely on the question we generate the light blue reasoning trace and blue response with Gemini, which we use for training.

Alice and Bob each have a coin and flip it until they get a heads. If Bob flipped his coin more times than Alice, what is the expected number of times Alice flipped her coin?

4/3

The problem asks for the expected number of times Alice flipped her coin, given that Bob flipped his coin more times than Alice.

Let X be the number of flips Alice makes until she gets a head.

Let Y be the number of flips Bob makes until he gets a head.

X and Y are independent random variables following a geometric distribution with parameter $p = 0.5$ (probability of getting a head).

The probability mass function for a geometric distribution is $P(K = k) = (1 - p)^{k-1}p$, for $k = 1, 2, \dots$.

In this case, $p = 0.5$, so $P(K = k) = (0.5)^{k-1}(0.5) = (0.5)^k = \frac{1}{2^k}$.

We are given the condition that Bob flipped his coin more times than Alice, which means $Y > X$.

We want to find the expected value of X given that $Y > X$, i.e., $E[X|Y > X]$.

The formula for conditional expectation is $E[X|A] = \sum_x xP(X = x|A)$.

Also, $P(X = x|A) = \frac{P(X=x \cap A)}{P(A)}$.

In our case, A is the event $Y > X$.

We need to find $P(Y > X)$.

$$P(Y > X) = \sum_{x=1}^{\infty} \sum_{y=x+1}^{\infty} P(X = x, Y = y)$$

Since X and Y are independent, $P(X = x, Y = y) = P(X = x)P(Y = y) = \frac{1}{2^x} \frac{1}{2^y} = \frac{1}{2^{x+y}}$.

$$P(Y > X) = \sum_{x=1}^{\infty} \sum_{y=x+1}^{\infty} \frac{1}{2^{x+y}} = \sum_{x=1}^{\infty} \frac{1}{2^x} \sum_{y=x+1}^{\infty} \frac{1}{2^y}$$

The inner sum is a geometric series: $\sum_{y=x+1}^{\infty} (\frac{1}{2})^y = (\frac{1}{2})^{x+1} + (\frac{1}{2})^{x+2} + \dots$

This is a geometric series with first term $a = (\frac{1}{2})^{x+1}$ and common ratio $r = \frac{1}{2}$.

$$\text{The sum is } \frac{a}{1-r} = \frac{(\frac{1}{2})^{x+1}}{1-\frac{1}{2}} = \frac{(\frac{1}{2})^{x+1}}{\frac{1}{2}} = (\frac{1}{2})^x.$$

$$\text{So, } P(Y > X) = \sum_{x=1}^{\infty} \frac{1}{2^x} (\frac{1}{2})^x = \sum_{x=1}^{\infty} (\frac{1}{4})^x.$$

This is another geometric series with first term $a = \frac{1}{4}$ and common ratio $r = \frac{1}{4}$.

$$\text{The sum is } \frac{a}{1-r} = \frac{\frac{1}{4}}{1-\frac{1}{4}} = \frac{\frac{1}{4}}{\frac{3}{4}} = \frac{1}{3}.$$

Now, we need to find $P(X = x \cap Y > X) = P(X = x, Y > x)$.

$P(X = x, Y > x) = P(X = x)P(Y > x)$, due to independence.

$$P(Y > x) = \sum_{y=x+1}^{\infty} P(Y = y) = \sum_{y=x+1}^{\infty} \frac{1}{2^y} = (\frac{1}{2})^{x+1} + (\frac{1}{2})^{x+2} + \dots = (\frac{1}{2})^x.$$

$$\text{So, } P(X = x, Y > x) = \frac{1}{2^x} \times (\frac{1}{2})^x = (\frac{1}{4})^x.$$

$$\text{Now, we can find } P(X = x|Y > X) = \frac{P(X=x \cap Y > X)}{P(Y > X)} = \frac{(\frac{1}{4})^x}{\frac{1}{3}} = 3(\frac{1}{4})^x.$$

Finally, we can calculate the conditional expectation:

$$E[X|Y > X] = \sum_{x=1}^{\infty} xP(X = x|Y > X) = \sum_{x=1}^{\infty} x \cdot 3(\frac{1}{4})^x = 3 \sum_{x=1}^{\infty} x(\frac{1}{4})^x.$$

Consider the series $S = \sum_{x=1}^{\infty} xr^x$, where $|r| < 1$.

$$S = r + 2r^2 + 3r^3 + 4r^4 + \dots$$

$$\frac{S}{r} = 1 + 2r + 3r^2 + 4r^3 + \dots$$

Consider the geometric series $G = 1 + r + r^2 + r^3 + \dots = \frac{1}{1-r}$.

Differentiating with respect to r :

$$\frac{dG}{dr} = 1 + 2r + 3r^2 + 4r^3 + \dots = \frac{d}{dr} \left(\frac{1}{1-r} \right) = \frac{1}{(1-r)^2}.$$

$$\text{So, } \frac{S}{r} = \frac{1}{(1-r)^2}, \text{ which means } S = \frac{r}{(1-r)^2}.$$

In our case, $r = \frac{1}{4}$.

$$\sum_{x=1}^{\infty} x \left(\frac{1}{4}\right)^x = \frac{\frac{1}{4}}{(1-\frac{1}{4})^2} = \frac{\frac{1}{4}}{(\frac{3}{4})^2} = \frac{\frac{1}{4}}{\frac{9}{16}} = \frac{1}{4} \times \frac{16}{9} = \frac{4}{9}.$$

Therefore, $E[X|Y > X] = 3 \times \frac{4}{9} = \frac{12}{9} = \frac{4}{3}$.

Alternative approach: Symmetry.

Consider the events $Y > X$, $X > Y$, and $X = Y$.

$P(Y > X) = P(X > Y)$ due to symmetry.

$$P(X = Y) = \sum_{k=1}^{\infty} P(X = k, Y = k) = \sum_{k=1}^{\infty} P(X = k)P(Y = k) = \sum_{k=1}^{\infty} \left(\frac{1}{2^k}\right)^2 = \sum_{k=1}^{\infty} \left(\frac{1}{4}\right)^k = \frac{\frac{1}{4}}{1-\frac{1}{4}} = \frac{\frac{1}{4}}{\frac{3}{4}} = \frac{1}{3}.$$

We have $P(Y > X) + P(X > Y) + P(X = Y) = 1$.

$$P(Y > X) + P(Y > X) + \frac{1}{3} = 1.$$

$$2P(Y > X) = 1 - \frac{1}{3} = \frac{2}{3}.$$

$P(Y > X) = \frac{1}{3}$. This confirms our previous calculation.

Let $E[X|Y > X] = \mu$.

We are looking for the expected number of flips Alice made, given Bob flipped more times.

Consider the case where the first flip for both is tails. Then the process restarts, and the condition remains.

Let A_1 be Alice's first flip, B_1 be Bob's first flip.

$$P(A_1 = H) = 1/2, P(A_1 = T) = 1/2.$$

$$P(B_1 = H) = 1/2, P(B_1 = T) = 1/2.$$

Case 1: $A_1 = H, B_1 = H$. $X = 1, Y = 1$, so $Y > X$ is false.

Case 2: $A_1 = H, B_1 = T$. Alice stops at 1, Bob continues. $Y > 1$.

Case 3: $A_1 = T, B_1 = H$. Bob stops at 1, Alice continues.

Case 4: $A_1 = T, B_1 = T$. Both continue.

Consider the conditional probabilities given $Y > X$.

Let $E = E[X|Y > X]$.

If the first flips are HH, the condition $Y > X$ is not met.

If the first flips are HT, Alice's number of flips is 1.

If the first flips are TH, Bob's number of flips is 1, Alice's is at least 2, so $Y < X$.

If the first flips are TT, the problem restarts, and the expected number of additional flips for Alice is still E .

Let N_A be the number of flips Alice makes, N_B be the number of flips Bob makes.

We are given $N_B > N_A$.

Consider the first flips:

HH (prob 1/4): Condition not met.

HT (prob 1/4): Alice flips 1 time.

TH (prob 1/4): Bob flips 1 time, Alice > 1 , so $N_A > N_B$, condition not met.

TT (prob 1/4): Both continue.

Let E be the expected number of Alice's flips given Bob flipped more.

If the first flips are HT, Alice flipped 1 time, and the condition is met.

If the first flips are TT, the situation is the same as the beginning, so the expected number of additional flips for Alice is E .

Consider the event $Y > X$.

Conditioning on the first flips:

$$E[X|Y > X] = E[X|Y > X, HH]P(HH|Y > X) + E[X|Y > X, HT]P(HT|Y > X) + E[X|Y > X, TH]P(TH|Y > X) + E[X|Y > X, TT]P(TT|Y > X)$$

$$P(Y > X|HH) = 0.$$

$$P(Y > X|HT) = 1.$$

$$P(Y > X|TH) = 0.$$

$P(Y > X|TT)$ depends on the future flips.

Let's use the definition of conditional expectation directly.

$$E[X|Y > X] = \sum_{x=1}^{\infty} x P(X = x|Y > X) = \sum_{x=1}^{\infty} x \frac{P(X=x, Y>x)}{P(Y>X)}$$

Consider the probabilities of the first flips given $Y > X$.

$$P(HH|Y > X) = \frac{P(Y>X|HH)P(HH)}{P(Y>X)} = \frac{0 \cdot 1/4}{1/3} = 0.$$

$$P(HT|Y > X) = \frac{P(Y>X|HT)P(HT)}{P(Y>X)} = \frac{1 \cdot 1/4}{1/3} = \frac{3}{4}.$$

$$P(TH|Y > X) = \frac{P(Y>X|TH)P(TH)}{P(Y>X)} = \frac{0 \cdot 1/4}{1/3} = 0.$$

$$P(TT|Y > X) = \frac{P(Y>X|TT)P(TT)}{P(Y>X)}$$

If the first flips are TT, the future behavior is the same, and the condition $Y > X$ holds if Bob takes more flips than Alice in the subsequent trials.

$$P(Y > X|TT) = P(\text{Bob needs more flips than Alice starting from scratch}) = P(Y > X) = 1/3.$$

$$P(TT|Y > X) = \frac{(1/3) \cdot (1/4)}{1/3} = \frac{1}{4}.$$

Sum of conditional probabilities: $0 + 3/4 + 0 + 1/4 = 1$.

Now consider the conditional expectations of X :

$E[X|Y > X, HH]$: Not relevant since $P(HH|Y > X) = 0$.

$E[X|Y > X, HT]$: Given HT and $Y > X$, Alice flipped 1 time. $E = 1$.

$E[X|Y > X, TH]$: Not relevant.

$E[X|Y > X, TT]$: Given TT and $Y > X$, Alice has already flipped once, and the expected number of additional flips is E .

So, the total number of flips is $1 + E$.

$$E = 0 \cdot 0 + 1 \cdot (3/4) + \text{undefined} \cdot 0 + (1 + E) \cdot (1/4)$$

$$E = 0 + 3/4 + 0 + 1/4 + E/4$$

$$E = 1 + E/4$$

$$E - E/4 = 1$$

$$3E/4 = 1$$

$$E = 4/3.$$

This confirms the previous result.

Let's think about the intuition. If we have the condition $Y > X$, it means Alice was "lucky" and got a head early, or Bob was "unlucky".

Consider the random variable $Z = Y - X$. We are given $Z > 0$.

We want $E[X|Z > 0]$.

Let $p = P(\text{head}) = 0.5$.

The number of tails before the first head follows a geometric distribution with parameter p .

$X - 1 \sim \text{Geom}(p)$, $Y - 1 \sim \text{Geom}(p)$.

$$P(X - 1 = k) = (1 - p)^k p.$$

$$P(X = x) = (1 - p)^{x-1} p.$$

Consider the joint distribution of X and Y .

$$P(X = x, Y = y) = p^2 (1 - p)^{x-1} (1 - p)^{y-1}$$

Consider the event $Y = X + k$, where $k \geq 1$.

$$P(Y = X + k) = \sum_{x=1}^{\infty} P(X = x, Y = x + k) = \sum_{x=1}^{\infty} p^2 (1 - p)^{x-1} (1 - p)^{x+k-1}$$

$$= p^2 (1 - p)^{k-1} \sum_{x=1}^{\infty} ((1 - p)^2)^{x-1} = p^2 (1 - p)^{k-1} \frac{1}{1 - (1 - p)^2}$$

$$= p^2 (1 - p)^{k-1} \frac{1}{1 - (1 - 2p + p^2)} = p^2 (1 - p)^{k-1} \frac{1}{2p - p^2} = p^2 (1 - p)^{k-1} \frac{1}{p(2 - p)}$$

$$= \frac{p(1 - p)^{k-1}}{2 - p}.$$

If $p = 0.5$, then $1 - p = 0.5$, $2 - p = 1.5$.

$$P(Y = X + k) = \frac{0.5(0.5)^{k-1}}{1.5} = \frac{(0.5)^k}{1.5} = \frac{(1/2)^k}{3/2} = \frac{1}{2^k} \cdot \frac{2}{3} = \frac{1}{3 \cdot 2^{k-1}}.$$

Check if $\sum_{k=1}^{\infty} P(Y = X + k) = P(Y > X) = 1/3$.

$$\sum_{k=1}^{\infty} \frac{1}{3 \cdot 2^{k-1}} = \frac{1}{3} \sum_{k=1}^{\infty} \left(\frac{1}{2}\right)^{k-1} = \frac{1}{3} (1 + 1/2 + 1/4 + \dots) = \frac{1}{3} \frac{1}{1 - 1/2} = \frac{1}{3} \cdot 2 = \frac{2}{3}.$$

Something is wrong here.

Let's recalculate $P(Y > X)$.

$$P(Y > X) = \sum_{x=1}^{\infty} \sum_{y=x+1}^{\infty} (1 - p)^{x-1} p (1 - p)^{y-1} p$$

$$= p^2 \sum_{x=1}^{\infty} (1 - p)^{x-1} \sum_{y=x+1}^{\infty} (1 - p)^{y-1}$$

$$\text{Inner sum: } (1 - p)^x + (1 - p)^{x+1} + \dots = \frac{(1 - p)^x}{1 - (1 - p)} = \frac{(1 - p)^x}{p}.$$

$$P(Y > X) = p^2 \sum_{x=1}^{\infty} (1 - p)^{x-1} \frac{(1 - p)^x}{p} = p(1 - p) \sum_{x=1}^{\infty} (1 - p)^{2(x-1)}$$

$$= p(1 - p) \sum_{x=1}^{\infty} ((1 - p)^2)^{x-1} = p(1 - p) \frac{1}{1 - (1 - p)^2}$$

$$= p(1 - p) \frac{1}{1 - (1 - 2p + p^2)} = p(1 - p) \frac{1}{2p - p^2} = p(1 - p) \frac{1}{p(2 - p)} = \frac{1 - p}{2 - p}.$$

If $p = 0.5$, $P(Y > X) = \frac{0.5}{1.5} = \frac{1}{3}$. Correct.

Now, let's find $E[X|Y > X]$.

$$E[X|Y > X] = \sum_{x=1}^{\infty} xP(X = x|Y > X) = \sum_{x=1}^{\infty} x \frac{P(X=x, Y>x)}{P(Y>X)}.$$

$$P(X = x, Y > x) = P(X = x)P(Y > x) \text{ (independence)}$$

$$P(X = x) = (1 - p)^{x-1} p.$$

$$P(Y > x) = \sum_{y=x+1}^{\infty} (1 - p)^{y-1} p = p[(1 - p)^x + (1 - p)^{x+1} + \dots] = p \frac{(1-p)^x}{1-(1-p)} = (1 - p)^x.$$

$$P(X = x, Y > x) = (1 - p)^{x-1} p(1 - p)^x = p(1 - p)^{2x-1}.$$

$$E[X|Y > X] = \frac{1}{P(Y>X)} \sum_{x=1}^{\infty} xp(1 - p)^{2x-1}$$

$$= \frac{2-p}{1-p} p(1 - p)^{-1} \sum_{x=1}^{\infty} x((1 - p)^2)^x \text{ (error in power)}$$

$$P(Y > x) = \frac{(1-p)^x}{1-(1-p)} p = (1 - p)^x.$$

$$E[X|Y > X] = \frac{1}{P(Y>X)} \sum_{x=1}^{\infty} xP(X = x)P(Y > x)$$

$$= \frac{1}{P(Y>X)} \sum_{x=1}^{\infty} x(1 - p)^{x-1} p(1 - p)^x$$

$$= \frac{p}{P(Y>X)} \sum_{x=1}^{\infty} x(1 - p)^{2x-1}$$

$$= \frac{p}{(1-p)/(2-p)} (1 - p)^{-1} \sum_{x=1}^{\infty} x((1 - p)^2)^x$$

$$= p \frac{2-p}{(1-p)^2} \sum_{x=1}^{\infty} x((1 - p)^2)^x.$$

$$\text{Let } r = (1 - p)^2. \sum_{x=1}^{\infty} xr^x = \frac{r}{(1-r)^2}.$$

$$1 - r = 1 - (1 - p)^2 = 1 - (1 - 2p + p^2) = 2p - p^2 = p(2 - p).$$

$$(1 - r)^2 = p^2(2 - p)^2.$$

$$\sum_{x=1}^{\infty} x((1 - p)^2)^x = \frac{(1-p)^2}{p^2(2-p)^2}.$$

$$E[X|Y > X] = p \frac{2-p}{(1-p)^2} \frac{(1-p)^2}{p^2(2-p)^2} = \frac{1}{p(2-p)}.$$

$$\text{If } p = 0.5, E[X|Y > X] = \frac{1}{0.5 \times 1.5} = \frac{1}{0.75} = \frac{1}{3/4} = 4/3.$$

Solution:

Let X be the number of flips Alice makes until she gets a head, and Y be the number of flips Bob makes until he gets a head. X and Y are independent geometric random variables with parameter $p = 0.5$. The probability mass function is $P(K = k) = (1 - p)^{k-1} p$.

We are interested in the expected number of times Alice flipped her coin, given that Bob flipped his coin more times than Alice, i.e., $E[X|Y > X]$.

Using the definition of conditional expectation, $E[X|Y > X] = \sum_{x=1}^{\infty} xP(X = x|Y > X)$.

$$P(X = x|Y > X) = \frac{P(X=x, Y>x)}{P(Y>X)}.$$

First, calculate $P(Y > X)$.

$$P(Y > X) = \sum_{x=1}^{\infty} \sum_{y=x+1}^{\infty} P(X = x, Y = y) = \sum_{x=1}^{\infty} P(X = x)P(Y > x).$$

$$P(X = x) = (0.5)^{x-1} (0.5) = (0.5)^x = \frac{1}{2^x}.$$

$$P(Y > x) = \sum_{y=x+1}^{\infty} (0.5)^{y-1} (0.5) = (0.5)^x.$$

$$P(Y > X) = \sum_{x=1}^{\infty} \frac{1}{2^x} \left(\frac{1}{2}\right)^x = \sum_{x=1}^{\infty} \left(\frac{1}{4}\right)^x = \frac{1/4}{1-1/4} = \frac{1/4}{3/4} = \frac{1}{3}.$$

$$\text{Next, calculate } P(X = x, Y > x) = P(X = x)P(Y > x) = \frac{1}{2^x} \left(\frac{1}{2}\right)^x = \left(\frac{1}{4}\right)^x.$$

$$\text{Now, find } P(X = x|Y > X) = \frac{P(X=x, Y>x)}{P(Y>X)} = \frac{(1/4)^x}{1/3} = 3\left(\frac{1}{4}\right)^x.$$

Finally, calculate the conditional expectation:

$$E[X|Y > X] = \sum_{x=1}^{\infty} xP(X = x|Y > X) = \sum_{x=1}^{\infty} x \cdot 3\left(\frac{1}{4}\right)^x = 3 \sum_{x=1}^{\infty} x\left(\frac{1}{4}\right)^x.$$

Using the formula $\sum_{x=1}^{\infty} xr^x = \frac{r}{(1-r)^2}$ with $r = 1/4$:

$$\sum_{x=1}^{\infty} x\left(\frac{1}{4}\right)^x = \frac{1/4}{(1-1/4)^2} = \frac{1/4}{(3/4)^2} = \frac{1/4}{9/16} = \frac{1}{4} \times \frac{16}{9} = \frac{4}{9}.$$

$$E[X|Y > X] = 3 \times \frac{4}{9} = \frac{12}{9} = \frac{4}{3}.$$

Final Answer: The final answer is $\boxed{4/3}$

s1: Simple test-time scaling

Table 10. s1K sample stemming from the astronomy subset of OlympicArena. The black text is the question and the blue text is the solution. Based solely on the question we generate the light blue reasoning trace and blue response with Gemini, which we use for training.

An often-repeated fun fact is that humans produce more power per unit volume than stars. If the sun were the same size, but it produced the same amount of power per unit volume as a human, what would its surface temperature be? Assume the "average human" produces 100 watts of power and has a volume of 66400 cubic centimeters.

- A: 3500 K
- B: 10000 K
- C: 25000 K
- D: 40000 K
- E: 50000 K

Using the numbers from the problem, the average human produces

$$u = \frac{100}{66400 \times 10^{-6}} = 1506 \text{ W/m}^3$$

The volume of the sun is $\frac{4}{3}\pi R_{\odot}^3$, so its new power output would be $P = \frac{4}{3}\pi R_{\odot}^3 u$. To find the equilibrium temperature, we use

$$P = \sigma AT^4 = 4\pi\sigma R_{\odot}^2 T^4$$

Solving for T , we get

$$T = \sqrt[4]{\frac{R_{\odot} u}{3\sigma}} = \sqrt[4]{\frac{(6.96 \times 10^8)(1506)}{3(5.67 \times 10^{-8})}} = 49823 \approx 50000 \text{ K.}$$

The problem asks for the surface temperature of the sun if it had the same size but produced power per unit volume as a human.

First, let's find the power density of a human.

Power produced by a human, $P_{human} = 100 \text{ W}$

Volume of a human, $V_{human} = 66400 \text{ cm}^3$

Convert the volume to cubic meters:

1 m = 100 cm

1 m³ = (100 cm)³ = 10⁶ cm³

$V_{human} = 66400 \text{ cm}^3 = 66400 \times 10^{-6} \text{ m}^3 = 0.0664 \text{ m}^3$

Power density of a human, $\rho_{power, human} = \frac{P_{human}}{V_{human}} = \frac{100 \text{ W}}{0.0664 \text{ m}^3}$

$\rho_{power, human} = 1506.024 \text{ W/m}^3$

Now, consider the sun with the same size as it currently is, but with a power density equal to that of a human.

We need the radius of the sun to calculate its volume. The average radius of the sun is $R_{sun} = 6.95 \times 10^8 \text{ m}$.

Volume of the sun, $V_{sun} = \frac{4}{3}\pi R_{sun}^3 = \frac{4}{3}\pi(6.95 \times 10^8 \text{ m})^3$

$V_{sun} = \frac{4}{3}\pi(337.159375 \times 10^{24}) \text{ m}^3$

$V_{sun} = 1410.24 \times 10^{24} \times \pi \text{ m}^3$

$V_{sun} = 4.4307 \times 10^{27} \text{ m}^3$

If the sun had the same power density as a human, the total power produced by this modified sun would be:

$P_{modified_sun} = \rho_{power, human} \times V_{sun}$

$P_{modified_sun} = 1506.024 \text{ W/m}^3 \times 4.4307 \times 10^{27} \text{ m}^3$

$P_{modified_sun} = 6.6726 \times 10^{30} \text{ W}$

s1: Simple test-time scaling

The surface temperature of a star is related to its luminosity (total power output) through the Stefan-Boltzmann law:

$$L = 4\pi R^2 \sigma T^4$$

where L is the luminosity (total power output), R is the radius of the star, σ is the Stefan-Boltzmann constant, and T is the surface temperature.

In this case, the luminosity of the modified sun is $P_{modified_sun}$. The radius of the modified sun is the same as the actual sun, R_{sun} .

The Stefan-Boltzmann constant, $\sigma = 5.67 \times 10^{-8} \text{ Wm}^{-2}\text{K}^{-4}$.

$$P_{modified_sun} = 4\pi R_{sun}^2 \sigma T^4$$

$$6.6726 \times 10^{30} \text{ W} = 4\pi (6.95 \times 10^8 \text{ m})^2 \times 5.67 \times 10^{-8} \text{ Wm}^{-2}\text{K}^{-4} \times T^4$$

Calculate the term $4\pi R_{sun}^2 \sigma$:

$$R_{sun}^2 = (6.95 \times 10^8)^2 = 48.3025 \times 10^{16} \text{ m}^2$$

$$4\pi R_{sun}^2 = 4\pi \times 48.3025 \times 10^{16} = 607.08 \times 10^{16} \text{ m}^2$$

$$4\pi R_{sun}^2 \sigma = 607.08 \times 10^{16} \text{ m}^2 \times 5.67 \times 10^{-8} \text{ Wm}^{-2}\text{K}^{-4}$$

$$4\pi R_{sun}^2 \sigma = 3441.93 \times 10^8 \text{ WK}^{-4} = 3.44193 \times 10^{11} \text{ WK}^{-4}$$

Now, substitute this back into the equation:

$$6.6726 \times 10^{30} = 3.44193 \times 10^{11} \times T^4$$

Solve for T^4 :

$$T^4 = \frac{6.6726 \times 10^{30}}{3.44193 \times 10^{11}} = 1.9386 \times 10^{19}$$

Solve for T :

$$T = (1.9386 \times 10^{19})^{1/4} = (193.86 \times 10^{17})^{1/4}$$

$$T = (1.9386)^{1/4} \times (10^{19})^{1/4} = (1.9386)^{0.25} \times 10^{4.75}$$

Calculate $(1.9386)^{0.25}$:

$$\text{Let } y = 1.9386^{0.25}, \text{ then } \ln y = 0.25 \ln(1.9386)$$

$$\ln(1.9386) \approx 0.6619$$

$$\ln y = 0.25 \times 0.6619 = 0.165475$$

$$y = e^{0.165475} \approx 1.1799$$

$$\text{So, } T = 1.1799 \times 10^{4.75} = 1.1799 \times 10^4 \times 10^{0.75}$$

$$10^{0.75} = 10^{3/4} = (10^3)^{1/4} = (1000)^{1/4}$$

We know $5^4 = 625$ and $6^4 = 1296$, so $(1000)^{1/4}$ is between 5 and 6.

$$\text{Alternatively, } 10^{0.75} = 10^{0.5} \times 10^{0.25} = \sqrt{10} \times 10^{0.25} \approx 3.16 \times 1.778 = 5.62$$

$$T = 1.1799 \times 10^4 \times 5.62 = 6.63 \times 10^4 \text{ K} = 66300 \text{ K}$$

Let's double-check the calculations.

$$\text{Power density of human: } \rho_{power, human} = 1506.02 \text{ W/m}^3$$

$$\text{Volume of sun: } V_{sun} = 4.43 \times 10^{27} \text{ m}^3$$

$$\text{Power of modified sun: } P_{modified_sun} = 1506.02 \times 4.43 \times 10^{27} = 6671.67 \times 10^{27} = 6.67 \times 10^{30} \text{ W}$$

$$\text{Stefan-Boltzmann law: } P = 4\pi R^2 \sigma T^4$$

$$T^4 = \frac{P}{4\pi R^2 \sigma}$$

$$4\pi R_{sun}^2 \sigma = 3.44 \times 10^{11}$$

$$T^4 = \frac{6.67 \times 10^{30}}{3.44 \times 10^{11}} = 1.939 \times 10^{19}$$

$$T = (1.939 \times 10^{19})^{1/4} = (193.9 \times 10^{17})^{1/4}$$

$$T = (193.9)^{0.25} \times (10^{17})^{0.25} = (193.9)^{0.25} \times 10^{4.25}$$

Calculate $(193.9)^{0.25}$:

$$\text{Let } y = 193.9^{0.25}, \text{ then } \ln y = 0.25 \ln(193.9)$$

$$\ln(193.9) \approx 5.267$$

$$\ln y = 0.25 \times 5.267 = 1.31675$$

$$y = e^{1.31675} \approx 3.73$$

$$T = 3.73 \times 10^{4.25} = 3.73 \times 10^4 \times 10^{0.25} = 37300 \times 1.778 = 66329 \text{ K}$$

The result is around 66000 K. This is not among the options. Let's review the assumptions and calculations.

Assumption: The sun radiates as a black body, which is reasonable for estimating surface temperature.

Consider potential errors in calculations.

Let's try a simpler approach by setting up ratios.

The power per unit volume of the modified sun is equal to that of a human.

$$\frac{P_{\text{modified_sun}}}{V_{\text{sun}}} = \frac{P_{\text{human}}}{V_{\text{human}}}$$

We also know $P_{\text{modified_sun}} = 4\pi R_{\text{sun}}^2 \sigma T_{\text{modified_sun}}^4$.

$$\frac{4\pi R_{\text{sun}}^2 \sigma T_{\text{modified_sun}}^4}{\frac{4}{3}\pi R_{\text{sun}}^3} = \frac{P_{\text{human}}}{V_{\text{human}}}$$

$$\frac{3\sigma T_{\text{modified_sun}}^4}{R_{\text{sun}}} = \rho_{\text{power, human}}$$

$$T_{\text{modified_sun}}^4 = \frac{\rho_{\text{power, human}} R_{\text{sun}}}{3\sigma}$$

Substitute the values:

$$\rho_{\text{power, human}} = 1506.02 \text{ W/m}^3$$

$$R_{\text{sun}} = 6.95 \times 10^8 \text{ m}$$

$$\sigma = 5.67 \times 10^{-8} \text{ Wm}^{-2}\text{K}^{-4}$$

$$T_{\text{modified_sun}}^4 = \frac{1506.02 \times 6.95 \times 10^8}{3 \times 5.67 \times 10^{-8}}$$

$$T_{\text{modified_sun}}^4 = \frac{10466.839 \times 10^8}{17.01 \times 10^{-8}} = \frac{1.0466 \times 10^{12}}{1.701 \times 10^{-7}} = 0.6153 \times 10^{19} = 6.153 \times 10^{18}$$

$$T_{\text{modified_sun}} = (6.153 \times 10^{18})^{1/4} = (6153 \times 10^{15})^{1/4}$$

$$T_{\text{modified_sun}} = (6153)^{0.25} \times (10^{15})^{0.25} = (6153)^{0.25} \times 10^{3.75}$$

Calculate $(6153)^{0.25}$:

$$\text{Let } y = 6153^{0.25}, \text{ then } \ln y = 0.25 \ln(6153)$$

$$\ln(6153) \approx 8.724$$

$$\ln y = 0.25 \times 8.724 = 2.181$$

$$y = e^{2.181} \approx 8.85$$

$$T_{\text{modified_sun}} = 8.85 \times 10^{3.75} = 8.85 \times 10^3 \times 10^{0.75} = 8850 \times 5.62 = 49737 \text{ K}$$

This is close to option E: 50000 K.

Let's re-check the units and calculations carefully.

$$\text{Power density of human: } \frac{100 \text{ W}}{0.0664 \text{ m}^3} = 1506.02 \text{ W/m}^3$$

$$\text{The formula derived was } T^4 = \frac{\rho_{\text{power, human}} R_{\text{sun}}}{3\sigma}.$$

Units check:

$$[\rho_{\text{power, human}}] = \text{W/m}^3$$

$$[R_{\text{sun}}] = \text{m}$$

$$[\sigma] = \text{Wm}^{-2}\text{K}^{-4}$$

$$\frac{(\text{W/m}^3) \times \text{m}}{\text{Wm}^{-2}\text{K}^{-4}} = \frac{\text{W/m}^2}{\text{Wm}^{-2}\text{K}^{-4}} = \frac{\text{W}}{\text{m}^2} \times \frac{\text{m}^2 \text{K}^4}{\text{W}} = \text{K}^4$$

The units match for T^4 .

Numerical calculation check:

$$\text{Numerator: } 1506.02 \times 6.95 \times 10^8 = 10466.839 \times 10^8 = 1.0466 \times 10^{12}$$

$$\text{Denominator: } 3 \times 5.67 \times 10^{-8} = 17.01 \times 10^{-8}$$

$$\text{Ratio: } \frac{1.0466 \times 10^{12}}{17.01 \times 10^{-8}} = 0.061528 \times 10^{20} = 6.1528 \times 10^{18}$$

$$T^4 = 6.1528 \times 10^{18}$$

$$T = (6.1528 \times 10^{18})^{1/4} = (6152.8 \times 10^{15})^{1/4}$$

$$T = (6152.8)^{0.25} \times 10^{3.75}$$

Let's use logarithms for precision.

$$\log_{10}(6152.8) \approx 3.789$$

$$0.25 \times 3.789 = 0.94725$$

$$10^{0.94725} \approx 8.856$$

$$T = 8.856 \times 10^{3.75} = 8.856 \times 10^3 \times 10^{0.75} = 8856 \times 5.623 = 49806 \text{ K}$$

This is very close to 50000 K.

Possible sources of minor discrepancies: rounding errors, precision of constants.

Let's verify the formula derivation.

$$\text{Power per unit volume} = \frac{\text{Total Power}}{\text{Volume}}$$

$$\rho_{power} = \frac{L}{V}$$

$$L = 4\pi R^2 \sigma T^4$$

$$V = \frac{4}{3}\pi R^3$$

$$\rho_{power} = \frac{4\pi R^2 \sigma T^4}{\frac{4}{3}\pi R^3} = \frac{3\sigma T^4}{R}$$

If the modified sun has the power density of a human:

$$\rho_{power,human} = \frac{3\sigma T_{modified_sun}^4}{R_{sun}}$$

$$T_{modified_sun}^4 = \frac{\rho_{power,human} R_{sun}}{3\sigma}$$

The formula derivation seems correct.

Let's use approximate values to check the order of magnitude.

$$\rho_{power,human} \approx 10^3 \text{ W/m}^3$$

$$R_{sun} \approx 7 \times 10^8 \text{ m}$$

$$\sigma \approx 6 \times 10^{-8} \text{ Wm}^{-2}\text{K}^{-4}$$

$$T^4 \approx \frac{10^3 \times 7 \times 10^8}{3 \times 6 \times 10^{-8}} = \frac{7 \times 10^{11}}{18 \times 10^{-8}} = 0.38 \times 10^{19} = 3.8 \times 10^{18}$$

$$T \approx (3.8 \times 10^{18})^{1/4} = (3800 \times 10^{15})^{1/4}$$

$$T \approx (3800)^{0.25} \times 10^{3.75}$$

$$(3800)^{0.25}: 7^4 = 2401, 8^4 = 4096. \text{ So, between 7 and 8.}$$

$$\approx 7.8$$

$$T \approx 7.8 \times 10^{3.75} = 7800 \times 5.6 = 43680 \text{ K}$$

The order of magnitude seems consistent with the detailed calculation.

The problem statement is straightforward and doesn't seem to have any hidden complexities. The assumptions made are standard for such problems.

Consider the precision of the given values.

Power of human: 100 W (exact)

Volume of human: 66400 cm³ (exact)

The result obtained is very close to option E. Given the nature of multiple-choice questions, the closest option is likely the intended answer.

If there were any misinterpretations of the question, it would likely be in the setup. However, the phrase "If the sun were the same size, but it produced the same amount of power per unit volume as a human" seems clear.

The surface temperature is calculated using the Stefan-Boltzmann law, assuming black-body radiation.

Double-check the provided options:

A: 3500 K

B: 10000 K

C: 25000 K

D: 40000 K

E: 50000 K

Our calculated value is approximately 49800 K, which is closest to 50000 K.

If we used more precise values for the constants, the result might be slightly different, but likely not enough to shift to another option.

The fun fact mentioned in the question implies that the power density of a human is higher than that of the sun. Let's verify this.

$$\text{Power output of the sun: } 3.846 \times 10^{26} \text{ W}$$

$$\text{Volume of the sun: } 4.43 \times 10^{27} \text{ m}^3$$

$$\text{Power density of the sun: } \frac{3.846 \times 10^{26}}{4.43 \times 10^{27}} = 0.868 \text{ W/m}^3$$

$$\text{Power density of human: } 1506 \text{ W/m}^3$$

Indeed, the power density of a human is significantly higher than that of the sun.

Final check of the calculation steps and logic. The approach of equating the power density of the modified sun to that of a human and then using the Stefan-Boltzmann law seems correct.

s1: Simple test-time scaling

Solution:

The power produced by an average human is $P_{human} = 100 \text{ W}$, and the volume of an average human is $V_{human} = 66400 \text{ cm}^3 = 0.0664 \text{ m}^3$.

The power density of a human is $\rho_{power, human} = \frac{P_{human}}{V_{human}} = \frac{100 \text{ W}}{0.0664 \text{ m}^3} \approx 1506.02 \text{ W/m}^3$.

If the sun were the same size but produced the same amount of power per unit volume as a human, its power density would be $\rho_{power, modified_sun} = \rho_{power, human}$.

The radius of the sun is $R_{sun} = 6.95 \times 10^8 \text{ m}$.

The volume of the sun is $V_{sun} = \frac{4}{3}\pi R_{sun}^3$.

The power density of the modified sun is given by $\rho_{power, modified_sun} = \frac{P_{modified_sun}}{V_{sun}}$.

We also know that $P_{modified_sun} = 4\pi R_{sun}^2 \sigma T^4$, where T is the surface temperature of the modified sun.

Equating the power density:

$$\rho_{power, human} = \frac{4\pi R_{sun}^2 \sigma T^4}{\frac{4}{3}\pi R_{sun}^3} = \frac{3\sigma T^4}{R_{sun}}$$

Solving for T^4 :

$$T^4 = \frac{\rho_{power, human} R_{sun}}{3\sigma}$$

Substitute the values:

$$T^4 = \frac{1506.02 \text{ W/m}^3 \times 6.95 \times 10^8 \text{ m}}{3 \times 5.67 \times 10^{-8} \text{ Wm}^{-2}\text{K}^{-4}}$$

$$T^4 = \frac{1.0466 \times 10^{12}}{1.701 \times 10^{-7}} = 6.1528 \times 10^{18} \text{ K}^4$$

Solving for T :

$$T = (6.1528 \times 10^{18})^{1/4} = (6152.8)^{0.25} \times 10^{18/4} = (6152.8)^{0.25} \times 10^{4.5}$$

Using logarithms:

$$\log_{10}(6152.8) \approx 3.789$$

$$0.25 \times 3.789 = 0.94725$$

$$(6152.8)^{0.25} = 10^{0.94725} \approx 8.856$$

$$T = 8.856 \times 10^{4.5} = 8.856 \times 10^4 \times 10^{0.5} = 88560 \times \sqrt{10} \approx 88560 \times 3.16 = 280000 \text{ K}$$

Let's redo the exponent calculation: $18/4 = 4.5$.

$$T = 8.856 \times 10^{4.5} = 8.856 \times 10^4 \times 10^{0.5} \text{ - error in previous step.}$$

$$T = (6.1528 \times 10^{18})^{0.25} = 49806 \text{ K}$$

The surface temperature would be approximately 49806 K, which is closest to 50000 K.

Final Answer: The final answer is E

D. Test-time scaling details

D.1. Sequential scaling ablations

<lim_start>user	<lim_start>user
What is the answer to Life, the Universe and Everything?	What is the answer to Life, the Universe and Everything?
Think for up to 2048 tokens.	Think for up to 64 steps.
<lim_start>assistant	<lim_start>assistant
<lim_start>think	<lim_start>64 steps left
Let me break down this question into the three parts it is asking for: 1) Life 2) Universe 3) Everything	Let me break down this question into the three parts it is asking for: 1) Life 2) Universe 3) Everything
Let me start with life...	<lim_start>63 steps left Let me start with life...
<lim_start>answer	<lim_start>answer
The answer is...	The answer is...

Figure 10. **Token and step instruction data formats for controlling test-time compute.** We only train our model on the [reasoning trace](#) and the [answer](#).

Table 11. **Scaling thinking time via tokens-conditional control.** All metrics are averaged over the 30 questions in AIME24.

Tokens instructed (\rightarrow)	1024	2048	4096	8192	16384
<i>No intervention at test-time</i>					
Thinking tokens	7939	7158	8263	7108	7500
Answer tokens	689	669	659	722	724
AIME24	26.7	30.0	33.3	33.3	40.0
<i>Forcing end of thinking when token budget is reached</i>					
Thinking tokens	1024	2048	4031	5664	6330
Answer tokens	15	15	142	722	691
AIME24	3.3	30.0	33.3	33.3	40.0

Token-conditional control One general approach is to simply tell a model in the prompt precisely how many tokens it should generate. Ideally, the model can keep track of its token count and adjust its generation to finish within the desired limits. We experiment with this approach by training a model with token instructions using the format in Figure 10 (left). We bucket the lengths of the reasoning traces from our 1,000 training examples into powers of two (rounded upwards) and add a corresponding instruction to the user prompt. For example, if the instruction says “Think for up to 2048 tokens”, then the reasoning trace has anywhere between 1024 and 2048 tokens. In Table 11, we show that after training the model hardly follows the token instruction. It does sometimes generate more tokens when given a higher limit but often overshoots the limit. This may not be unique to our model as prior work suggests that OpenAI o1-mini can also not follow token instructions (Zhang & Chen, 2024). To prevent exceeding the limit, we test budget forcing the thinking to end once the limit is reached. This leads to perfect control (Table 11 (lower)). With budget forcing, the scaling trend is also clearer as the model can no longer overshoot the limit when given a small thinking budget. This leads to better test-time scaling values for *Token Prompting + budget forcing* in Table 3. To compute Control reported in Table 3 for token-conditional control variants we divide the number of times the thinking tokens in Table 11 are less than the upper limit by the total evaluations (2/5 for without intervention; 5/5 for with intervention).

Step-conditional control Token instructions fail as current models cannot count tokens. To accommodate this lack of capability, we experiment with making the counting more coarse-grained. We partition the reasoning traces into steps and ask the model to think for a specific number of steps rather than tokens. We split our reasoning traces on double newlines into steps, which we find act as intuitive separators based on manual inspection of samples. We bucket our training samples into powers of 2 depending on their number of steps and add a corresponding step instruction following the format in Figure 10 (right). This format is based on early experiments, where we found the model to be more likely to adhere to the step limit

Table 12. **Scaling thinking time via step-conditional control.** All metrics are averaged over the 30 samples in AIME24. Token counts ignore the thinking and step delimiters.

Steps instructed (→)	16	32	64	128	256
<i>No intervention at test-time</i>					
Steps used	123	90	80	82	136
Tokens per step	60	70	69	66	56
Thinking tokens	7252	6277	5396	5552	7551
Answer tokens	665	653	735	777	754
AIME24	33.3	23.3	33.3	36.7	33.3
<i>Forcing end of thinking when 0 steps are reached</i>					
Steps used	16	32	59	78	136
Tokens per step	96	94	80	70	56
Thinking tokens	1517	2963	4636	5409	7551
Answer tokens	1111	788	799	794	754
AIME24	23.3	23.3	33.3	36.7	33.3

Table 13. **Scaling thinking time via class-conditional control.** We report “accuracy / average thinking tokens per sample”; the higher the accuracy and the fewer the thinking tokens (inference cost) the better.

Prompt appended to the question after two newlines	AIME24	MATH	GPQA
<i>Answer after a short amount of thinking. Do not spend excessive time double-checking your work.</i>	30.0% / 8033	90.4% / 2537	56.6% / 4177
<i>Answer after a long amount of thinking. If you feel like you are finished early, spend the extra time trying to double-check your work until you are absolutely sure that you have the correct answer.</i>	36.7% / 9651	91.4% / 3875	51.0% / 4827
Without generic prompt appending	50.0% / 6109	93.0% / 3298	57.6% / 3510

when counting down (“3 steps left...2 steps left”) rather than counting up (“Step2...Step3...”). This is likely because if counting down, the final step is always 1, which will act as a strong prior to the model to finish its generation. If counting up, the final step before the answer varies, thus if the model does not remember the original step instruction, it may fail to stop. We conclude the following from our results in Table 12: **(1)** The model still struggles to adhere to the step limit. The model sometimes simply continues counting into negative steps, e.g. “-1 steps left”. To solve this issue, we automatically stop the thinking process once 0 steps are reached and then force the model to transition to answering mode by appending the answer token delimiter (§3). This leads to perfect step adherence (lower half of Table 12), yet problems remain. **(2)** The model compensates for fewer steps by making each step longer. For example, when forced to use up to 16 steps vs 256 steps, the model generates an average of 96 tokens per step vs 56. Despite this issue, more steps still clearly correlate with more total thinking tokens in Table 12 and better performance leading to a positive slope **(3)** Step instructions are more costly than other methods. The step delimiters require around 6 tokens each which for e.g. 64 steps adds up to a total of around 380 tokens. When ignoring the step delimiters in token counts as in Table 12, the model still requires 7551 thinking tokens on average to achieve only 33.3% on AIME24. To compute Control reported in Table 3 for step-conditional control variants, we first decide that 100 tokens are an upper limit per step and then multiply this number by the steps instructed to arrive at a proxy total token limit, e.g. 1600 for 16 steps instructed. We then check whether the thinking tokens in Table 12 fit within the respective limit for each evaluation run (3/5 for without intervention; 5/5 for with intervention). For the model in Figure 7, we use a model with step-conditional control trained on an earlier version of our data and using an earlier version of our evaluation codebase.

Class-conditional control OpenAI exposes test-time compute control to users via a “reasoning_effort” API parameter with three possible settings: low, medium, and high.³ The OpenAI documentation also states that “Reducing reasoning effort *can* result in faster responses and fewer tokens used on reasoning in a response.” suggesting that they are unable to control test-time compute with guarantees. Thus, maybe OpenAI simply adjusts the prompt or system instruction depending on the reasoning effort desired. In Table 13, we show that separate prompts for short and long thinking allow us to control thinking time to some extent: Prompting the model to think for longer leads to longer thinking. However, it does not reliably improve performance and control is not precise. The current adherence to control may suffice when we only have three classes, but it might not scale to finer-grained classes. To compute Control reported in Table 3 for this method, we assume that prompting the model to think for a short time in Table 13 should produce fewer tokens than the default for AIME24, while the long prompt should produce more. As $8033 > 6109$ and $9651 > 6109$, one out of two follows our expected control thus Control is 50%.

D.2. Examples for rejection sampling ablation

³https://github.com/openai/openai-python/blob/44d6210f101abedeb2dd68507fcffcb329df70ea/src/openai/types/chat/completion_create_params.py#L172

Table 14. Answers generated by an earlier version of s1-32B when rejection sampling on AIME24. The black text is the question and the yellow text is the solution. Based solely on the question we generate the light blue reasoning trace and blue response with s1-32B using a temperature of 1. We generate until the reasoning trace has less than 4000 tokens for the first and less than 8000 tokens for the second example. It required on average 199 (1) tries per example until thinking was ≤ 4000 (≤ 8000 tokens).

Let $O(0, 0)$, $A(\frac{1}{2}, 0)$, and $B(0, \frac{\sqrt{3}}{2})$ be points in the coordinate plane. Let \mathcal{F} be the family of segments \overline{PQ} of unit length lying in the first quadrant with P on the x -axis and Q on the y -axis. There is a unique point C on \overline{AB} , distinct from A and B , that does not belong to any segment from \mathcal{F} other than \overline{AB} . Then $OC^2 = \frac{p}{q}$, where p and q are relatively prime positive integers. Find $p + q$.

23

[Correct generation with 3981 thinking tokens and 1055 answer tokens]

The problem asks for a point C on the segment \overline{AB} that is not contained in any other segment from the family \mathcal{F} , except for \overline{AB} itself.

The points O, A, B form a triangle in the first quadrant.

$$O = (0, 0)$$

$$A = (\frac{1}{2}, 0)$$

$$B = (0, \frac{\sqrt{3}}{2})$$

The segment \overline{AB} connects $A(\frac{1}{2}, 0)$ and $B(0, \frac{\sqrt{3}}{2})$.

The equation of the line containing \overline{AB} can be found using the two points:

$$\text{Slope } m = \frac{\frac{\sqrt{3}}{2} - 0}{0 - \frac{1}{2}} = -\sqrt{3}$$

Using the point-slope form $y - y_1 = m(x - x_1)$ with point $A(\frac{1}{2}, 0)$:

$$y - 0 = -\sqrt{3}(x - \frac{1}{2})$$

$$y = -\sqrt{3}x + \frac{\sqrt{3}}{2}$$

The segment \overline{AB} lies in the first quadrant and connects $(\frac{1}{2}, 0)$ to $(0, \frac{\sqrt{3}}{2})$.

The family \mathcal{F} consists of segments \overline{PQ} of unit length, where P is on the x -axis and Q is on the y -axis. Let $P = (a, 0)$ and $Q = (0, b)$.

The length of \overline{PQ} is $\sqrt{(a - 0)^2 + (0 - b)^2} = \sqrt{a^2 + b^2} = 1$.

So $a^2 + b^2 = 1$.

Since P is on the positive x -axis and Q is on the positive y -axis, we have $a > 0$ and $b > 0$.

The segment \overline{PQ} connects $(a, 0)$ and $(0, b)$. The equation of the line containing \overline{PQ} is $\frac{x}{a} + \frac{y}{b} = 1$.

The region covered by the family \mathcal{F} is the area bounded by the lines containing these segments. The endpoints $(a, 0)$ and $(0, b)$ vary such that $a^2 + b^2 = 1$.

Consider the parametrization $a = \cos \theta$, $b = \sin \theta$, where $0 < \theta < \frac{\pi}{2}$.

The segment \overline{PQ} connects $(\cos \theta, 0)$ and $(0, \sin \theta)$. The equation of the line is $\frac{x}{\cos \theta} + \frac{y}{\sin \theta} = 1$.

We are looking for a unique point C on \overline{AB} , distinct from A and B , that does not belong to any segment from \mathcal{F} other than \overline{AB} .

Let C be a point on \overline{AB} . We can parametrize the points on \overline{AB} as $(1 - t)A + tB$ for $0 \leq t \leq 1$.

$$C = (1 - t)(\frac{1}{2}, 0) + t(0, \frac{\sqrt{3}}{2}) = (\frac{1}{2} - \frac{1}{2}t, \frac{\sqrt{3}}{2}t)$$

Since C is distinct from A and B , we have $0 < t < 1$.

Suppose the point C lies on some segment $\overline{PQ} \in \mathcal{F}$, where $P = (\cos \theta, 0)$ and $Q = (0, \sin \theta)$.

The point C satisfies the equation $\frac{x}{\cos \theta} + \frac{y}{\sin \theta} = 1$.

Plugging in the coordinates of C :

$$\frac{\frac{1-t}{2}}{\cos \theta} + \frac{\frac{\sqrt{3}t}{2}}{\sin \theta} = 1$$

$$\frac{1-t}{2 \cos \theta} + \frac{\sqrt{3}t}{2 \sin \theta} = 1$$

Multiply by 2:

$$\frac{1-t}{\cos \theta} + \frac{\sqrt{3}t}{\sin \theta} = 2$$

$$(1-t) \sin \theta + \sqrt{3}t \cos \theta = 2 \sin \theta \cos \theta$$

$$\sin \theta - t \sin \theta + \sqrt{3}t \cos \theta = \sin(2\theta)/2$$

We are looking for a point C on \overline{AB} such that the only segment from \mathcal{F} containing C is \overline{AB} itself.

The segment \overline{AB} is part of the family \mathcal{F} .

For \overline{AB} , $P = A = (\frac{1}{2}, 0)$ and $Q = B = (0, \frac{\sqrt{3}}{2})$.

Here $a = \frac{1}{2}$, $b = \frac{\sqrt{3}}{2}$.

$$a^2 + b^2 = (\frac{1}{2})^2 + (\frac{\sqrt{3}}{2})^2 = \frac{1}{4} + \frac{3}{4} = 1.$$

The line segment \overline{AB} connects $(\frac{1}{2}, 0)$ and $(0, \frac{\sqrt{3}}{2})$.

The equation of the line is $\frac{x}{1/2} + \frac{y}{\sqrt{3}/2} = 1$, which simplifies to $2x + \frac{2}{\sqrt{3}}y = 1$, or $\sqrt{3}x + y = \frac{\sqrt{3}}{2}$.

This matches the equation $y = -\sqrt{3}x + \frac{\sqrt{3}}{2}$.

Consider the envelope of the family of lines $\frac{x}{\cos \theta} + \frac{y}{\sin \theta} = 1$.

Differentiating with respect to θ :

$$-\frac{x \sin \theta}{\cos^2 \theta} + \frac{y \cos \theta}{\sin^2 \theta} = 0$$

$$\frac{y \cos \theta}{\sin^2 \theta} = \frac{x \sin \theta}{\cos^2 \theta}$$

$$y \cos^3 \theta = x \sin^3 \theta$$

$$\frac{y}{x} = \tan^3 \theta$$

$$\tan \theta = (\frac{y}{x})^{1/3}$$

From the line equation: $y \sin \theta = \sin \theta \cos \theta - x \sin \theta$

$$y = \cos \theta - x$$

$$\text{Substitute } \cos \theta = \frac{1}{\sqrt{1+\tan^2 \theta}} = \frac{1}{\sqrt{1+(y/x)^2/3}}$$

$$\cos \theta = \frac{x^{1/3}}{(x^{2/3} + y^{2/3})^{1/2}}$$

$$\sin \theta = \tan \theta \cos \theta = (\frac{y}{x})^{1/3} \frac{x^{1/3}}{(x^{2/3} + y^{2/3})^{1/2}} = \frac{y^{1/3}}{(x^{2/3} + y^{2/3})^{1/2}}$$

Substitute back into the line equation:

$$\frac{x}{\cos \theta} + \frac{y}{\sin \theta} = 1$$

$$x(x^{2/3} + y^{2/3})^{1/2}/x^{1/3} + y(x^{2/3} + y^{2/3})^{1/2}/y^{1/3} = 1$$

$$x^{2/3}(x^{2/3} + y^{2/3})^{1/2} + y^{2/3}(x^{2/3} + y^{2/3})^{1/2} = 1$$

$$(x^{2/3} + y^{2/3})^{3/2} = 1$$

$$x^{2/3} + y^{2/3} = 1$$

The envelope of the family \mathcal{F} is the astroid $x^{2/3} + y^{2/3} = 1$.

The segments from \mathcal{F} are tangent to this astroid.

The point C on \overline{AB} that we are looking for is the point where \overline{AB} is tangent to the astroid.

The equation of \overline{AB} is $y = -\sqrt{3}x + \frac{\sqrt{3}}{2}$.

Substitute into the astroid equation:

$$x^{2/3} + (-\sqrt{3}x + \frac{\sqrt{3}}{2})^{2/3} = 1$$

Let $u = x^{1/3}$ and $v = y^{1/3}$. The astroid is $u^2 + v^2 = 1$.

The point C lies on both the line \overline{AB} and the astroid.

Differentiating the astroid equation implicitly:

$$\frac{2}{3}x^{-1/3} + \frac{2}{3}y^{-1/3}y' = 0$$

$$y' = -\frac{y^{1/3}}{x^{1/3}} = -(\frac{y}{x})^{1/3}$$

The slope of the tangent to the astroid at a point (x, y) is $-\sqrt[3]{\frac{y}{x}}$.

The slope of the line \overline{AB} is $-\sqrt{3}$.

So, at the point of tangency, $-\sqrt[3]{\frac{y}{x}} = -\sqrt{3}$.

$$\sqrt[3]{\frac{y}{x}} = \sqrt{3}$$

$$\frac{y}{x} = (\sqrt{3})^3 = 3\sqrt{3}$$

The point C lies on the line $y = -\sqrt{3}x + \frac{\sqrt{3}}{2}$ and satisfies $\frac{y}{x} = 3\sqrt{3}$.

$$\text{So } y = 3\sqrt{3}x.$$

Substitute into the line equation:

$$3\sqrt{3}x = -\sqrt{3}x + \frac{\sqrt{3}}{2}$$

$$3x = -x + \frac{1}{2}$$

$$4x = \frac{1}{2}$$

$$x = \frac{1}{8}$$

$$\text{Then } y = 3\sqrt{3}\left(\frac{1}{8}\right) = \frac{3\sqrt{3}}{8}.$$

The point C is $\left(\frac{1}{8}, \frac{3\sqrt{3}}{8}\right)$.

We need to check if this point lies on the segment \overline{AB} .

The point C is of the form $\left(\frac{1}{2} - \frac{1}{2}t, \frac{\sqrt{3}}{2}t\right)$.

$$\frac{1}{2} - \frac{1}{2}t = \frac{1}{8} \implies 4 - 4t = 1 \implies 3 = 4t \implies t = \frac{3}{4}.$$

$$\frac{\sqrt{3}}{2}t = \frac{\sqrt{3}}{2} \cdot \frac{3}{4} = \frac{3\sqrt{3}}{8}.$$

So C lies on \overline{AB} .

We need to make sure $0 < t < 1$, which is true for $t = \frac{3}{4}$.

Now, we need to check if this point C does not belong to any other segment from \mathcal{F} .

The point C lies on the astroid. The segment \overline{AB} is tangent to the astroid at C .

Any other segment from \mathcal{F} that contains C as an interior point, not a tangent point.

Consider the parametrization of the family \mathcal{F} .

A point (x, y) belongs to some segment in \mathcal{F} iff there exists θ such that $\frac{x}{\cos \theta} + \frac{y}{\sin \theta} = 1$.

For the point $C = \left(\frac{1}{8}, \frac{3\sqrt{3}}{8}\right)$, we have:

$$\frac{1/8}{\cos \theta} + \frac{3\sqrt{3}/8}{\sin \theta} = 1$$

$$\frac{1}{\cos \theta} + \frac{3\sqrt{3}}{\sin \theta} = 8$$

$$\sin \theta + 3\sqrt{3} \cos \theta = 8 \sin \theta \cos \theta$$

$$\sin \theta + 3\sqrt{3} \cos \theta = 4 \sin(2\theta)$$

We know that C lies on \overline{AB} , which corresponds to some specific segment in \mathcal{F} .

The problem statement assumes the existence and uniqueness of such a point C .

The unique point C on \overline{AB} , distinct from A and B , that does not belong to any segment from \mathcal{F} other than \overline{AB} .

This means that if C lies on another segment $\overline{P'Q'} \in \mathcal{F}$, then $\overline{P'Q'} = \overline{AB}$.

The point C is the point of tangency of \overline{AB} with the astroid.

Now we need to find OC^2 .

$$OC^2 = \left(\frac{1}{8}\right)^2 + \left(\frac{3\sqrt{3}}{8}\right)^2 = \frac{1}{64} + \frac{27}{64} = \frac{28}{64} = \frac{7}{16}.$$

Here $p = 7$ and $q = 16$.

p and q are relatively prime.

$$p + q = 7 + 16 = 23.$$

Final check of the reasoning:

The family \mathcal{F} consists of unit-length segments with endpoints on the axes.

The envelope of this family is the astroid $x^{2/3} + y^{2/3} = 1$.

The segments from \mathcal{F} are tangent to the astroid.

The segment \overline{AB} is also a member of the family \mathcal{F} .

We are looking for a point C on \overline{AB} that lies on the astroid. 40

This point C is the point of tangency of \overline{AB} with the astroid.

If a point on \overline{AB} lies on the astroid, it belongs to the tangent segment at that point. Since \overline{AB} is the tangent segment, this point does not belong to any other segment from \mathcal{F} .

Consider the case when the segment \overline{AB} intersects the astroid at two points.

If the segment \overline{AB} is not tangent to the astroid, then there are two points of intersection.

Let the points of intersection be C_1 and C_2 .

If C_1 lies on \overline{AB} , then the tangent to the astroid at C_1 is the segment \overline{AB} .

If C_2 lies on \overline{AB} , then the tangent to the astroid at C_2 is the segment \overline{AB} .

The slope of \overline{AB} is $-\sqrt{3}$.

We found the point on the astroid with tangent slope $-\sqrt{3}$.

The problem statement guarantees the uniqueness of such a point C .

The point C must be interior to \overline{AB} , so $0 < t < 1$.

The parameter $t = \frac{3}{4}$ is in this range.

The point C is distinct from A and B .

If $C = A$, then $t = 0$, $C = (\frac{1}{2}, 0)$.

If $C = B$, then $t = 1$, $C = (0, \frac{\sqrt{3}}{2})$.

The point of tangency C is the unique point on \overline{AB} (excluding endpoints) that lies on the astroid.

Solution:

Let the family of segments \mathcal{F} be defined by segments \overline{PQ} of unit length with P on the positive x -axis and Q on the positive y -axis. Let $P = (a, 0)$ and $Q = (0, b)$. The length condition gives $a^2 + b^2 = 1$. The segment \overline{PQ} lies on the line $\frac{x}{a} + \frac{y}{b} = 1$.

Using the parametrization $a = \cos \theta$, $b = \sin \theta$ with $0 < \theta < \frac{\pi}{2}$, the equation of the line is $\frac{x}{\cos \theta} + \frac{y}{\sin \theta} = 1$.

The envelope of this family of lines is the astroid $x^{2/3} + y^{2/3} = 1$.

The segments from \mathcal{F} are tangent to this astroid.

The segment \overline{AB} connects $A(\frac{1}{2}, 0)$ and $B(0, \frac{\sqrt{3}}{2})$. The equation of the line containing \overline{AB} is $y = -\sqrt{3}x + \frac{\sqrt{3}}{2}$. This segment is part of the family \mathcal{F} .

We are looking for a unique point C on \overline{AB} , distinct from A and B , that does not belong to any segment from \mathcal{F} other than \overline{AB} . This means C is the point where \overline{AB} is tangent to the astroid.

The slope of the tangent to the astroid at a point (x, y) is $-\sqrt[3]{\frac{y}{x}}$. The slope of \overline{AB} is $-\sqrt{3}$.

Setting the slopes equal: $-\sqrt[3]{\frac{y}{x}} = -\sqrt{3} \implies \frac{y}{x} = 3\sqrt{3}$.

The point C lies on the line $y = -\sqrt{3}x + \frac{\sqrt{3}}{2}$ and satisfies $y = 3\sqrt{3}x$.

Substituting, $3\sqrt{3}x = -\sqrt{3}x + \frac{\sqrt{3}}{2} \implies 4\sqrt{3}x = \frac{\sqrt{3}}{2} \implies x = \frac{1}{8}$.

Then $y = 3\sqrt{3}(\frac{1}{8}) = \frac{3\sqrt{3}}{8}$.

The point C is $(\frac{1}{8}, \frac{3\sqrt{3}}{8})$.

We need to check if C lies on \overline{AB} . The points on \overline{AB} are $(\frac{1}{2} - \frac{1}{2}t, \frac{\sqrt{3}}{2}t)$ for $0 \leq t \leq 1$.

For $x = \frac{1}{8}$, $\frac{1}{2} - \frac{1}{2}t = \frac{1}{8} \implies t = \frac{3}{4}$.

For $y = \frac{3\sqrt{3}}{8}$, $\frac{\sqrt{3}}{2}t = \frac{3\sqrt{3}}{8} \implies t = \frac{3}{4}$.

Since $0 < \frac{3}{4} < 1$, C is an interior point of \overline{AB} .

The point C is the unique point on \overline{AB} (excluding endpoints) that lies on the astroid. The tangent to the astroid at C is the segment \overline{AB} . Thus, C does not belong to any other segment from \mathcal{F} .

Finally, we calculate $OC^2 = (\frac{1}{8})^2 + (\frac{3\sqrt{3}}{8})^2 = \frac{1}{64} + \frac{27}{64} = \frac{28}{64} = \frac{7}{16}$.

We have $p = 7$ and $q = 16$. These are relatively prime.

$p + q = 7 + 16 = 23$.

Final Answer: The final answer is 23

[Incorrect generation with 5923 thinking tokens and 754 answer tokens]

The problem asks for a point C on the segment \overline{AB} such that C is not on any other segment from the family \mathcal{F} , except \overline{AB} itself. The family \mathcal{F} consists of segments \overline{PQ} of unit length, with P on the x -axis and Q on the y -axis in the first quadrant. Let $P = (x, 0)$ and $Q = (0, y)$, where $x > 0$ and $y > 0$. The length of the segment \overline{PQ} is 1, so the distance between P and Q is 1.

$$\sqrt{(x-0)^2 + (0-y)^2} = 1$$

$$\sqrt{x^2 + y^2} = 1$$

$$x^2 + y^2 = 1$$

The segment \overline{PQ} lies in the first quadrant, so $x > 0$ and $y > 0$.

The equation $x^2 + y^2 = 1$ represents the quarter circle in the first quadrant, with endpoints at $(1, 0)$ and $(0, 1)$.

The points on the segment \overline{PQ} can be parameterized as $(1-t)x + t(0)$, $(1-t)0 + ty) = (x(1-t), yt)$, where $0 \leq t \leq 1$.

The segment \overline{AB} connects $A(\frac{1}{2}, 0)$ and $B(0, \frac{\sqrt{3}}{2})$.

The equation of the line containing \overline{AB} can be found using the two points:

$$\text{Slope } m = \frac{\frac{\sqrt{3}}{2} - 0}{0 - \frac{1}{2}} = \frac{\frac{\sqrt{3}}{2}}{-\frac{1}{2}} = -\sqrt{3}.$$

Using point-slope form with point $A(\frac{1}{2}, 0)$:

$$y - 0 = -\sqrt{3}(x - \frac{1}{2})$$

$$y = -\sqrt{3}x + \frac{\sqrt{3}}{2}$$

The segment \overline{AB} lies in the first quadrant, between $x = 0$ and $x = \frac{1}{2}$.

Alternatively, we can parameterize the points on \overline{AB} .

Let C be a point on \overline{AB} . Then $C = (1-\lambda)A + \lambda B$ for some $0 \leq \lambda \leq 1$.

$$C = (1-\lambda)(\frac{1}{2}, 0) + \lambda(0, \frac{\sqrt{3}}{2}) = (\frac{1}{2} - \frac{1}{2}\lambda, \frac{\sqrt{3}}{2}\lambda).$$

We are looking for a unique point C on \overline{AB} , distinct from A and B , that does not belong to any segment from \mathcal{F} other than \overline{AB} .

Consider a segment from \mathcal{F} , with endpoints $P = (x, 0)$ and $Q = (0, y)$, where $x^2 + y^2 = 1$.

A point on this segment is of the form $(x(1-t), yt)$, where $0 \leq t \leq 1$.

We want to find a point C on \overline{AB} , $C \neq A, B$, such that if C lies on a segment $\overline{PQ} \in \mathcal{F}$, then $\overline{PQ} = \overline{AB}$.

Let $C = (\frac{1}{2} - \frac{1}{2}\lambda, \frac{\sqrt{3}}{2}\lambda)$, where $0 < \lambda < 1$.

If C lies on a segment \overline{PQ} from \mathcal{F} , then there exist $x, y > 0$ with $x^2 + y^2 = 1$, and $t \in [0, 1]$ such that:

$$\frac{1}{2} - \frac{1}{2}\lambda = x(1-t)$$

$$\frac{\sqrt{3}}{2}\lambda = yt$$

$$\text{From the first equation, } 1-t = \frac{\frac{1}{2} - \frac{1}{2}\lambda}{x} = \frac{1-\lambda}{2x}.$$

$$\text{From the second equation, } t = \frac{\frac{\sqrt{3}}{2}\lambda}{y} = \frac{\sqrt{3}\lambda}{2y}.$$

Since $t \in [0, 1]$, we have $1-t \in [0, 1]$.

Also, $x > 0$, so $\frac{1-\lambda}{2x} > 0$, which implies $1-\lambda > 0$, or $\lambda < 1$. This is consistent with the condition for point on \overline{AB} .

$$\text{We have } 1-t = \frac{1-\lambda}{2x} \text{ and } t = \frac{\sqrt{3}\lambda}{2y}.$$

$$\text{Adding these equations: } 1 = \frac{1-\lambda}{2x} + \frac{\sqrt{3}\lambda}{2y}$$

$$2xy = (1-\lambda)y + \sqrt{3}\lambda x$$

We know $x^2 + y^2 = 1$.

If the point C belongs to the segment \overline{AB} itself, then the endpoints of the segment are A and B .

So, the segment is from $(\frac{1}{2}, 0)$ to $(0, \frac{\sqrt{3}}{2})$.

Here, $x = \frac{1}{2}$ and $y = \frac{\sqrt{3}}{2}$.

Check if $x^2 + y^2 = 1$: $(\frac{1}{2})^2 + (\frac{\sqrt{3}}{2})^2 = \frac{1}{4} + \frac{3}{4} = 1$. So $\overline{AB} \in \mathcal{F}$.

If C belongs to another segment \overline{PQ} from \mathcal{F} , with endpoints $P = (x, 0)$ and $Q = (0, y)$, where $(x, y) \neq (\frac{1}{2}, \frac{\sqrt{3}}{2})$.

Consider the geometric interpretation. The family \mathcal{F} consists of segments of unit length with endpoints on the axes. The midpoints of these segments lie on the circle $(x - \frac{1}{2})^2 + (y - \frac{1}{2})^2 = \frac{1}{2}$.

Let the point C correspond to some λ .

If C lies on \overline{PQ} , then $C = (x(1 - t), yt)$.

So, $\frac{1}{2} - \frac{1}{2}\lambda = x(1 - t)$ and $\frac{\sqrt{3}}{2}\lambda = yt$.

We need to find a $\lambda \in (0, 1)$ such that the only solution to these equations, with $x^2 + y^2 = 1$, $x, y > 0$, is $x = \frac{1}{2}$ and $y = \frac{\sqrt{3}}{2}$.

From the equations, $1 - t = \frac{1-\lambda}{2x}$ and $t = \frac{\sqrt{3}\lambda}{2y}$.

Substitute these into $x^2 + y^2 = 1$.

Try a different approach. Consider the tangents to the family of segments.

The segments are formed by points $(x, 0)$ and $(0, y)$ with $x^2 + y^2 = 1$.

The equation of the line containing the segment \overline{PQ} is $\frac{x}{x} + \frac{y}{y} = 1$, or $\frac{x}{x} + \frac{y}{y} = 1$.

The equation of the line is $\frac{x}{x} + \frac{y}{y} = 1$.

Consider the equation of the segment in parametric form: $(x(1 - t), yt)$.

If a point C lies on this segment, then $C = (x_c, y_c)$, where $x_c = x(1 - t)$ and $y_c = yt$.

So, $\frac{x_c}{x} = 1 - t$ and $\frac{y_c}{y} = t$.

$\frac{x_c}{x} + \frac{y_c}{y} = 1 - t + t = 1$.

The segments from \mathcal{F} are parts of the lines $\frac{x}{x_0} + \frac{y}{y_0} = 1$, where $x_0^2 + y_0^2 = 1$, $x_0, y_0 > 0$.

Consider the point $C = (\frac{1}{2} - \frac{1}{2}\lambda, \frac{\sqrt{3}}{2}\lambda)$.

If C lies on a segment from \mathcal{F} with endpoints $(x, 0)$ and $(0, y)$, then:

$$\frac{\frac{1}{2} - \frac{1}{2}\lambda}{x} + \frac{\frac{\sqrt{3}}{2}\lambda}{y} = 1$$

$$\frac{1-\lambda}{2x} + \frac{\sqrt{3}\lambda}{2y} = 1$$

We need to find a unique $\lambda \in (0, 1)$ such that the only solution (x, y) to this equation, with $x^2 + y^2 = 1$, $x, y > 0$, is $(\frac{1}{2}, \frac{\sqrt{3}}{2})$.

Substitute $x = \frac{1}{2}$ and $y = \frac{\sqrt{3}}{2}$ into the equation:

$$\frac{1-\lambda}{2(\frac{1}{2})} + \frac{\sqrt{3}\lambda}{2(\frac{\sqrt{3}}{2})} = 1$$

$$1 - \lambda + \lambda = 1$$

$$1 = 1$$

This shows that any point on \overline{AB} lies on the segment \overline{AB} itself.

Consider the line containing \overline{AB} : $y = -\sqrt{3}x + \frac{\sqrt{3}}{2}$.

If a point C on \overline{AB} also lies on another segment from \mathcal{F} with endpoints $(x, 0)$ and $(0, y)$, then:

$$\frac{x_c}{x} + \frac{y_c}{y} = 1.$$

Let the point C divide \overline{AB} in the ratio $\mu : (1 - \mu)$, where $0 < \mu < 1$.

$$C = (1 - \mu)A + \mu B = (1 - \mu)(\frac{1}{2}, 0) + \mu(0, \frac{\sqrt{3}}{2}) = (\frac{1}{2} - \frac{1}{2}\mu, \frac{\sqrt{3}}{2}\mu).$$

If C lies on a segment with endpoints $(x, 0)$ and $(0, y)$, then:

$$\frac{\frac{1}{2} - \frac{1}{2}\mu}{x} + \frac{\frac{\sqrt{3}}{2}\mu}{y} = 1.$$

We are looking for a point C such that the line passing through C with the form $\frac{x}{x_0} + \frac{y}{y_0} = 1$, where $x_0^2 + y_0^2 = 1$, is unique.

Consider the tangents to the unit circle centered at the origin. The lines of the form $\frac{x}{x_0} + \frac{y}{y_0} = 1$ are tangents to the circle $x^2 + y^2 = r^2$.

Consider the dual problem. The family of segments corresponds to points on the quarter circle $x^2 + y^2 = 1$ in the first quadrant.

The lines containing the segments are $\frac{x}{x_0} + \frac{y}{y_0} = 1$.

The envelope of these lines is the curve whose tangents are these lines.

The equation $\frac{x}{x_0} + \frac{y}{y_0} = 1$, with the constraint $x_0^2 + y_0^2 = 1$.

Let $x_0 = \cos \theta$, $y_0 = \sin \theta$, where $0 < \theta < \frac{\pi}{2}$.

The equations of the lines are $x \cos \theta + y \sin \theta = 1$.

The envelope of the family of lines $x \cos \theta + y \sin \theta = 1$ is the circle $x^2 + y^2 = 1$.

The segments from $\overline{\mathcal{F}}$ are parts of the tangents to the unit circle in the first quadrant.

The point C on \overline{AB} that does not belong to any other segment from \mathcal{F} means that the tangent to the unit circle passing through C is unique.

Consider the point $C = (\frac{1}{2} - \frac{1}{2}\lambda, \frac{\sqrt{3}}{2}\lambda)$.

The tangents to the unit circle passing through C have the form $xx_C + yy_C = 1$.

If the tangent is unique, then C lies on the unit circle.

$$\begin{aligned} (\frac{1}{2} - \frac{1}{2}\lambda)^2 + (\frac{\sqrt{3}}{2}\lambda)^2 &= 1 \\ (\frac{1}{4} - \frac{1}{2}\lambda + \frac{1}{4}\lambda^2) + \frac{3}{4}\lambda^2 &= 1 \\ \frac{1}{4} - \frac{1}{2}\lambda + \lambda^2 &= 1 \\ 4\lambda^2 - 2\lambda + 1 &= 4 \\ 4\lambda^2 - 2\lambda - 3 &= 0 \end{aligned}$$

Solve for λ :

$$\lambda = \frac{-(-2) \pm \sqrt{(-2)^2 - 4(4)(-3)}}{2(4)} = \frac{2 \pm \sqrt{4+48}}{8} = \frac{2 \pm \sqrt{52}}{8} = \frac{2 \pm 2\sqrt{13}}{8} = \frac{1 \pm \sqrt{13}}{4}.$$

We need $0 < \lambda < 1$.

$$\sqrt{13} \approx 3.6.$$

$$\frac{1+3.6}{4} = \frac{4.6}{4} > 1.$$

$$\frac{1-3.6}{4} = \frac{-2.6}{4} < 0.$$

Something is wrong. The point C is inside the unit circle.

Let's rephrase the condition. There is a unique point C on \overline{AB} such that if C lies on a segment $\overline{PQ} \in \mathcal{F}$, then $\overline{PQ} = \overline{AB}$.

Let the point C on \overline{AB} be $(\frac{1}{2} - \frac{1}{2}\lambda, \frac{\sqrt{3}}{2}\lambda)$.

Consider a segment from \mathcal{F} with endpoints $(x, 0)$ and $(0, y)$, $x^2 + y^2 = 1$.

The parametric form of the segment is $(x(1-t), yt)$.

If C is on this segment, then for some $t \in [0, 1]$:

$$\frac{1}{2} - \frac{1}{2}\lambda = x(1-t)$$

$$\frac{\sqrt{3}}{2}\lambda = yt$$

If the segment is unique, then the values of x and y are unique.

The only solution to $\frac{1-\lambda}{2x} + \frac{\sqrt{3}\lambda}{2y} = 1$, with $x^2 + y^2 = 1$, $x, y > 0$, should be $x = \frac{1}{2}, y = \frac{\sqrt{3}}{2}$.

Consider the intersection of the line containing \overline{AB} with the boundary of the region formed by the segments in \mathcal{F} .

The boundaries are the x -axis, y -axis, and the quarter circle $x^2 + y^2 = 1$.

Consider the dual problem again. The family of lines $\frac{x}{x_0} + \frac{y}{y_0} = 1$, where $x_0^2 + y_0^2 = 1$, $x_0, y_0 > 0$.

The envelope of these lines is the circle $x^2 + y^2 = 1$.

A point belongs to a unique segment from \mathcal{F} if it lies on the circle $x^2 + y^2 = 1$.

The point C on \overline{AB} satisfies $C = tA + (1-t)B$.

Let's consider the case where the segment is \overline{AB} . Here $x = \frac{1}{2}, y = \frac{\sqrt{3}}{2}$.

The point C can be represented as $(\frac{1}{2}(1-s), \frac{\sqrt{3}}{2}s)$ for $0 \leq s \leq 1$.

We are looking for a point C on \overline{AB} that does not lie on any other segment from \mathcal{F} .

Consider the geometry. The family \mathcal{F} forms a region bounded by the axes and the quarter circle.

The segments are chords of circles centered on the line $y = x$, tangent to the axes.

Let the endpoints of a segment be $(\cos \theta, 0)$ and $(0, \sin \theta)$.

A point on the segment is $(\cos \theta(1 - t), \sin \theta t)$.

The point $C = (\frac{1}{2} - \frac{1}{2}\lambda, \frac{\sqrt{3}}{2}\lambda)$.

If C lies on such a segment, then $\frac{\frac{1}{2} - \frac{1}{2}\lambda}{\cos \theta} = 1 - t$ and $\frac{\frac{\sqrt{3}}{2}\lambda}{\sin \theta} = t$.

$$\frac{1-\lambda}{2\cos\theta} + \frac{\sqrt{3}\lambda}{2\sin\theta} = 1.$$

We need a unique $\lambda \in (0, 1)$ such that the only solution $(\cos \theta, \sin \theta)$ is $(\frac{1}{2}, \frac{\sqrt{3}}{2})$, which corresponds to $\theta = \frac{\pi}{3}$.

Consider the function $f(\theta) = \frac{1}{2\cos\theta} - \frac{\lambda}{2\cos\theta} + \frac{\sqrt{3}\lambda}{2\sin\theta}$.

We need $f(\theta) = 1$.

If $\lambda = \frac{1}{2}$, then $C = (\frac{1}{4}, \frac{\sqrt{3}}{4})$.

$$\frac{1-1/2}{2\cos\theta} + \frac{\sqrt{3}(1/2)}{2\sin\theta} = 1$$

$$\frac{1}{4\cos\theta} + \frac{\sqrt{3}}{4\sin\theta} = 1$$

$$\frac{1}{\cos\theta} + \frac{\sqrt{3}}{\sin\theta} = 4$$

$$\sin\theta + \sqrt{3}\cos\theta = 4\sin\theta\cos\theta$$

$$\sin\theta + \sqrt{3}\cos\theta = 2\sin(2\theta)$$

Divide by 2: $\frac{1}{2}\sin\theta + \frac{\sqrt{3}}{2}\cos\theta = \sin(2\theta)$

$$\sin(\theta + \frac{\pi}{3}) = \sin(2\theta).$$

$$\theta + \frac{\pi}{3} = 2\theta + 2\pi k, \text{ or } \theta + \frac{\pi}{3} = \pi - 2\theta + 2\pi k.$$

$$\theta = \frac{\pi}{3} - 2\pi k, \text{ so } \theta = \frac{\pi}{3}.$$

$$3\theta = \pi - \frac{\pi}{3} + 2\pi k = \frac{2\pi}{3} + 2\pi k.$$

$$\theta = \frac{2\pi}{9} + \frac{2\pi k}{3}.$$

If $k = 0$, $\theta = \frac{2\pi}{9}$.

If $k = 1$, $\theta = \frac{2\pi}{9} + \frac{2\pi}{3} = \frac{2\pi+6\pi}{9} = \frac{8\pi}{9}$.

If $\lambda = \frac{1}{2}$, the point is $(\frac{1}{4}, \frac{\sqrt{3}}{4})$.

This point lies on segments corresponding to $\theta = \frac{\pi}{3}$ and $\theta = \frac{2\pi}{9}$.

The unique point C means that for other values of λ , there is more than one solution for (x, y) .

Consider the tangent to the unit circle passing through C .

If the tangent is unique, C is on the unit circle.

This leads to $\lambda = \frac{1 \pm \sqrt{13}}{4}$, neither of which is in $(0, 1)$.

Consider the geometric interpretation of the family \mathcal{F} . The segments connect points on the axes such that the distance is 1.

The locus of the centers of these segments is the circle $(x - \frac{1}{2})^2 + (y - \frac{1}{2})^2 = \frac{1}{2}$, in the first quadrant.

If a point C lies on a segment from \mathcal{F} , then C is on a line segment connecting $(x, 0)$ and $(0, y)$ with $x^2 + y^2 = 1$.

The line containing the segment is $\frac{x}{x_0} + \frac{y}{y_0} = 1$.

If C belongs to a unique segment, then there is a unique line of this form passing through C .

The point C on \overline{AB} is $(\frac{1}{2} - \frac{1}{2}\lambda, \frac{\sqrt{3}}{2}\lambda)$.

We need a unique (x_0, y_0) with $x_0^2 + y_0^2 = 1$, $x_0, y_0 > 0$, such that $\frac{\frac{1}{2} - \frac{1}{2}\lambda}{x_0} + \frac{\frac{\sqrt{3}}{2}\lambda}{y_0} = 1$.

Let the point C be such that the line passing through C with the form $\frac{x}{x_0} + \frac{y}{y_0} = 1$ is unique, subject to $x_0^2 + y_0^2 = 1$.

This line is tangent to the unit circle.

The point C lies on the intersection of the line containing \overline{AB} and the unit circle.

$$(\frac{1}{2} - \frac{1}{2}\lambda)^2 + (\frac{\sqrt{3}}{2}\lambda)^2 = 1.$$

We found no solution for $\lambda \in (0, 1)$.

s1: Simple test-time scaling

The unique point C means that if any other segment passes through C , it must be \overline{AB} .

Consider the slope of the line containing the segment connecting $(x, 0)$ and $(0, y)$. Slope is $-\frac{y}{x}$.

The equation is $y = -\frac{y}{x}x + y$.

If C lies on the segment, then $\frac{1-\lambda}{2x} + \frac{\sqrt{3}\lambda}{2y} = 1$.

Consider the geometric mean.

Let the point C have coordinates (a, b) . The segment connecting $(x, 0)$ and $(0, y)$ passes through (a, b) .

$$\frac{a}{x} + \frac{b}{y} = 1.$$

If C is on \overline{AB} , then $b = -\sqrt{3}a + \frac{\sqrt{3}}{2}$.

$$a = \frac{1}{2} - \frac{1}{2}\lambda, b = \frac{\sqrt{3}}{2}\lambda.$$

The point C is tangent to the envelope of the family of segments.

Solution:

Let the family of segments be \mathcal{F} . The segments have endpoints $P = (x, 0)$ and $Q = (0, y)$ with $x^2 + y^2 = 1$ and $x, y > 0$.

The points on the segment \overline{PQ} satisfy $\frac{x}{x} + \frac{y}{y} = 1$. The segments lie on the lines $\frac{x}{x_0} + \frac{y}{y_0} = 1$, where $x_0^2 + y_0^2 = 1$, $x_0, y_0 > 0$.

The segment \overline{AB} has endpoints $A(\frac{1}{2}, 0)$ and $B(0, \frac{\sqrt{3}}{2})$. The equation of the line containing \overline{AB} is $y = -\sqrt{3}x + \frac{\sqrt{3}}{2}$.

A point C on \overline{AB} can be parameterized as $C = (\frac{1}{2} - \frac{1}{2}\lambda, \frac{\sqrt{3}}{2}\lambda)$, where $0 \leq \lambda \leq 1$.

If C belongs to a segment from \mathcal{F} with endpoints $(x, 0)$ and $(0, y)$, then $\frac{\frac{1}{2} - \frac{1}{2}\lambda}{x} + \frac{\frac{\sqrt{3}}{2}\lambda}{y} = 1$.

We are looking for a unique point C on \overline{AB} , distinct from A and B , that does not belong to any segment from \mathcal{F} other than \overline{AB} . This means that the only solution (x, y) to the equation with $x^2 + y^2 = 1$, $x, y > 0$, is $(\frac{1}{2}, \frac{\sqrt{3}}{2})$.

The segments from \mathcal{F} are parts of the tangents to the unit circle. The point C must be tangent to the envelope of the family of segments. The envelope is the unit circle itself.

The unique point C on \overline{AB} , distinct from A and B , that lies on the unit circle. We need to solve:

$$(\frac{1}{2} - \frac{1}{2}\lambda)^2 + (\frac{\sqrt{3}}{2}\lambda)^2 = 1$$

$$\lambda = \frac{1}{2}. \text{ The point } C = (\frac{1}{4}, \frac{\sqrt{3}}{4}).$$

$$OC^2 = (\frac{1}{4})^2 + (\frac{\sqrt{3}}{4})^2 = \frac{1}{16} + \frac{3}{16} = \frac{4}{16} = \frac{1}{4}.$$

$$OC^2 = \frac{1}{4} = \frac{p}{q}, \text{ so } p = 1, q = 4.$$

p and q are relatively prime.

$$p + q = 1 + 4 = 5.$$

Final Answer: The final answer is 5
